ROLE OF BLUE ON YELLOW AND LOW LUMINANCE ACHROMATIC mfVEP IN PREPERIMETRIC GLAUCOMA, AND THEIR STRUCTURAL AND FUNCTIONAL CORRELATES

Radha Govind

Australian School of Advanced Medicine

Faculty of Human Sciences

A thesis submitted to Macquarie University in fulfilment of the requirements for the degree of Doctor of Philosophy

2017

Supervisors

Prof. Stuart L Graham

A/Prof Alexander Klistorner

Dr Hema Arvind

TABLE OF CONTENTS

LIST OF TABLES

LIST OF FIGURES

DECLARATION OF ORIGINALITY

I hereby declare that this thesis is my original work. To the best of my knowledge, this thesis does not contain material that has been accepted for the award of any other degree or diploma at the University or any other tertiary institution. An Ethics committee approval was obtained from the University of Sydney (HREC No: 2012/743) and Macquarie University (HREC Approval number: 05-2009/11594) prior to commencement of the study. Data collection included in this thesis was performed at Save Sight Institute, University of Sydney, The Eye Associates and Australian School of Advanced Medicine, Macquarie University.

I give consent for the thesis to be made available for photocopying and loan if accepted for the award of the degree.

Radha Govind

June 2017

ACKNOWLEDGEMENTS

It takes a village to raise a child and complete a PhD! I am truly indebted to all the wonderful people that have supported me during this amazing journey.

I would like to express my sincere gratitude to my amazing supervisors Prof Stuart Graham and Dr Alexander Klistorner for their great insight, firm yet kind guidance, Dr Hema Arvind for her warmth and kindness and statistical support. I would like to thank all my supervisors for their unwavering support, patience and guidance throughout my research. Their clarity and vision even when I couldn't see past the hurdles has brought me this far.

I wish to acknowledge Macquarie University for having offered support in terms of funding under the Australian Postgraduate Award (APA) and the Postgraduate Research Fund (PGRF) Scholarship. I appreciate the support of the friendly staff at the university, Eye Associates, Save Sight Institute and the Macquarie University Eye clinic. A special thanks to Angela and Theresa for their kindness and positivity.

I would like to thank my dear friends Prema and Deepa for their constant encouragement, love and support throughout this journey. Thanks for putting up with my million phone calls at odd hours, answering my silly questions and checking on me constantly. Thank you both for never giving up on me and taking me through this with the kind of love and understanding that only those who have walked this path before possess.

My family has been my rock in every aspect of my life. I am forever indebted to my amazing husband Govind who has stood by me through the highs and lows, my beautiful kids Surabhi and Sashwath for being there for me every step of the way. Your smiles have picked me up every time I tripped over and have given me hope. I will always remember Surabhi's pep talks, motivating words and love, Sashu's cuddles and optimism. I am forever indebted to my mother Lalitha for everything she has given me in my life, and being my Dad and Mum rolled into one, my dearest Vivek who has been a kind and supportive brother, best friend, and spiritual mate.

My sincere thanks to my in-laws Mr. Narayanan and Mrs. Rajalakshmi, my family in India and the US – Srikanth anna, Uma, Meera and Maalu papa, my soul sisters Renjini and Irene, all my friends and extended family here in Sydney for your constant love and support.

Finally, I dedicate this piece of work to my father, my anchor and my guiding light, Late. Mr. Mahadevan, and my dear mate Arvind smiling from above!

THESIS SUMMARY

Glaucoma is a progressive optic neuropathy characterized by a specific pattern of optic disc damage and ganglion cell loss. It is one of the leading causes of blindness in the world. The gold standard for the diagnosis of glaucoma is the detection of characteristic optic disc changes and identification of visual field loss on Standard Automated Perimetry (SAP), which is subjective and often unreliable. It is also evident that due to the redundancy of the visual system, there exists a time gap in the detection of structural versus functional glaucomatous changes.

The use of multifocal visual evoked potential (mfVEP) to objectively detect glaucomatous visual field defects has been well demonstrated. Building on this, a Blue on Yellow mfVEP (BonY mfVEP) that targets the Koniocellular pathway and Low Luminance Achromatic mfVEP (LLA mfVEP) that targets the Magnocellular pathway of the visual system have been developed. The sensitivities of these specialized multifocal techniques have also been recently studied.

This project seeks to establish the long-term changes associated with these objective perimetry tests and identify the role of both BonY and LLA mfVEP as potential markers in the detection of pre-perimetric glaucoma to establish alternative methods to standard perimetry techniques that offer early detection of functional visual loss. Furthermore, establishing a relationship between these mfVEP techniques to other subjective perimetry techniques and high resolution retinal imaging techniques will help decide on a combination of structural and functional tests that will optimally detect change early as no single test appears to be definitely superior to others.

HYPOTHESIS

- SAP is currently the gold standard for detecting functional visual loss associated with glaucoma. Both BonY mfVEP and LLA mfVEP show the potential to detect functional visual loss associated with early glaucoma prior to changes on SAP.
- Scotomas detected by BonY and LLA mfVEP reflect local structural and functional glaucomatous defects as detected by visual field testing with SAP and imaging techniques such as OCT, HRT and Stereo photography.
- With the conventional understanding that latency delay would more likely reflect demyelination while amplitude would reflect axonal loss, we hypothesize that the BonY and LLA mfVEP latency may have the potential for identifying glaucoma progression earlier than conventional perimetry.
- A combination of specialized mfVEP technique and structural imaging will be the key identifying early glaucomatous changes and detecting progression thereby enabling a confident treatment plan to prevent irreversible vision loss.

This research will set to answer the following questions in each chapter.

- **Chapters 1 and 2** will look at the wealth of research and information available to support the aims of the thesis and to establish the research methods; clinical investigations performed, and enlist the parameters addressed in both normal and diseased eyes.

- Several subjective and objective psychophysical tests have been designed based on the Magnocellular and Koniocellular visual pathways and aim to detect early functional loss in glaucoma. In **Chapter 3**, I will be comparing the performance of subjective and objective perimetry tests based on each pathway and to determine if tests targeting one pathway are better than the other in detecting early functional loss.

- In **Chapter 4** the baseline latency values of BonY and LLA mfVEP are compared between the preperimetric glaucoma subjects that had a worsening visual field defect over time and those that remained stable with no field progression, to assess if latency delay can be an early indicator of future progression. The role of BonY and LLA amplitudes and its correlation with other structural and functional parameters is assessed.

- **Chapter 5** evaluates the combination of structural and functional parameters, which will optimally detect early glaucoma and also monitor progression effectively thereby facilitating early intervention to prevent loss of vision. Prediction of future glaucomatous defects from baseline structural and functional tests by calculating the Positive Predictive Values (PPV) and Negative Predictive Values for combination of structural and functional tests is presented.

- **Chapter 6** summarizes the results of the study and looks at future directions.

CHAPTER 1

INTRODUCTION AND REVIEW OF LITERATURE

1.1 Organization of the Human Retina

The human retina is a thin multilayered tissue that contains three developmentally distinct, interconnected cell groups that form signal processing networks[1] namely the sensory neuroepithelium (SNE) containing Photoreceptors and Bipolar Cells (BC), the Multipolar neurons consisting of Ganglion Cells, Amacrine Cells and Axonal cells and the Gliaform Neurons consisting the Horizontal cells (HC). These are arranged and adapted within the different layers of the retina to meet the various functional requirements (*Fig1.1)*.

The Photoreceptors and Bipolar Cells form the first stage of the vertical chain of the neural pathways in visual processing. The retinal pigment epithelium (RPE) has a highly specialized organization related to its functional role as an intermediary between the choroid and the neural retina. RPE cells are polarized and are involved in diverse activities essential to retinal homeostasis and visual function. Coding of visual information begins with conversion of light energy to membrane potential changes in photoreceptors. Rods have exquisite sensitivity to light and can detect even a single photon and hence responsible for dim light vision. Cones are 100 times less sensitive than rods, but exhibit much faster response kinetics during photo transduction[2,3]. The photoreceptors are connected to the ganglion cells by via the Bipolar cells which get inputs either from rods or cones[4,5,6]. The axons of the Retinal Ganglion Cells (RGCs) carry all the visual information from the inner retina to the brain through the two optic nerves[1].

Fig 1.1: Anatomical layers of the retina comprising the cells contributing the signal processing networks. *RPE- Retinal Pigment Epithelium, OLM- Outer Limiting Membrane, ONL- Outer Nuclear Layer, OPL- Outer Plexiform layer, INL- Inner Plexiform Layer, GCL- Ganglion Cell Layer, NFL- Nerve Fibre Layer, ILM- Internal Limitng Membrane*

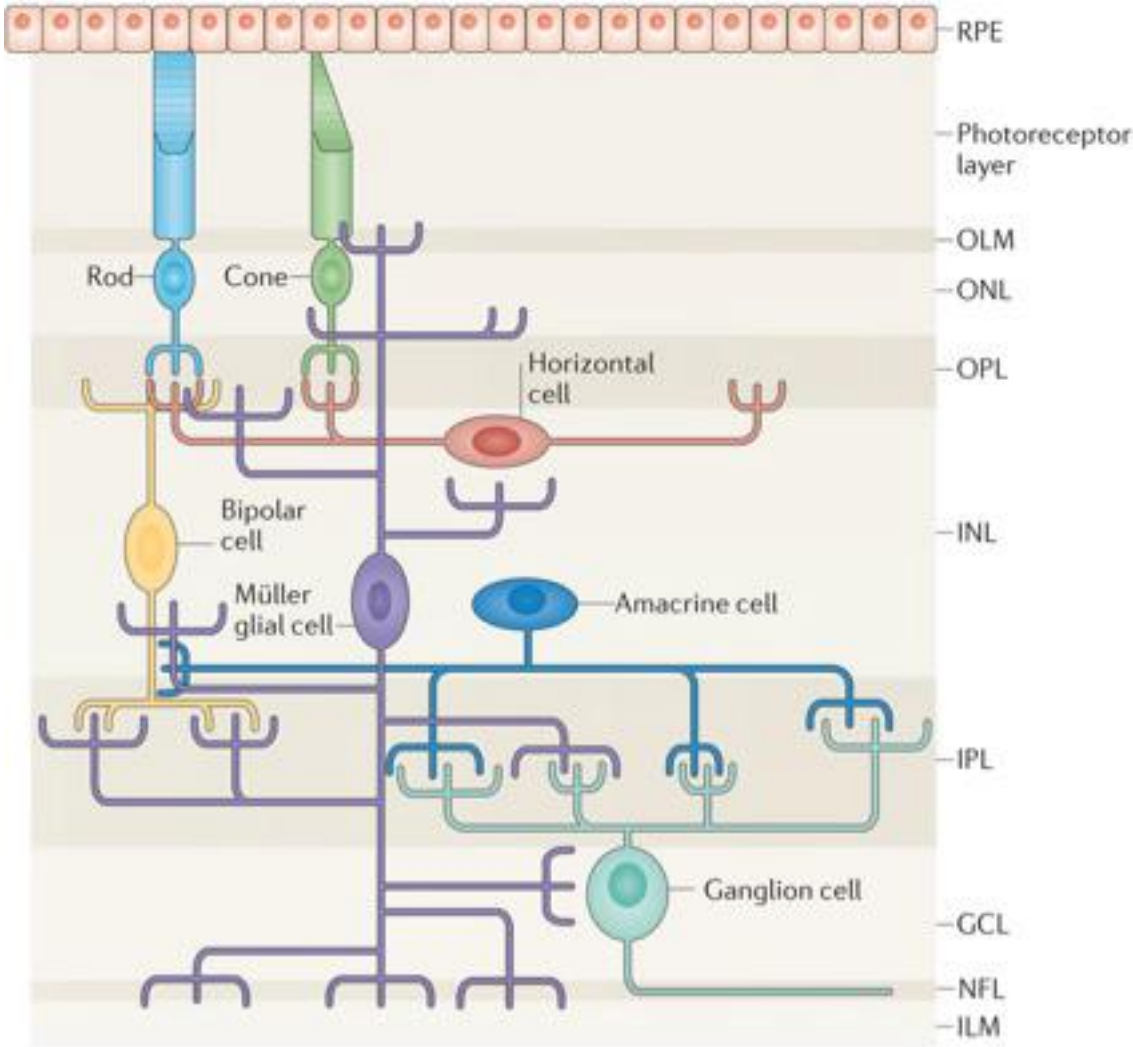

1.2 The Optic Nerve Head

The Optic disc consists of the RGC axons (retinal nerve fibers) converging to exit the eye, forming the neuroretinal rim (NRR) and a central cup, which can vary in size, together with retinal arteries and veins. The RGC axons near the center of the visual field move away from the fovea towards the optic disc in an arcuate pattern entering in the superior and inferior portions of the disc. This prevents the axons from crossing the highly sensitive fovea resulting in a horizontal raphe temporal to the macula (*Fig 1.2)*.

The fibers arising from the RGCs both superior and inferior to the horizontal raphe follow a strict segregation and any injury to these specific locations produces characteristic visual field defects, patterns of neuronal rim loss and optic disc pallor[7,8,9].

Fig 1.2: Orientation of the optic nerve fiber bundles in the right eye. *M- Macula, P- Optic disc, R- Horizontal Raphe, PM- Papillomacular fibres, AF- Arcuate fibres, T- Temporal side, N- Nasal side (Millodot Dictionary of Optometry and Visual Science, 7th edition, 2009, Butterworth-Heinemann)*

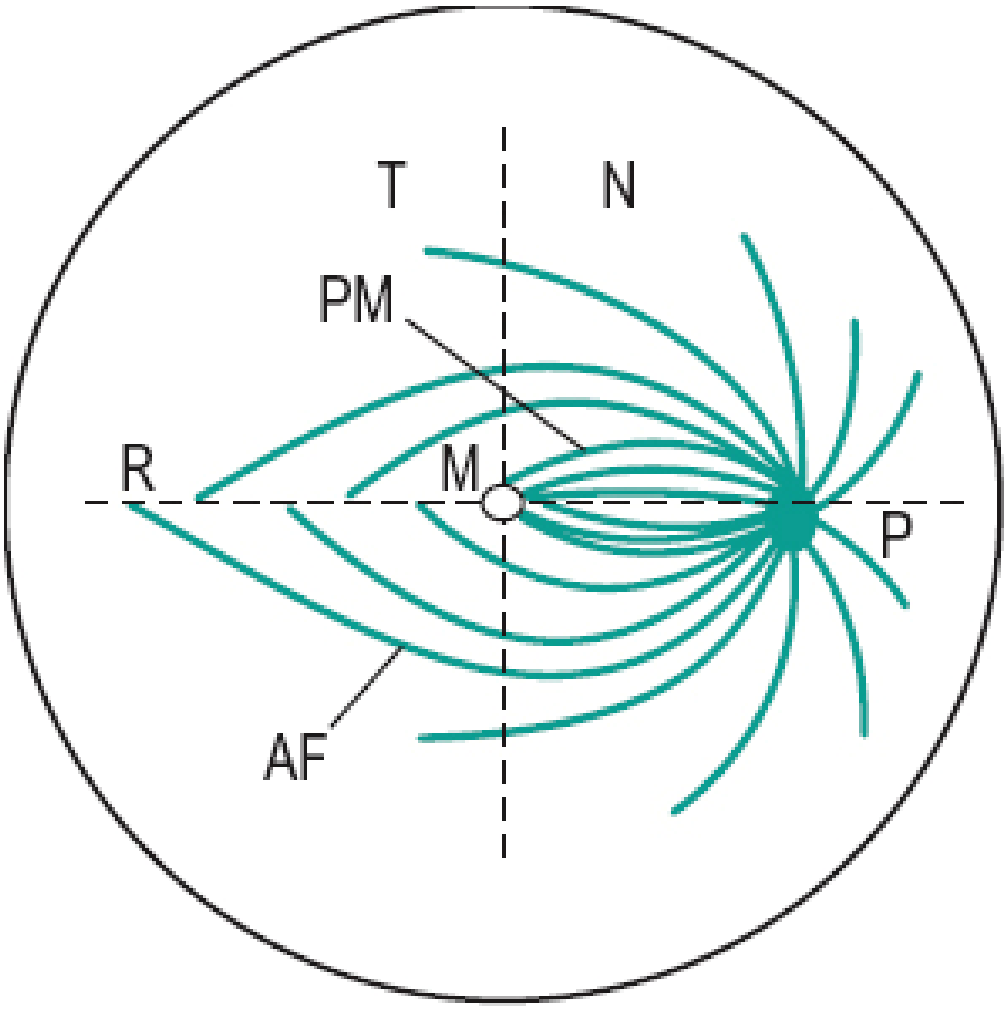

1.3 The Visual Pathways

Many distinct pathways of visual information originate from the retina in order to process multiple distinct visual signals emerging from the photoreceptors. Along with the five major types of RGCs namely ON and OFF parasol, ON and OFF midget, and small bistratified cells which project to the Lateral Geniculate Nucleus (LGN), several additional cell types with distinctive morphology have been identified[10,11,12]. Recent studies postulate that there can be many more visual functional pathways present than the 3 established pathways widely accepted, namely, Parvocellular, Magnocellular and Koniocellular pathways[10,13,14] (*fig 1.3)*.

THE MAGNOCELLULAR (M) PATHWAY originates in the retina largely with the parasol cells, which comprise about 10% of all retinal ganglion cells. Parasol cells have large dendritic and receptive fields and selectively project to the magnocellular layers of the LGN. Functionally, the M pathway is thought to be important for the perception of high frequency flicker[15,16]. They enhance the peripheral retina's ability to pick up motion and low contrast information and also respond to luminance contrast, high temporal and low spatial frequency stimuli[17]. Due to the low prevalence of the magnocellular RGCs, they are considered non-redundant.

THE PARVOCELLULAR PATHWAY begins with the retinal midget cells, comprising approximately 80% of all ganglion cells. Midget cells of the retina have relatively small dendritic and receptive fields and form the major projection to the parvocellular layers of the LGN. The P pathway appears to be important for the high visual acuity [18,19,20]. The parvocellular RGCs are wavelength selective and respond to high spatial frequency, low contrast sensitivity and low temporal frequency stimuli.

THE KONIOCELLULAR PATHWAY sends signals through the LGN to the primary visual cortex[21,22,23]. There is evidence that Koniocellular ganglion cell types are present in the central retina[24]. Koniocellular pathways receive input from the cones serving the central-most degrees of the visual field and it is possible that the cones in the rod-free area of the foveola exclusively serve the midget-parvocellular pathway[25,26]. They have a variable receptive field organization, large dendritic field size and receive stimulation from blue wavelengths[1].

The structure–function relations of other koniocellular populations are less directly established. Two classes of atypical ('ON–OFF' and 'suppressed-by-contrast') receptive fields were reported in the central retina[27,15,28] and in the central visual field representation in the LGN. Due to the smaller population, Koniocellular cells are also considered to be a part of non-redundant group of RGCs.

Fig 1.3: Parallel pathways from the retina to the cortex[29]. *Midget, Parasol and bistratified ganglion cells linked to parallel pathways that remain anatomically separate through the LGN into the Primary Visual Cortex (V1). Midget ganglion cells project to the parvocellular layers of the LGN and on to layer 4Cβ of V1 (red). Parasol ganglion cells project to magnocellular layers of the LGN and on to layer 4Cα of V1 (yellow). Small and large bistratified ganglion cells project to Koniocellular layers of the LGN and on to layer 2/3 (blue).*

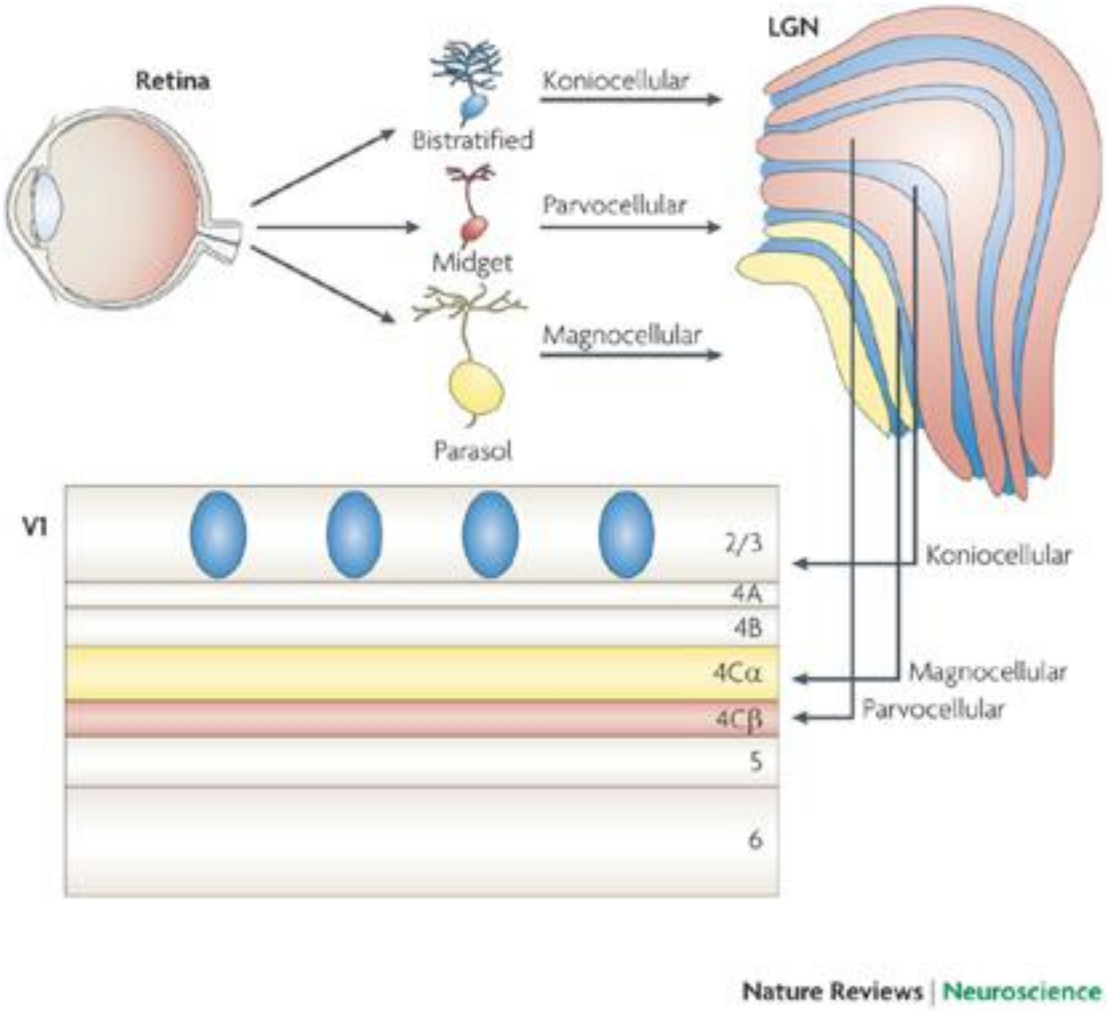

1.4 Glaucomatous Optic Neuropathy

Glaucoma is the leading cause of preventable irreversible blindness in the world. It is a progressive optic neuropathy characterized by a specific pattern of optic disc damage and ganglion cell loss. Early detection and lowering the intraocular pressure remain the most important factors for clinicians. Primary Open Angle Glaucoma (POAG) is the most common type of glaucoma in the Western world, affecting population of over 40 years of age and remains one of the three major causes of blind registrations in Australia[30]. There seems to be an increasing incidence of the disease with increase in age and half of those affected in any population studies are undiagnosed. With the ageing population on the rise in Australia, there will be a steep rise in the financial burden both for the individual and the medical system with the diagnosis of glaucoma. Severe and irreversible damage has usually occurred to the visual field in one or both eyes by the time the disease is detected and a treatment course is started. Earlier studies[31,32] have demonstrated beyond doubt that irreversible nerve fibre loss occurs before SAP detects visual field defects. The rate of progression of the visual field defect varies in patients, and treatment efficacy is variable. Several recent studies[33,34] have established that while treatment slows the disease, treated patients may still show slow advancement of visual field loss.

The following are the common signs that exist in isolation or together that suggest the diagnosis of glaucoma

- Increased cup-disc ratio of >0.6
- Asymmetry in the CD ratio between eyes, >0.2
- Vertical elongation of the Optic disc rim denoting loss of rim superiorly or inferiorly
- Notching or focal loss of the neuroretinal rim,
- Localized wedge defects on the nerve fiber layer
- Associated disc hemorrhages
- Peripapapillary atrophy

Developing neuroretinal rim loss or developing/ progressing visual field loss usually points to the diagnosis of glaucoma. There is a great variability in diagnosing and correlating

progressive structural changes correlating with functional changes. Intraocular pressure (IOP) of greater than 21mmHg is the most reproducible and largely accepted risk factor for Primary Open Angle Glaucoma. Other significant factors include family history, myopia, altered optic nerve head blood supply and increasing age.

The course of glaucomatous progression is highly variable. Identifying factors that predict progression can help guide clinical practice and patient treatment and monitoring. It has been estimated that the incidence of blindness 20 years after the initial diagnosis of POAG is 27% for one eye and 9% for both eyes in a primarily white population[35]. Data from population-based, cross-sectional studies revealed that for patients with POAG, the mean change in visual field testing for European-derived, Hispanic, African-derived and Chinese was –1.12, –1.26, –1.33 and –1.56 dB/year, respectively. The differences in the mean deviation (MD) were not statistically significant by ethnicity. Because some participants were treated, the data cannot be used to represent the natural history of POAG[35].

The Early Manifest Glaucoma Trial (EMGT) and the Collaborative Normal Tension Glaucoma Study (CNTGS) have provided important data on the natural course of POAG and on its risk factors for progression and are progressive studies that tested large groups of people with glaucoma without treatment. Patients need to be monitored carefully after being diagnosed with glaucoma to determine the rapidity of glaucoma progression. Individualised treatment plans must be tailored to patients and to their rate of progression.

The EMGT[36] study was randomised to the no-treatment group studied in detail about the natural course of POAG and can be used to predict the likelihood of visual loss from glaucoma. 49% of the individuals without treatment progressed, compared with 30% with treatment (an average IOP lowering of 25%)[37,38] . 68% of the untreated patients showed definite visual field progression, with an overall median time to progression of 42.8 months after a 6 year follow up. There was a significant variation in time to progression among the subjects after 4 years of follow up. In some cases, the disease deteriorated within 1 year but most of the time, it took several years to demonstrate progression.

The Collaborative Normal Tension Glaucoma Study (CNTGS)[39] found that there was a wide variability in the clinical course of the disease and documented the natural course of untreated Normal Tension Glaucoma (NTG). The focus was on patients with glaucomatous optic nerve damage and visual field loss accompanied by an IOP within the normal range. This study established that the level of IOP still influences the course of NTG. Both these studies

indicate that treatment should be personalized based of the stage of disease and rate of progression.

1.5 Structural Assessments in Glaucoma

1.5.1 Stereo disc photography

The evaluation of the optic nerve and retinal nerve fiber layer (RNFL) is essential to the recognition of glaucomatous damage and remains the most important technique in the evaluation of the subject with glaucoma with objective documentation of the disc where possible. Morphological examination of the optic nerve head using stereoscopic photos is a cost effective and simple method that is clinically mandatory in glaucoma diagnosis monitor progression.

An optic nerve or RNFL abnormality is often, but not always, the first sign of glaucomatous damage. Early glaucomatous damage can be difficult to detect, requiring careful observation of the optic nerve and RNFL. Optic disc photography or optic nerve and RNFL imaging (see below) should be performed at the initial visit and yearly thereafter to document the optic nerve and RNFL status[40].

A thorough optic nerve examination should be used along with perimetry to diagnose glaucoma and to assess disease severity. Staging the disease and consideration of risk factors for glaucoma progression enables the clinician to establish a target intraocular pressure. The structural assessment (optic nerve and RNFL) and functional evaluation (perimetry) are used together to monitor for change over time as well restage the patient's condition. Optic disc and RNFL assessment should include the evaluation of optic disc size, rim shape and area, presence of RNFL loss, peripapillary atrophy (PPA), and retinal or optic disc hemorrhages. This will improve the ability to diagnosis and manage glaucoma[41].

The Ocular Hypertension Treatment Study (OHTS)[42], EMGT and European glaucoma prevention study[43] have all used the optic disc photography as a method for assessment of optic disc damage in their randomized clinical trials. Standardizing the optic disc evaluation enables reproducibility in the evaluation of optic disc photographs[44,45]

By subjectively assessing the optic nerve, the clinician can make note of the other disease processes that can affect the functional evaluation. It also enables comprehensive evaluation of parameters such as disc hemorrhages, and disc pallor. There have also been several advances in computer-based technologies that can provide the examiner with reproducible assessments of the ONH.

Fig 1.4: Progression of optic nerve cupping in the left eye of a patient with glaucoma. The image on the left shows a relatively normal optic cup indicated by the arrow. The image on the right shows progression of the disease in the same subject after 5 years.

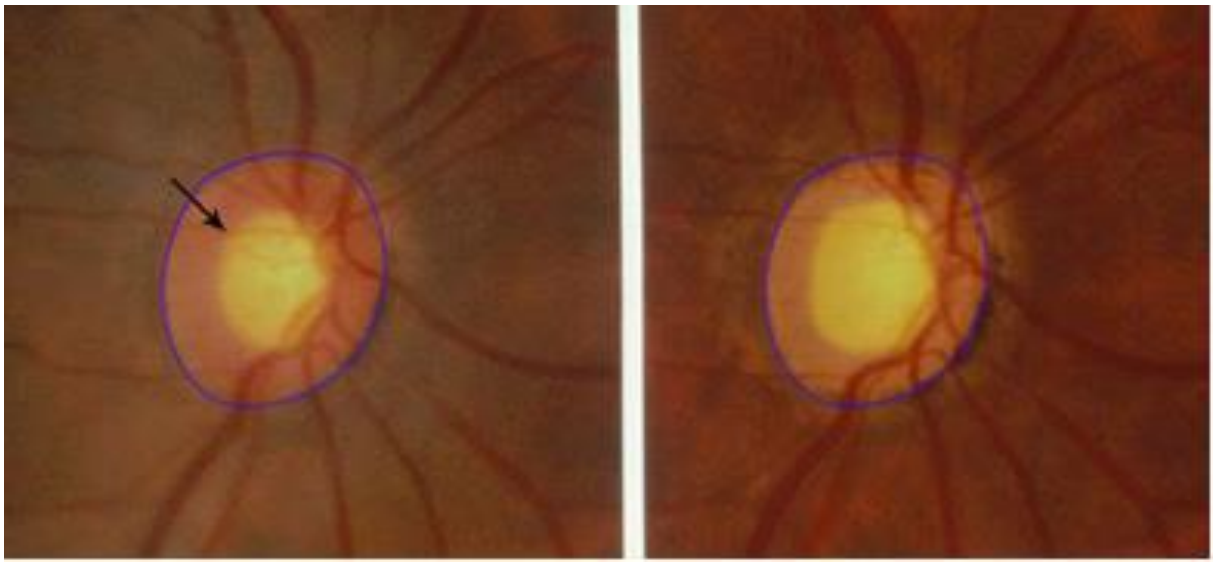

Detecting change and monitoring progression:

Monitoring the optic disc change can be achieved by comparing the serial photographs over time. Comparing the trajectory of the blood vessels on the optic disc between stereo photographs helps in detecting change. Estimating the cup/disc ratio is insufficient for monitoring structural changes. Presence of beta-zone PPA and enlargement of beta-zone PPA have been shown to be associated with glaucoma progression[46,47,48].

Limitations: There is a lot of variability in classifying the optic nerve head as glaucomatous between practitioners and between visits[36]. There is also a high inter and intra observer variability in disc assessment. Increasing media opacities can hamper the comparison of serial photographs. Clarity of the media and patient cooperation is also essential in obtaining a good quality image.

1.5.2 Scanning Laser Ophthalmoscopy using Heidelberg Retinal Tomograph II (HRT II)

HRT provides a real-time imaging technique that produces multiple coronal optical cross-sections of the retina and optic nerve head. These are combined to give a three-dimensional image of the optic nerve.

The Heidelberg Retina Tomograph (HRT; Heidelberg Engineering, Heidelberg, Germany) is a widely used CSLO device. The HRT uses a diode laser beam (wavelength, 670 nm) and captures a series of 32 sequential two-dimensional scans in a total acquisition time of 1.6 seconds. The optical transverse resolution of the HRT is 10 μm and the axial resolution 300 μm.

The HRT II uses a higher resolution and measures a 15-degree scan area and automatically adjusts the fine focus and scan depth. This also keeps the axial resolution of the scan at 62 μm by varying the number of imaging planes. This ensures constant digital resolution despite the differences in the depth or size of optic disc.

The HRT II calculates stereometric parameters, including cup shape, cup volume, rim area, rim volume, mean retinal nerve fiber layer (RNFL) thickness, mean height of contour, mean contour elevation, mean cup depth, and mean height inside contour line, and compares them to the normal ranges.

The Glaucoma Probability Score (GPS) can distinguish between healthy and glaucomatous eyes. GPS is an operator-independent algorithm at least with respect to defining the disc margin. In addition to the numeric GPS score, the Moorfields Regression Analysis (MRA) shows a graphical representation of the GPS with a) red crosses that indicate an 'outside normal limits' disc sector, b) yellow exclamation mark indicating a 'borderline' disc sector and c) green check marks indicating a 'within normal limits' disc sector. These classifications cannot be used in isolation and all other clinical features should be taken into consideration.

If the GPS classification changes between repeated tests in the absence of glaucomatous progression, the test should be considered unreliable[49,50]. GPS classification is based on the manufacturer suggested cutoff values. Borderline classifications should be interpreted with a degree of caution as eyes close to the lower and higher cutoffs may well be differently classified on repeat testing[51]. Change in GPS over time (linear regression) is in moderate agreement with change in rim area and change in visual sensitivity[51].

The MRA compares the topography of the optic disc to that of a normative database. An advantage of the MRA is that it can be used to compare the neuroretinal rim areas in six sectors to the corresponding areas of visual field and provide a global comparison of the data. The six segments are the superior half of disc, inferior half of disc, superior temporal segment, inferior temporal segment, superior segment and inferior segment[52].

HRT-II software also performs Topographic Change Analyses (TCA) on the topographic parameters obtained. TCA compares topographic values in discrete areas of the image and utilizes a comparison of each follow-up image to its baseline, and represents change with a pixel plot. The HRT automatically performs the TCA if there is one mean baseline image and at least two follow-up images. TCA is a powerful analysis that can often detect very small changes in the optic disc tomography.

Limitations*:* Mean pixel height standard deviation (MPHSD) provides an objective measurement of HRT image quality. Factors affecting the image quality are age, high myopia, and increased visual impairment and media opacities. The acceptable cut off for good image quality is 40 μm. Higher cut off value of MPHSD increases test-retest variability[53,54,55] and may result in inaccurate measurements for some optic disc structures.

The test provides topography of the disc but cannot directly measure RNFL thickness, but rather uses an arbitrary level of 50um below the paillomacular bundle as its reference plane to calculate RNFL thickness.

Despite the limitations, several studies show that measurements with the HRT are highly reproducible and accurate in determining the optic disc topography in numerous studies[56,45,57,58,59].

Fig 1.5: Heidelberg Retinal Tomograph (HRT II) scan report showing MRA. The image on top shows the topographic map of the optic disc. Dark colors are elevated and light colors appear deeper. Red indicates the cup, while the blue and green areas demonstrate the sloping and non-sloping neuroretinal rim (NRR), respectively. The bottom figure shows the MRA as utilized by the HRT II in a healthy optic nerve. MRA compares the sectoral NRR areas to the corresponding areas of the visual field in six different sectors, as shown in the analysis at the bottom of the figure.

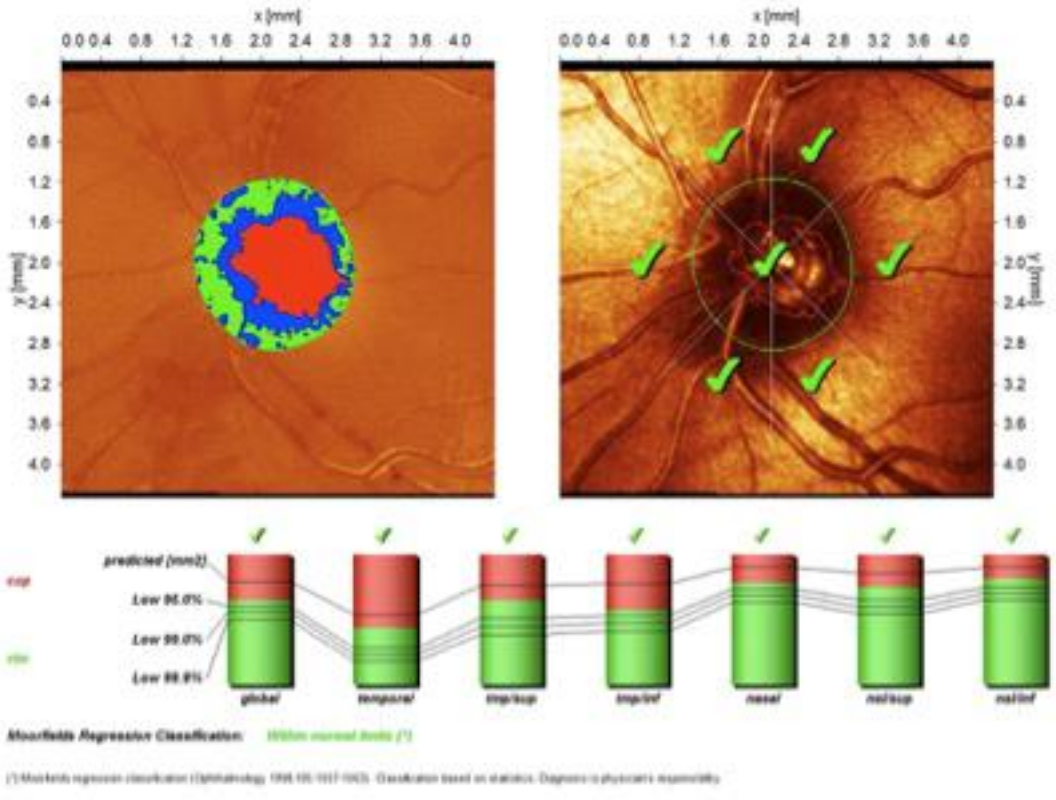

Rim Area	global	temporal	tmp/sup	tmp/inf	nasal	nal/sup	nal/inf
actual (mm2)	1.41	0.23	0.18	0.16	0.41	0.21	0.22
predicted (mm2)	1.71	0.29	0.22	0.20	0.47	0.23	0.24
low 95.0% CI lim. (mm2)	1.31	0.15	0.15	0.13	0.38	0.19	0.20
low 99.0% CI lim. (mm2)	1.20	0.12	0.13	0.14	0.36	0.18	0.19
low 99.9% CI lim. (mm2)	1.09	0.10	0.11	0.12	0.33	0.15	0.17
actual/disc area (%)	65.56	44.30	65.34	57.35	78.51	75.19	81.51
predicted (%)	79.62	54.38	76.50	77.78	90.56	85.65	90.52
low 95.0% CI lim. (%)	60.84	28.43	51.36	53.62	73.71	65.44	74.90
low 99.0% CI lim. (%)	55.69	23.17	45.30	47.69	69.06	60.12	70.54
low 99.9% CI lim. (%)	50.63	18.26	39.13	41.60	64.05	54.46	65.81

1.5.3 Spectral Domain-Optical Coherence Tomography (SD-OCT)

OCT is a non-contact, non-invasive imaging technique that provides high resolution, cross sectional images of the posterior segment of the eye.

Spectral domain OCT (SD-OCT) has enabled clinicians to obtain very high-resolution images of the ONH and RNFL structures and the technique are much faster than the earlier time domain OCT techniques. Several studies advocate macular imaging[60,61] as a useful tool for structural assessment of glaucomatous damage as the macula has the highest concentration of ganglion cells[60]. This technique also provides reproducible measurements in normal and glaucomatous eyes. Inter-test variability of SDOCT is also excellent. Average RNFL measurements showed the best reproducibility[60,62]. No relationship was found between the severity of glaucoma and variability of OCT RNFL measurements[63]. However, in advanced disease the RNFL reaches a "floor' or lower limit and is therefore less useful to detect further change.

The strength of the OCT technologies lies in its ability to measure structural parameters without the need for a reference plane or magnification correction and their ability to image all three scanning areas namely, RNFL, ONH, and macula. The Spectralis SD-OCT (Heidelberg Eng.) has an axial resolution of 3.9μm with a transverse resolution of 14μm and scan depth of 1.9mm. The dual-beam scanning system consists of a confocal scanning laser ophthalmoscopy (CSLO) reference beam to acquire reference scans for eye movement tracking and a second beam to simultaneously acquire OCT images. The system provides a "RNFL change report" that shows the individual baseline and follow-up scans for the overall and sectoral RNFL measurements[64].

Progression on OCT has been defined as a reproducible mean RNFL thinning of >20μm[65]. The guided progression analysis (GPA) evaluates and compares scans acquired longitudinally and gives a summary analysis after considering the expected test-retest variability. The corresponding rate of change and a p value is given. Rate of change on Time-Domain OCT is -0.72μm/ year and -1.26 to -2.12 μm/ year on Spectral Domain OCT[66,67,68] Evaluation of GPA is a better tool than assessing the ONH and macular thickness parameters in detecting change over time[69]. RNFL thickness declines with time in normal (around 0.2-0.5um per year, but much faster in glaucoma cases [67]. In clinical practice however, faster rates can be frequently seen[70,71,72,73]. It does not correlate well with the decline of Visual Field Index (VFI) on perimetry[74].

Limitations of OCT*:* As for all optical imaging technologies, image quality may be compromised in patients with media opacities. The signal strength influences the measurements taken. Another major drawback is the non-compatibility of current SDOCT technology with the earlier OCT technologies. There is also a lack of ethnicity-specific normative database. There is currently a progression analysis software available in the OCT but this was under trial and was unavailable for the analysis of this study.

Fig 1.6: Spectralis SD-OCT scans and RNFL change report of a glaucoma subject with baseline and follow-up showing progressive loss of the RNFL

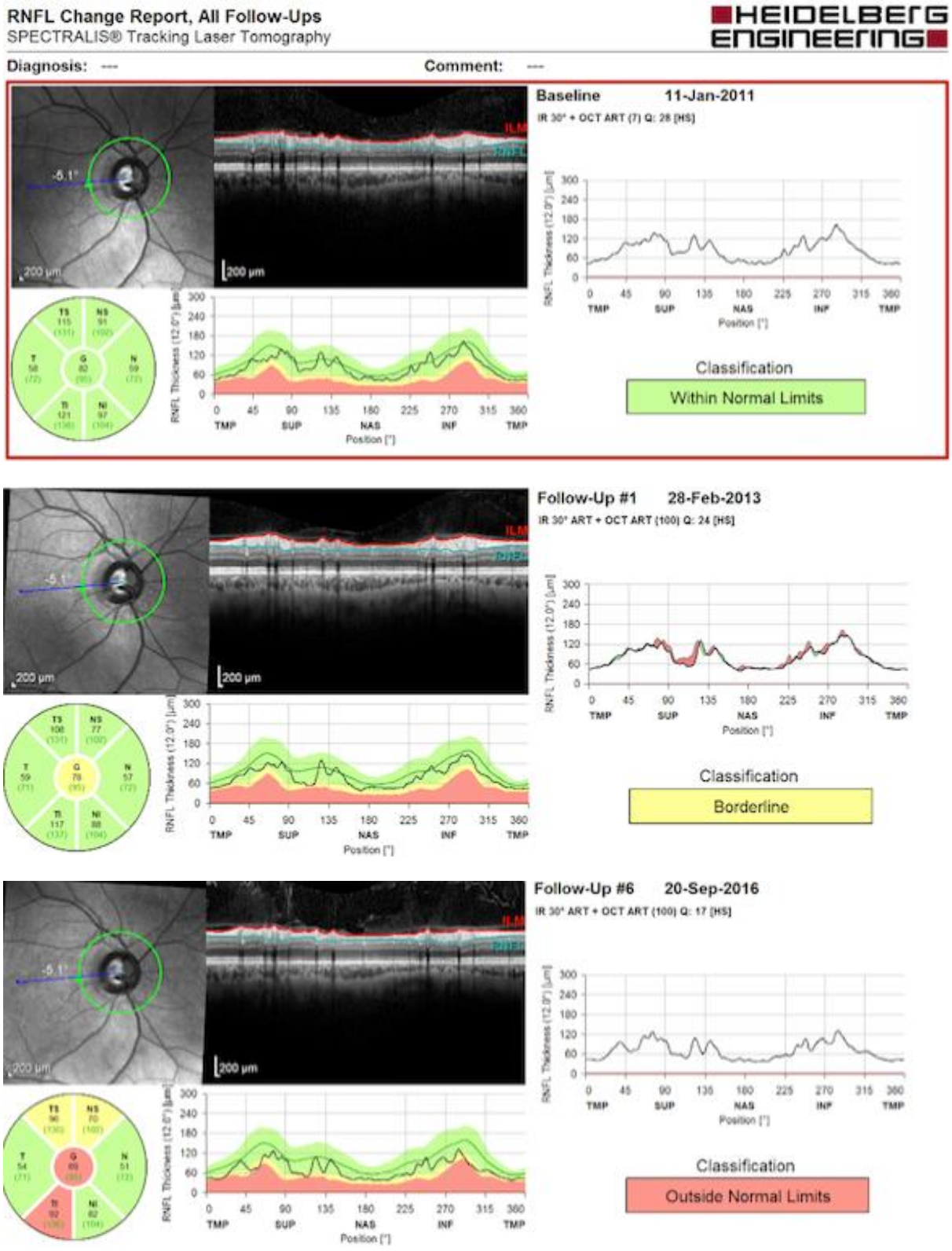

1.6 Functional Assessments in Glaucoma

1.6.1 Standard Automated Perimetry

Automated perimetry has become an integral tool in the management of glaucoma and is widely used as the metric to determine functional loss. The Humphrey Visual Field Analyzer (HFA II-i) is the most widely used automated perimeter among clinicians. Standard threshold automated perimetry (SAP) involves determining the minimum luminance necessary for the patient to detect the presentation of a static white light stimulus of constant size in various locations of the visual field. The value of automated perimetry testing depends on the reliability of the patient's responses and careful administration of the test by the investigator[75].

There is significant inter-test variability in individual glaucoma patients and the presence of high risk factors for developing glaucomatous damage that makes it difficult to determine the presence of damage with statistical confidence. It is also difficult to distinguish between true progression and fluctuation unless the test is repeated multiple times[76]. Repeating the test is a tedious process often not followed in common practice, despite the published evidence[31, 76].

SAP uses a static achromatic stimulus. It is thought to nonselectively invoke all the primary RGC types responsible for vision. Since there is considerable overlap in the receptive fields of retinal ganglion cells, a test with a nonselective stimulus may not be highly sensitive for the earliest loss of retinal ganglion cells due to the considerable redundancy in the coverage of a given location in the retina[77]. Therefore, unless the damage is very localized, standard threshold automated perimetry may not detect visual field loss until the optic nerve has already suffered considerable damage[32].

The presence of changes in RNFL, site and severity of the defects, peripapillary changes, changes in the neuroretinal rim and vasculature were assessed in various cross-sectional studies on structure-function relationships in glaucoma. The results indicate a strong correlation between subjective assessment of the optic disc using disc photography and standard automated perimetry[78]. The incidence of field progression was significantly higher in subjects defined as having glaucomatous optic discs at baseline, indicating that structural changes were likely to be present before visual field changes[34].

Several factors that influence variability of the visual field results such as patient performance, poor reliability indices, fatigue, media opacities, learning effects, uncorrected refractive error and true physiological variability together account for only one third of the variability found in testing[79,80].[81]. Swedish Interactive Threshold Algorithm (SITA) is a testing strategy that greatly reduces the testing time and variability compared to the full threshold testing. In addition, SITA STANDARD algorithm also uses the Guided Progression Analysis (GPA) on the HFA to identify the progression of the existing defect. This is based on the progression analysis developed for the Early Manifest Glaucoma Trial (EMGT)[82].

Measuring the rate of VF progression

Subjective judgment of visual field printouts is unreliable and agreement among clinicians is poor[83]. Statistical analysis in the perimeter or stand-alone software is advantageous to measure progression.

Progression of a glaucomatous visual field loss is defined as a reproducible drop in the visual field mean deviation of at least 2dB[84]. Both local and global metrices such as Mean Deviation (MD) or Visual Field Index (VFI) are needed for assessing progression. Total Deviation based methods are more sensitive to cataract while pattern deviation methods may underestimate progression rates.

Various scoring systems are used to measure visual field loss progression in clinical trials. The Advanced Glaucoma Intervention Study (AGIS)[44] used the actual difference in the threshold values from normal. The Collaborative Initial Glaucoma Treatment Study (CIGTS)[85] used the probability values associated with these differences. This scoring design assigns weights to the probability values and uses nearest locations to establish the severity and the depth of the defect. Both systems grade the severity of visual field loss. CIGTS scoring system has a higher temporal variability than AGIS system.

All Glaucoma clinicians and researchers use HVF perimetry to help with both the diagnosis of glaucomatous field loss and to assess the progression. Currently glaucoma progression analysis, progressor and VFI (Visual Field Index) are used for trend and event analysis. Most clinicians utilize a combination of trend and event analysis and there is consensus that better methods to detect progression are required.

Fig 1.7: Example HFA report of a patient with early glaucoma

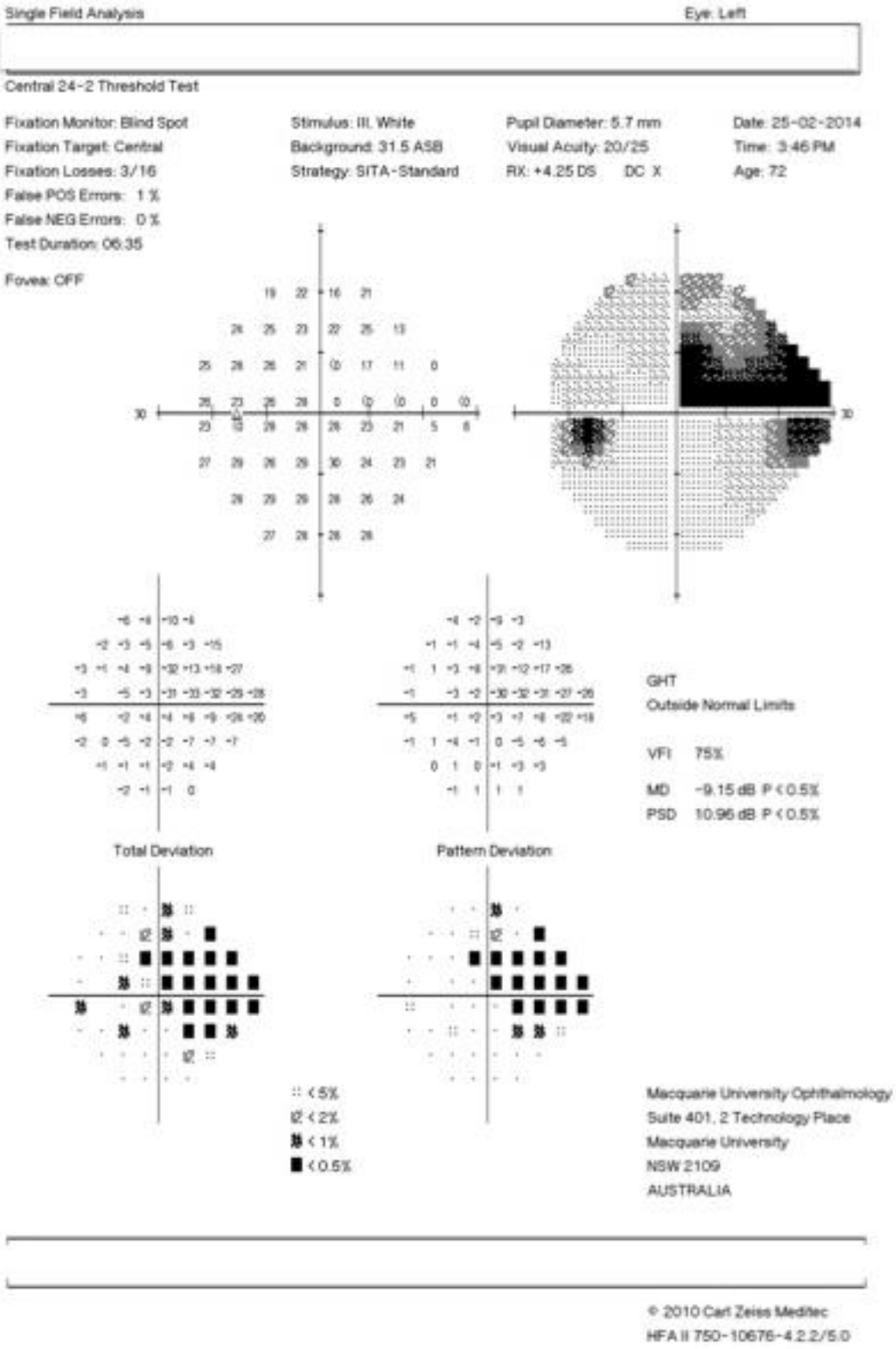

1.6.2 Short Wavelength Automated Perimetry (SWAP)

Blue-yellow perimetry, or SWAP, is designed to assess short wavelength loss, which is believed to be detectable earlier in glaucoma patients and is mediated by the midget small bistratified ganglion cells[86]. SWAP assesses the S cone visual field under yellow adaptation that reduces participation of the other cone systems. SWAP varies from SAP in that a narrow-band size V blue-light stimulus (peak sensitivity 440 nanometer [nm]) is presented on a broad-band yellow background illumination[87]. The development of SWAP as a visual field test was based on the finding that glaucomatous optic nerve damage may be associated with an acquired color vision deficit in the blue-yellow spectrum and/or red-green spectrum[88]. The clinical application of the technique was developed by Stiles to assess the blue-yellow chromatic channel[89].

The incidence of new glaucomatous visual field abnormalities when testing with SWAP is comparable to that detected with standard threshold automated perimetry. However, when a defect appears with SWAP, it may be more likely to persist in follow-up tests than when a defect appears in standard threshold automated perimetry[90,91,92].

Initial studies reported that localized short wavelength losses were more prevalent in patients who have ocular hypertension and glaucoma[93]. The short wavelength deficits are larger than the defects seen in standard threshold automated perimetry, and the rate of progression was twice as high in SWAP[94]. However more recent studies suggest that the performance of SAP was equal to or slightly better than SWAP and not significantly different from FDT[95]. There is a higher variability between tests and intratest in SWAP than in standard threshold automated perimetry[91]. This indicates that larger deviations from normal values are required for statistical significance. For subjects with established glaucomatous visual field loss on SAP, the area of visual field loss is larger on SWAP[96, 97]. In another study by Johnson et al[78], the defects on SWAP were larger in the progressing group as opposed to those that were stable. The findings of this study also indicated that SWAP results could predict the development of glaucomatous visual field loss 3 to 5 years earlier[98]. This was identical to an earlier study by Sample et al[97]. Despite the correlation of the structural changes on the ONH to the functional defects detected on SWAP, increasing evidence suggests that the structural changes precede the functional visual loss[99, 100].

Several longitudinal studies indicate that SWAP detects functional loss 3-5 years prior to the abnormalities being detected on SAP[101, 102, 103]. In eyes with established visual field defects, the progression of the defect on SWAP is faster than SAP. However, a more recent study by Van de Schoot et al. suggests that SAP appears to be as sensitive as SWAP to conversion in a large majority of the eyes[92].

Limitations of the SWAP technique are the long test duration, influence of media opacities and a greater magnitude of long-term fluctuation compared with standard threshold automated perimetry, making it difficult to assess progression accurately. SWAP is now considered less valuable for the detection and monitoring of glaucomatous progression[92].

Fig 1.8: Example SWAP report of a patient with early glaucoma

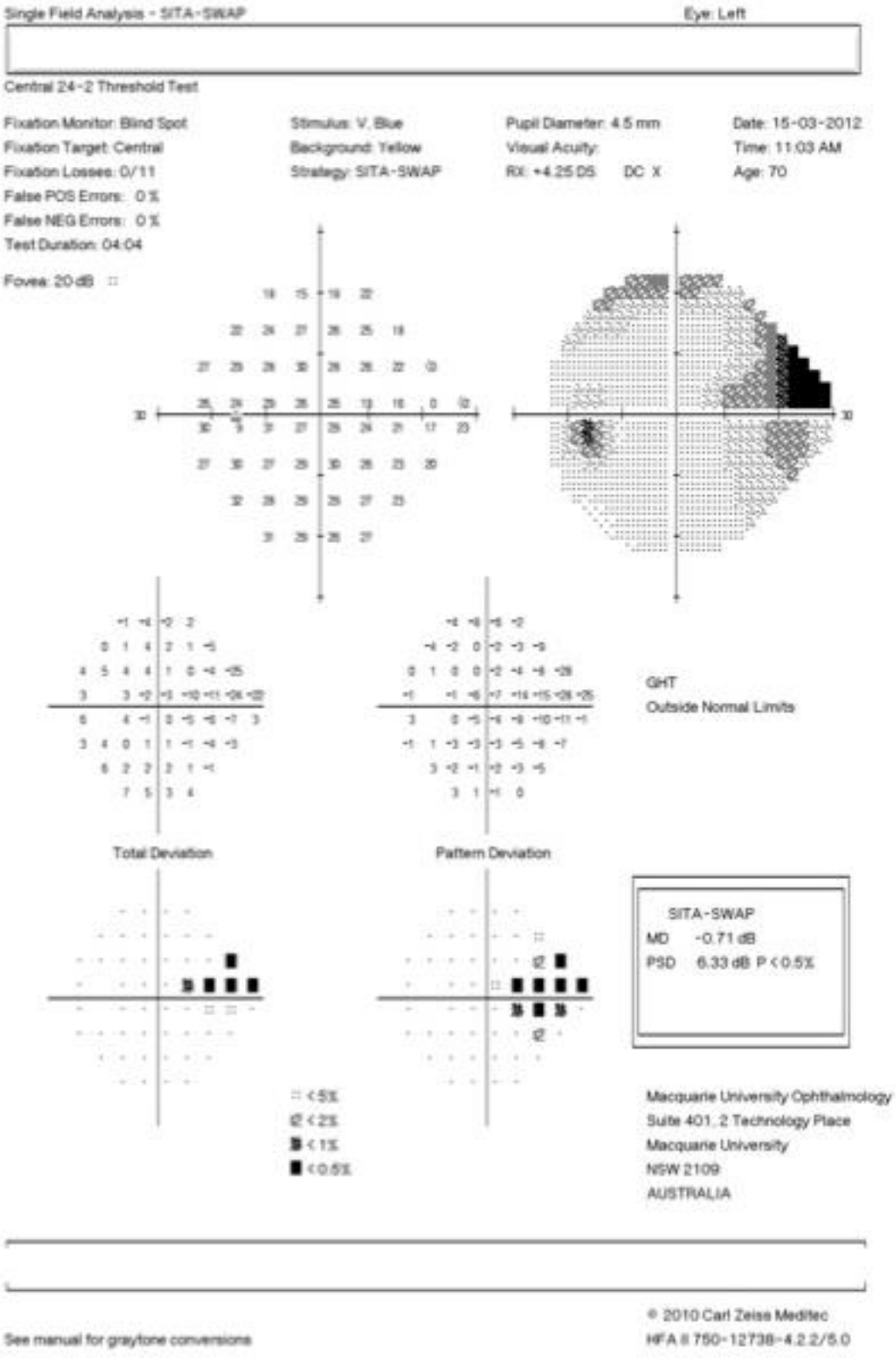

1.6.3 Frequency Doubling Technology (FDT) Perimetry

This rapid visual function test exploits the frequency doubling illusion[104] where the alternating light and dark bars appear to have twice the actual number of bars when shown at low spatial frequency (less than 1 cpd) and high temporal frequency (greater than 15 Hz) counterface flicker. The large-diameter ganglion cells in the magnocellular visual pathway mediate this process. FDT perimetry is a contrast threshold test with a more complex target than standard threshold automated perimetry.

In general, FDT is a useful tool for the detection of glaucoma for both full threshold testing and as a screening device. A number of studies show that the FDP has a high sensitivity and specificity for the early glaucoma detection using the HFA as gold standard[105, 106, 95] for early glaucoma and a higher values for moderate and advanced glaucoma[107, 108].

Predicting Progression*:* In a recent study by Xin et al the change in mean deviation (MD) of HVF over time and the change in MD of FDT over time were compared. The agreement among tests on which eyes showed progression was poor[109]. Studies comparing FDT against SAP in eyes with glaucoma defined by structural damage to the optic disc, find that the diagnostic precision of the FDT is similar to or slightly better than SAP[110, 111].

The main advantages of FDT perimetry are the short testing time, resistance to blur and pupil size, and the convenience of a portable and relatively inexpensive instrument. Some of the disadvantages are the insufficient fixation checks, inability to store the data in memory, and poor printout quality. Data on reproducibility has been conflicting. While one study reported a poor reproducibility in borderline cases another indicated that reproducibility for FDT is better that for standard threshold automated perimetry for all cases from normal to advanced glaucoma. FDT perimetry is currently most useful as a screening tool, although further advances in this technology may allow it to become appropriate for long-term follow-up of patients.

The FDT was adapted to test a more conventional Humphrey 24-2 test grid pattern in the Matrix perimeter[112]. This provided more detailed topography for scotomas, with a similar or slightly lower sensitivity to SAP[113].

Fig 1.9: Example FDT report of a patient with early glaucoma

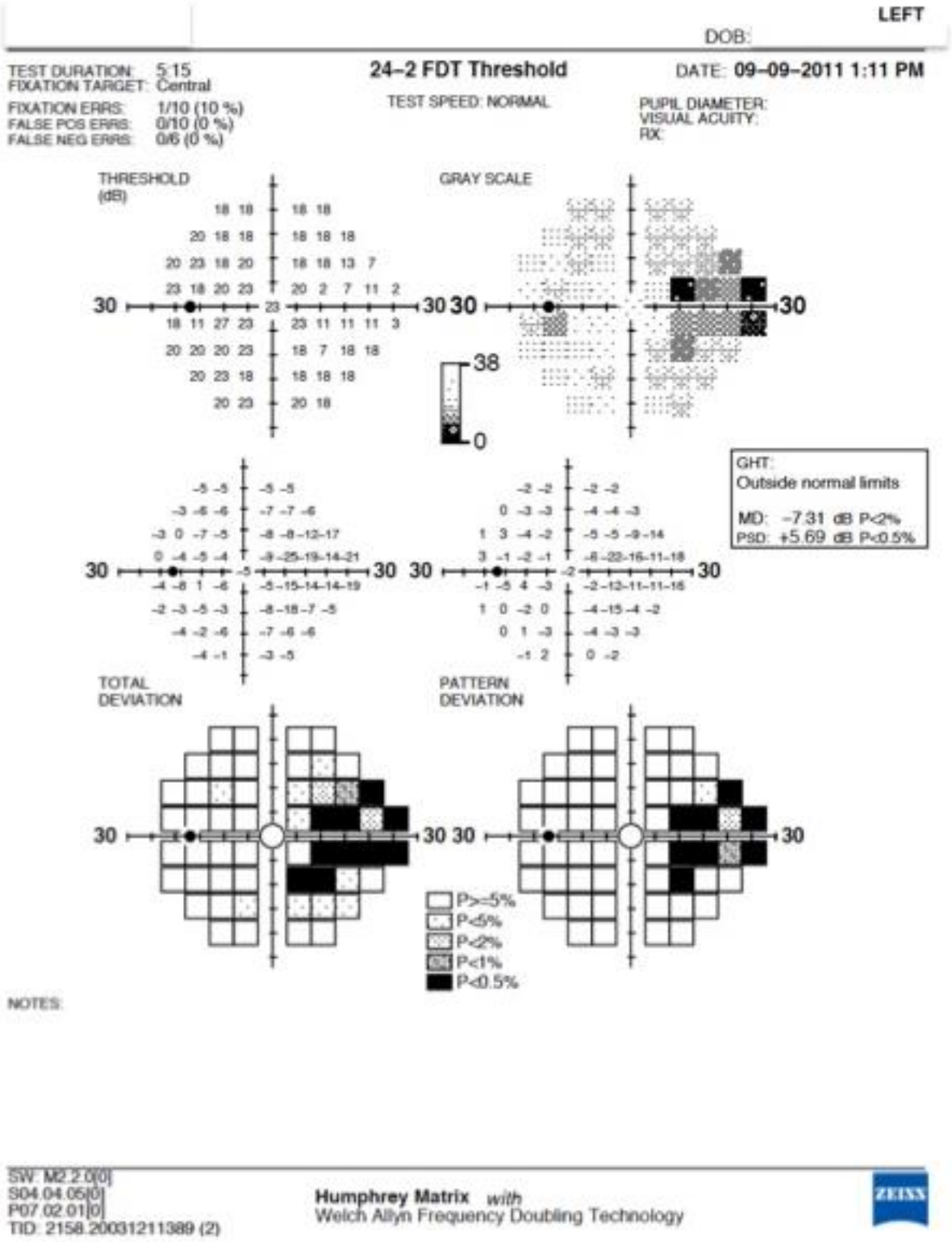

1.7 Electrophysiology in Glaucoma

With appropriate stimulation and recording techniques, electrophysiology allows the selective monitoring of the function of retinal pigment epithelial cells, rods, cones, retinal bipolar cells and ganglion cells, and of the optic nerve pathway to V1 and higher. All of these techniques have been examined in glaucoma.
The techniques can be broadly divided into Electroretinograms (ERG) and Visually Evoked Potentials (VEP). The full field ERG only shows minor changes in glaucoma and is therefore not useful in glaucoma [114].

The origin of the **MULTIFOCAL ELECTRORETINOGRAM** *(mfERG)* signals as a photopic stimulus is generated by the retinal bipolar cells, which are driven by the cones (*Fig 10a)*. There is strong evidence that even advanced glaucoma does not affect the basic mfERG components. Several further studies that tried to monitor the retinal ganglion cell (RGC) function with the mfERG have had somewhat limited success[115].

The **PHOTOPIC NEGATIVE RESPONSE** *(PhNR)* is recorded under photopic conditions, like a full-field ERG and appears as a slow negative wave after the positive b-wave (*Fig 10b)*. PhNR amplitudes are significantly reduced in glaucoma patients and a reduction of PhNR amplitudes correlates well with visual sensitivity losses as measured by automated static visual field testing[116, 117, 118].

The **PATTERN ELECTRORETINOGRAM** *(PERG)* (*Fig 10c)*. The signal is generated by using a high-contrast patterned reversing stimulus on a television monitor and is sensitive to changes in the health of the retinal ganglion cell (RGCs). Several studies have shown that PERG can be an early glaucoma indicator in ocular hypertension with a high sensitivity and specificity before conversion to demonstrable glaucomatous disease[119, 120, 121]. It is important to note that the levels of RGC dysfunction do not always correlate to the structural changes seen on OCT and the PERG signal relies on the normal functioning of the RGCs[122]. Longitudinal studies by Bode et al. and Bach et al. have shown that the PERG can predict visual field changes up to 4 years ahead of reliable field loss[123,121]. These findings also correlate well with the study by Banitt et al. that loss of retinal ganglion cell function precedes structural loss by 8 years in glaucoma suspects[124]. However, the signal is very small (4-8uV) and subject to many confounding factors including media opacities and refraction, with a high inter-test variability making its interpretation difficult clinically.

Fig 1.10: Examples of various electrophysiology recordings in the eye

a) Multifocal Electroretinogram traces and a 3-D plot reflecting the response density across the stimulated area of a normal eye

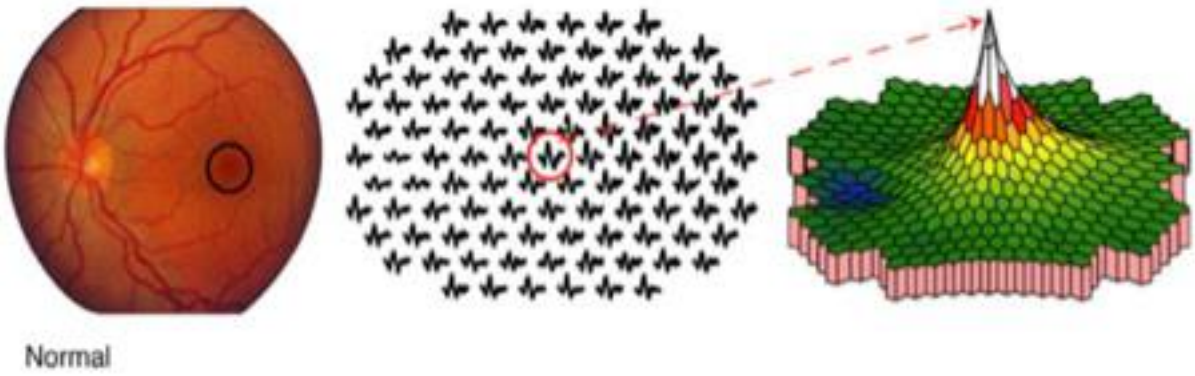

b) Characteristic waveform of the Photopic Negative Response ERG (PhNR)- is the slow negative potential following the b-wave in the Photopic ERG

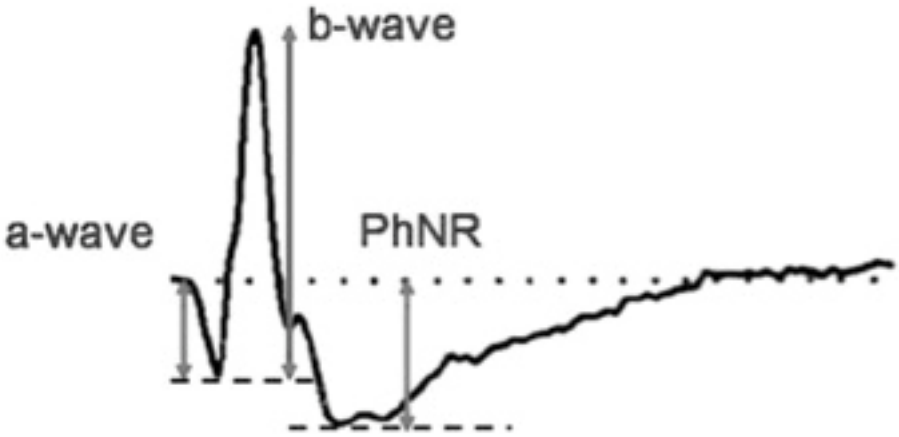

c) *Example of a Pattern Electroretinogram (PERG) response*

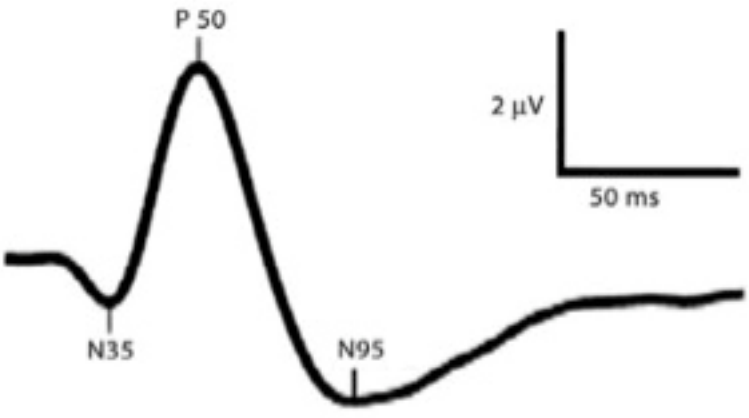

1.8 The Visual Evoked Potentials (VEP) in Glaucoma

The visually evoked potential is a summed electrical signal generated by the occipital region of the cortex in response to visual stimulation. It is measured similarly to the electroencephalogram (EEG) with scalp electrodes and is isolated from the background EEG by signal averaging.

a) The Flash Visual Evoked Potential (VEP) uses a diffuse flash presented in a Ganzfeldt bowl under photopic adaptation conditions. The flash VEP displays large inter-individual variation and is thus primarily used as a gross test of cortical response in uncooperative patients or in those with poor fixation. The major limitation of this technique in detecting glaucoma is that the evoked responses are dominated by foveal input, which has cortical over representation and is unable to detect abnormalities in the peripheral field[125, 126].

b) The Pattern VEP has been shown to be sensitive to optic nerve lesions caused by demyelinization[127], ischemia[128], and compression of the anterior visual pathway[129]. Glaucoma has also been reported to affect the VEP by causing both reductions in amplitude[130] and increases in latency[131, 132,]. Increased pattern VEP latency has been associated with optic disc cupping and the presence of visual field loss. In ocular hypertension the pattern VEP has been normal unless eccentric viewing or provocative techniques have been employed[133].

The standard stimulus used for the Pattern VEP is a checkerboard consisting of black and white squares, which alternate in regular phase frequency every 1-2 seconds with a certain fixation point. The optimal response is achieved with a spatial frequency of 10-20 minutes of arc with a temporal frequency of 8Hz[134, 135]. With current developments in the technique, changes in contrast, spatial and temporal frequency and chromatically varied gratings are now possible. It has been recorded that chromatic contrast stimuli usually elicits a small cortical response that can be difficult to detect[136, 137].

c) The Chromatic VEP: Blue yellow pattern VEPS have been demonstrated to primarily prolong the response peak time whilst the amplitude remains relatively unaltered. It has been established that full field chromatic (blue-yellow) pattern VEPs may be more sensitive than achromatic (black-white) in detecting glaucoma and may predict the clinical signs of glaucomatous progression[138, 139]. In a longitudinal study conducted by Horn et al. between glaucoma patients and normal controls, the peak time of the blue yellow VEPs in had a high sensitivity (90%) although the amplitude did not differ significantly between the two groups.

There was a significant prolongation of the latency in those with progressive disease at least two years before morphological changes arose indicating a role in monitoring progression of glaucoma[139].

Overall, the conventional VEP with pattern or chromatic stimuli show abnormal results in glaucoma but have not been established as being able to reliably diagnose early glaucoma. The tests only examine the central 10 degrees of visual field and provide a single response so are not useful for isolating defects in glaucoma. Graham et al did demonstrate that hemifield PERGs might be able to detect gross functional loss in glaucoma[140]. However, to obtain multiple VEPs at different retinal locations would be too time consuming. Therefore, a new topographic method of VEP recordings based upon Sutter's multifocal technology was developed to circumvent these problems[141, 142].

Fig 1.11: Normal Pattern-reversal VEP recorded from mid-occipital scalp 50-degree checkerboard pattern stimuli

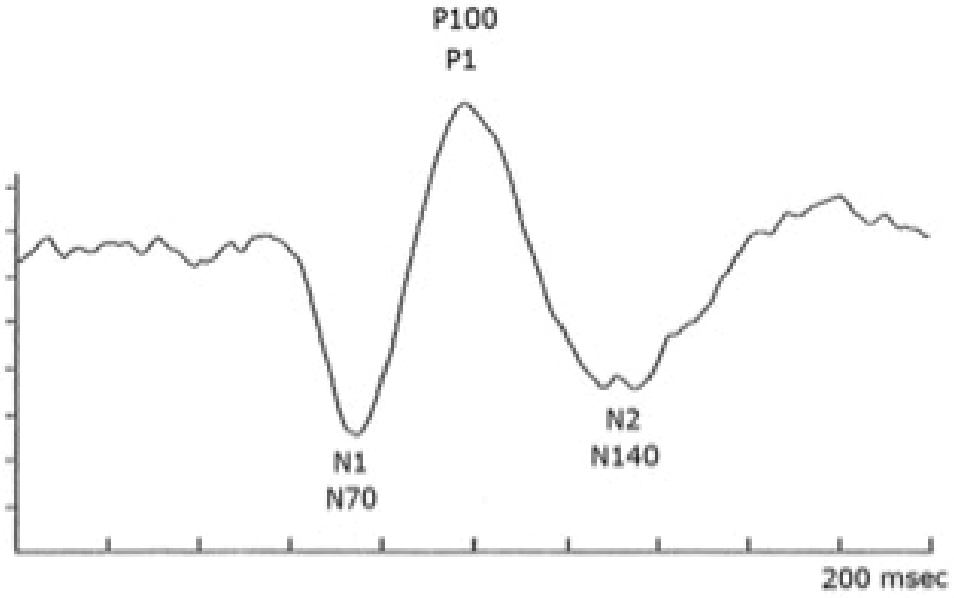

1.9 Multifocal Visual Evoked Potentials and its Role in Glaucoma

The standard visual evoked potential (VEP) originates from excitatory and inhibitory postsynaptic potentials in neurons of the (primary) visual cortex and provides a means of measuring the integrity of the visual pathway. The multifocal VEP (mfVEP) substantially adds to the information obtained, by providing a topographic map of VEP responses across the central visual field. It has the advantage of being able to detect responses from underlying signal generators with different orientations, which tend to cancel one another out when recording a summed response in the conventional VEP. Several studies have shown the relatively high sensitivity of mfVEP in detecting glaucomatous damage[143, 144, 145, 146, 147]. However, nearly all of this work has been based on amplitude measures of the mfVEP.

1.9.1 MULTIFOCAL STIMULATION is achieved by using pseudorandom stimulus presentation (M-sequences). Two opposite checkerboard-pattern conditions undergo pseudorandom binary exchange at 60 sites of the visual field. With this, there is a 50% probability for the checkerboard pattern to reverse its polarity every 15 millisecond (duration of every frame of stimulation display)[148, 149, 150, 151].

With multifocal visual evoked potentials (mfVEPs) the visual field can be sampled for response abnormalities. Thus, mfVEPs open the possibility of an objective visual field test. The issue, however, is greatly complicated by the variability of the responses across the visual field and between subjects. Cortical morphology dictates the mfVEP shape and influences mfVEP magnitude; consequently it is one important cause of the variability of mfVEPs[152]. To account for the cortical magnification of the visual field representation specifically scaled circular checkerboard patterns are used for stimulation. **The stimulus** has a dartboard configuration with 60 closely packed segments. These segments are cortically scaled with eccentricity to stimulate roughly equal areas of the striate cortical surface.

1.9.2 ORIGIN OF MFVEP SIGNALS: Evidence suggests that mfVEP signals are mostly generated in the V1 or striate cortex[153,154]. The responses do not all have the same waveform, which leads to the suggestion that other sources must be contributing. Fortune et al.[155] have in their study have suggested that like the pattern VEP, mfVEP has both striate and extrastriate contributions although the extrastriate component may be smaller in mfVEP.

VEP signals from all areas of the visual field up to 20 degrees of eccentricity can be recorded using horizontally oriented bipolar electrodes straddling the inion called the Bipolar Occipital Straddle (BOS). This facilitates the registration of the horizontally oriented dipoles from the base of the calcarine sulcus. Results are then obtained by using Kernel analysis. There is good correlation between the multifocal VEP (first slice of the second-order kernel) and the areas of visual field loss in patients with glaucoma, and optic atrophy[143, 156].

Multifocal VEP magnitude is particularly valuable for an objective visual field assessment in glaucoma patients. Multifocal VEP latency measures promise further insight into visual system abnormalities in patients with optic neuritis and multiple sclerosis[157, 158]. With the multifocal technique separate responses from many visual field locations (more than 50, can be obtained within a short time interval) per recording. Responses to different stimuli, e.g. flash or pattern reversal can be extracted from summed responses recorded with a single electrode pair.

1.9.3 VARIATIONS IN THE NORMAL MFVEP are present between the eyes of the same subject, across the visual field and across individuals. The variations in the folding and positioning of the brain in relation to the electrodes are the same for the representation of the two eyes. There is also a small inter ocular latency difference across the midline with the left eye leading in the left visual field and the right eye leading in the right visual field[159]. The mfVEP amplitude and waveform varies across the visual field in several ways. The responses from the upper and lower field are reversed in polarity in most subjects and are consistent with the anatomy of V1[143, 160]. The same studies showed that the waveform of the responses along the vertical meridian differs from the waveform of the other responses in several subjects. The responses also vary in amplitude even from areas at the same eccentricity. There is also a difference in size of the responses between the right and left eyes for corresponding sectors of the visual field. A latency difference between the eyes is also seen along the midline, which is likely due to the conduction time of the unmyelinated ganglion cell axons on the retinal surface[161].

In recent years, there has been many advancements in the mfVEP technique including changes in the electrode positions[162, 145, 144], multiple channel recordings[145, 163], pattern sequence[163], EEG scaling, dichoptic stimulation[164, 165], inter-eye asymmetry and analysis of

waveforms[166, 167], as well as improvement in the signal to noise ratio (SNR) and use of alternative stimuli patterns[166, 168].

In glaucoma, damage to the retinal ganglion cells causes visual field defects. At present, patients with suspected glaucoma, based on structural optic disc changes or high intraocular pressure, are assessed with static visual field perimetry, which requires the patients to judge the test stimuli subjectively. The possibility of an objective detection of glaucoma-induced visual field defects is opened by mfVEPs. It has been established that multifocal pattern VEP using a multi-channel bipolar recording technique shows a strong relationship between subjective visual field loss and the recorded cortical response. The technique can reliably map visual field loss in adults and children and the findings strongly correlate with subjective perimetry results[169, 170].

The mfVEP recordings for the two eyes of the same individuals are considered identical if there are no defects in either eye. While different strategies proved successful for the evaluation of mfVEP magnitude and latency, root-mean-square (RMS) calculations and correlations of the responses with reference traces have the advantage of being based on a number of points as opposed to single peak values and yield reliable estimates of response magnitude and latency. Estimates of mfVEP magnitude, latency, and cortical topography are valuable tools for the assessment of visual function[171].

The ratios of the RMS amplitudes for the responses from each eye are calculated if the mfVEP is significantly smaller in one eye than the other. The significance level can then be obtained by comparing this ratio to the mean and standard deviation (SD) of a group of normal subjects. Scaling of the probability plot of HVF and mfVEP has to be identical to be compared directly to each other[159].

Fig 1.12 a: mfVEP stimulus display of 60 cortically scaled sectors where each sector displays an independent pattern-reversing checkerboard[172]

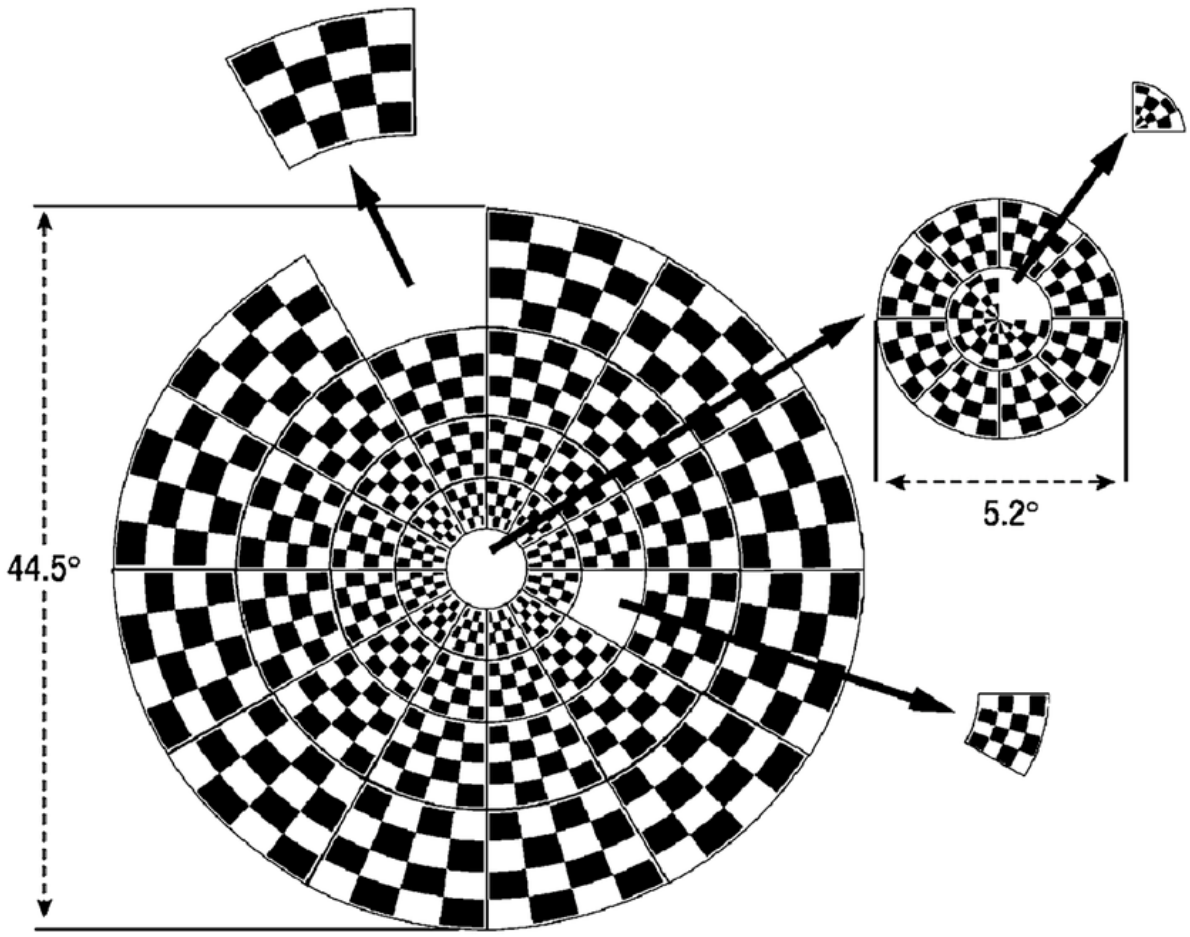

Fig 1.12 b: Cortically scaled dartboard black and white pattern stimulus with 58 segments and nasal step test region[172]

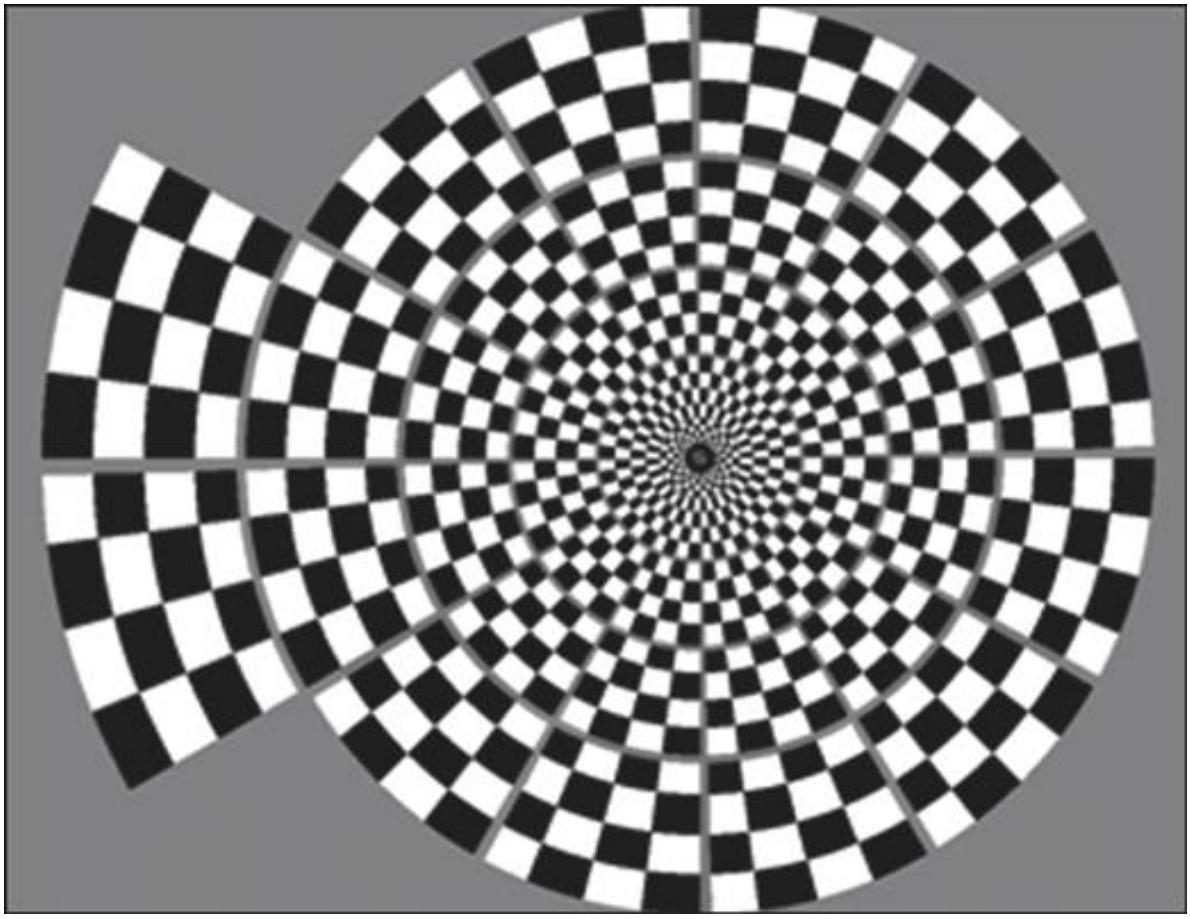

Fig 1.12 c: Local mfVEP responses. *Expanded traces from one of the segments demonstrated lower amplitude and delayed latency in a glaucomatous eye (bottom) compared with that in the fellow eye (top)*[172].

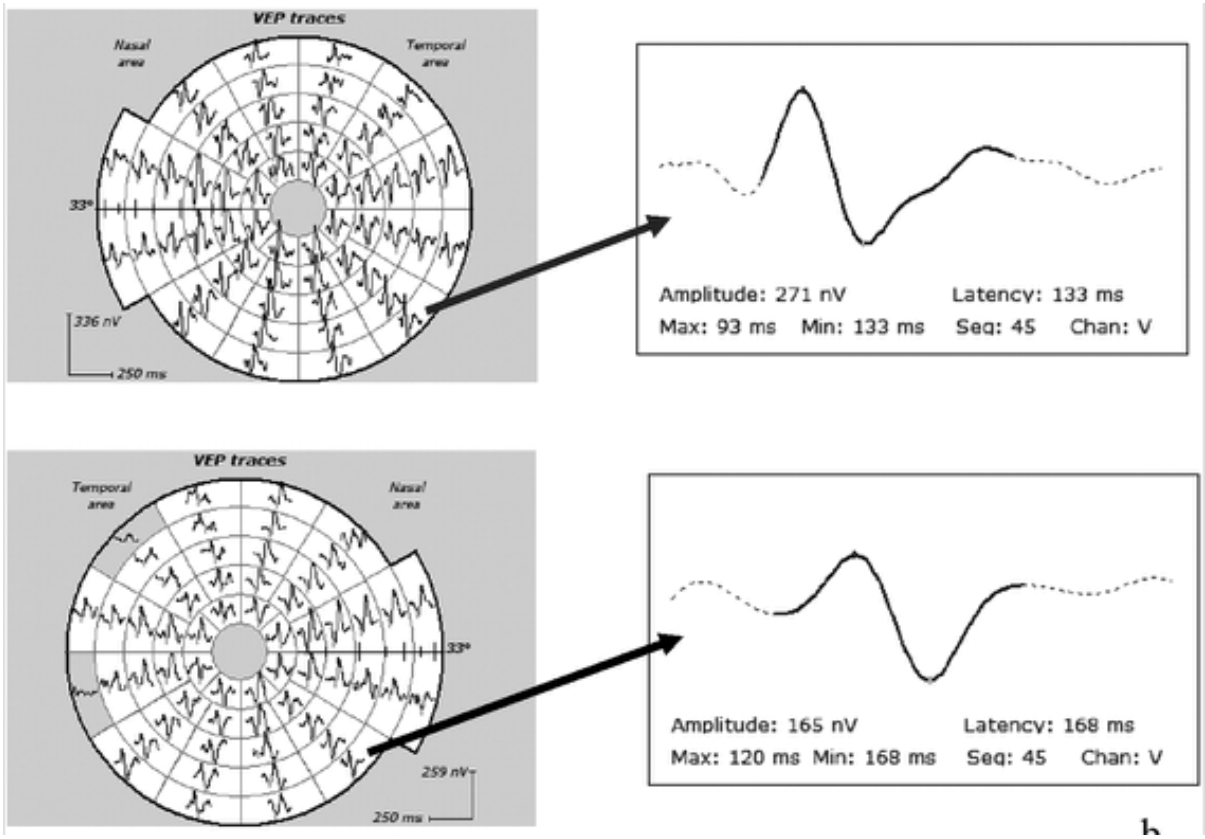

1.9.4 SPECIFICITY OF THE MFVEP AND REPRODUCIBILITY

Fortune et al. studied the effects of age, sex and race on mfVEP recordings on 100 healthy participants and concluded that there was no overall effect of age on the signal to noise ratio (SNR) of mfVEP recordings. There was no evidence of localized effects. There was no significant interaction between race and location. But the RMS amplitude was larger, on average, in females than in males. This sex difference has been reported for both conventional and multifocal recordings. The RMS amplitude of the noise, was also larger in females[173]. A study conducted by Nakamura et al on the effect of refractive errors on mfVEP responses concluded that high myopia reduces the SNR of mfVEP responses even with refractive correction[174]. The team also proposed that a normative database for high myopes should be established to evaluate mfVEP responses for highly myopic glaucoma patients.

Specificity of mfVEP was found to be excellent by using cluster criteria for monocular and inter-ocular tests.
Several studies by the same group were conducted to ascertain the reproducibility of mfVEP test on normal controls and subjects with glaucoma. Confirmation of an abnormal cluster is specifically indicative of a true defect on the mfVEP. It is also essential to note that confirmation of mfVEP abnormalities increases specificity because significant clusters are unlikely to repeat in controls[175, 176177].

The study by Klistorner et al. examined the source of variability in the mfVEP amplitude. The study aimed at establishing a relationship of this variability to the strength of the signal across the visual field. The variability of mfVEP was significant between tests despite care to replicate electrode position. The change in amplitude was also eccentricity dependent and there was increased variability towards the peripheral visual field. The study concludes that mfVEP is not useful in monitoring the deepening defect after 10dB but can be used to follow an expanding scotoma[178]. Studies by James et al. and Zhang et al. more recently are working towards improving the SNR by increasing amplitude and reducing noise of the mfVEP using the pattern-pulse mfVEP[167, 179].

Based on the fact that monocular mfVEP responses from the two eyes of healthy controls are almost identical, Graham et al[113] and Hood[112] proposed that the comparison of the two monocular mfVEP recordings from patients may allow the detection of early and localized damage of the ganglion cells or optic pathway. A small group of patients with ganglion cell

loss and optic nerve damage participated in the study along with healthy controls. There were marked differences between the mfVEP responses from the two eyes of all the participants with disease. The interocular analysis of the mfVEP allows for an objective identification of monocular field defects and also helps quantify the same[144]

Several studies indicate a great degree of correspondence between subjective and objective visual field measurements and anatomical measurements, which highlights the potential of mfVEPs to assist visual field perimetry in glaucoma patients[180,147,181,182,183]

1.9.5 LATENCY CHANGES IN MFVEP SECONDARY TO GLAUCOMATOUS DAMAGE

The latency of the conventional pattern-reversal VEP (cVEP) has been reported to increase with glaucomatous damage[184, 185]. The mean latency of the open angle glaucoma (OAG) (68 eyes with OAG) was 27.8 ms longer than that of their control group in a study conducted by Parisi et al.[186] All of their patients with OAG showed VEP latencies that were longer than any of the 80 control eyes and the sensitivity and specificity of the VEP was 100%. The increased latency correlated with both the severity and location of the visual field defects. This study was surprising, as previous reports had only shown mild delays in cVEP in glaucoma.

Rodarte et al.[158] demonstrated small mfVEP delays, i.e. of a few milliseconds rarely exceeding 10 ms, which affected only about 40% of the glaucoma patients tested. Further, the sensitivity was poor and there was a considerable overlap between the latencies of 100 eyes of 50 glaucoma patients (25 Normal Tension Glaucoma and 25 High Tension Glaucoma) and control (94 eyes of 47 subjects) groups. This contrasts with greater latency effects of glaucoma reported in a recent cVEP study[187]. The differences in the study population of these two studies does not justify the difference in their findings. But the differences in the two tests (test stimuli and recording technique), cVEP and mfVEP may account for at least some of the discrepancy in the results.

In a study by Grippo et al.[187] comparing the cVEP with mfVEP response in glaucomatous damage, the cVEP and the mfVEP latencies for the subjects with glaucoma were longer than the controls. Fewer than 12.3% of patients had latencies falling outside the range of the controls and the specificity values were contradicting with the study by Parisi et al[186] which reported a sensitivity and specificity of 100%.

Prolonged cVEP latency could provide a potential mode of detecting abnormal ganglion cells if a method for reliably measuring the latency could be developed. While trying to assess the abnormality of monocular mfVEP timing, a template method was suggested by Hood et al[188] by summing the responses across regions or using a cluster criterion to improve the specificity of a test for abnormal latency measures. The confidence levels used were also adjusted based on the SNR of the response. The group also proposed that inter-ocular latency differences of the mfVEP get larger with age. Despite a weak correlation, they suggested having age-matched controls[189].

Hood et al[181] also reported that the black and white mfVEP detects less than 90% of abnormal hemifields associated with early glaucoma and approximately 5% of cases are missed as compared with subjective achromatic standard perimetry . Hence, improvement of the multifocal technique was still needed in order to use it as an objective measure of assessing early glaucomatous functional loss.

1.9.6 BLUE ON YELLOW MULTIFOCAL VEP (BonY mfVEP)

The rationale for blue-on-yellow mfVEP design is similar to the one used for subjective SWAP targeting a blue and yellow subset of the visual pathway (Koniocellular pathway) which has a sparse neural representation and less functional redundancy[138, 139, 190].

Based on the fact that glaucoma and ocular hypertension can be associated with blue- color vision disturbances[191], Korth et al[190] attempted to isolate the blue-sensitive pathway with pattern VEP. They recorded the pattern-onset VEP in response to blue stripes (460nm) presented with or without a bright yellow adaptation light (570 nm), which were then compared against the visual field defects. The test was found to be highly specific (94%).

Horn et al[192] conducted a longitudinal study on perimetric and preperimetric patients with chronic open-angle glaucoma using VEP measurements using the blue-on-yellow pattern stimulation. A strong yellow (570nm) homogenous adaptation light was superimposed with a blue stripe pattern (460nm). The VEP peak times of subjects in the preperimetric group was significantly prolonged in patients with progressive disease and were detected 2 years before morphological changes were evident.

Following these earlier leads Klistorner et al.[169] investigated the sensitivity of a blue-on-yellow mfVEP in the detection of early glaucomatous field loss. 50 patients with early

glaucoma were tested with both black-and-white mfVEP and blue-on-yellow mfVEP (BonY mfVEP). The amplitude and latency values were compared to those of normal controls. Larger scotomata were noted on blue-on-yellow mfVEP compared with black-and-white mfVEP of the same eyes. The defects detected on SAP corresponded topographically with the amplitude reduction on BonY mfVEP with significant correlation. The technique was found to be highly (95%) specific. The group used the Accumap (ObjectiVision Pty. Ltd, Sydney, Australia) and the Opera software described elsewhere[147]. *Fig 13* shows the blue-on-yellow stimulus used for the mfVEP recordings adapting the sparse presentation technique described by James and Maddess[167]. The bright yellow background has a luminance of 125 cd/m^2 and the 4X4 grid of blue checks scaled proportional to the segment size had a luminance of 20 cd/m^2.

A subsequent study from the same group[193] analyzed the BonY mfVEP amplitude asymmetry and latency values of 30 patients with glaucomatous optic discs and normal standard visual fields (i.e. pre-perimetric patients). The amplitude asymmetry was significantly abnormal in over 45% of subjects. The defect was monocular and corresponded to the eye with the worse disc. The defect also corresponded to the location of the worst affected rim on OCT. With average field losses of -5dB or more, the median SNR (Signal to Noise Ratio) of mfVEP has already been reduced to a value that is in the range of noise. There is little or no signal in the mfVEP responses for losses of about -10dB or more[159].

Fig 1.13 The Blue-on-Yellow mfVEP stimulus based on sparse stimulus presentation[169].

Approximately one sixth of the segments are activated at any particular time.

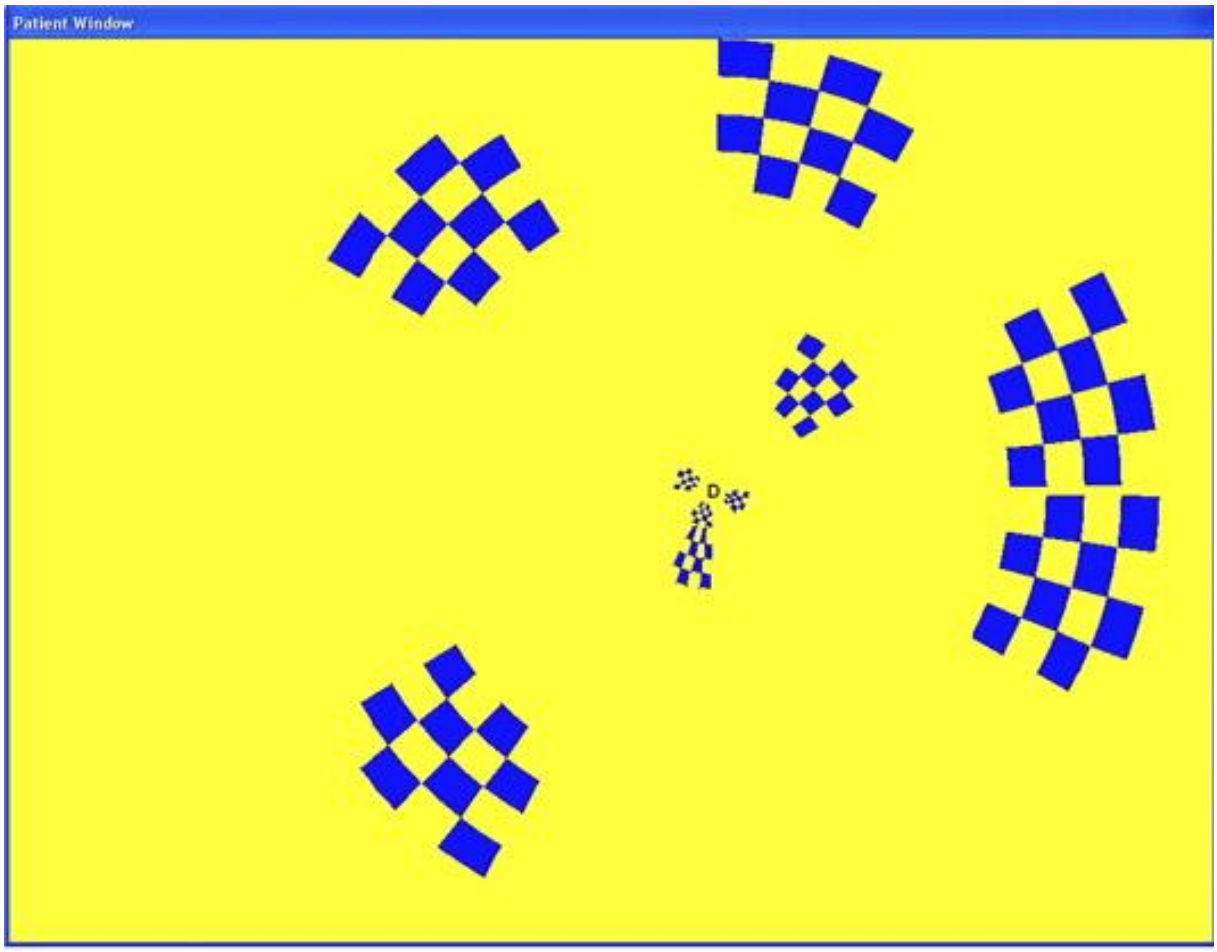

1.9.7 LOW LUMINANCE ACHROMATIC MULTIFOCAL VEP (LLA mfVEP)

Similar to the Koniocellular pathway, the Magnocellular pathway also involves a set of ganglion cells with less redundancy. This pathway conveys information about low contrast and low spatial frequency achromatic images. The contrast response functions of magnocellular neurons demonstrate saturation at low levels of luminance contrast[194]. FDT perimetry, which is available in the clinical setting, is based on the frequency doubling illusion and thought to be targeting the M pathway and is reported as sensitive in early glaucoma[195, 196].

In 1997, Klistorner et al[197] established that selective stimulation of the magnocellular pathway can be achieved using low-contrast stimuli. They demonstrated that it was possible to differentiate between magnocellular and parvocellular pathways using different contrast conditions. They also showed that magnocellular response changes early in the disease[198]. Therefore, based on the saturating nature of the contrast response function in the magnocellular pathway and taking into account the eccentricity of the early glaucomatous visual field defects (10 – 20 degrees), the team has designed the Low Luminance Achromatic mfVEP (LLA mfVEP).

The stimulus is identical with the BonY mfVEP but uses the equivalent in gray scale. The yellow background is replaced by light gray of the same luminance (125 cd/m^2) and the blue color of the checkerboard has been replaced by darker gray checkerboard with the same luminance (20 cd/m^2).

Arvind et al[199] compared the multifocal pattern onset VEPs using BonY, LLA and high-luminance contrast achromatic (HLA) stimulations in 30 normal subjects and 23 subjects with early glaucoma and found that BonY and LLA mfVEPs performed comparably, and both were significantly better than High- luminance achromatic mfVEP in identifying early glaucoma. They also assessed the specificity of BonY and LLA stimulation in 25 normal subjects and found that specificities for BonY and LLA were similar at 96% and was significantly higher than HLA mfVEP, which stood at 79.3%.

More recently, Sriram et al[200] studied the performance of LLA mfVEP in pre-perimetric glaucoma and also compared it to other functional and structural measures used in glaucoma detection. It was noted that LLA mfVEP identified approximately 50.6% of eyes with pre-perimetric glaucoma, significantly higher than other perimetric measures and similar to HRT. A combination of LLA mfVEP and HRT testing was proposed to be highly sensitive (76.5%) for pre-perimetric glaucoma.

Fig 1.14: The Low luminance achromatic mfVEP stimulus based on sparse stimulus presentation testing the magnocellular pathway[199]

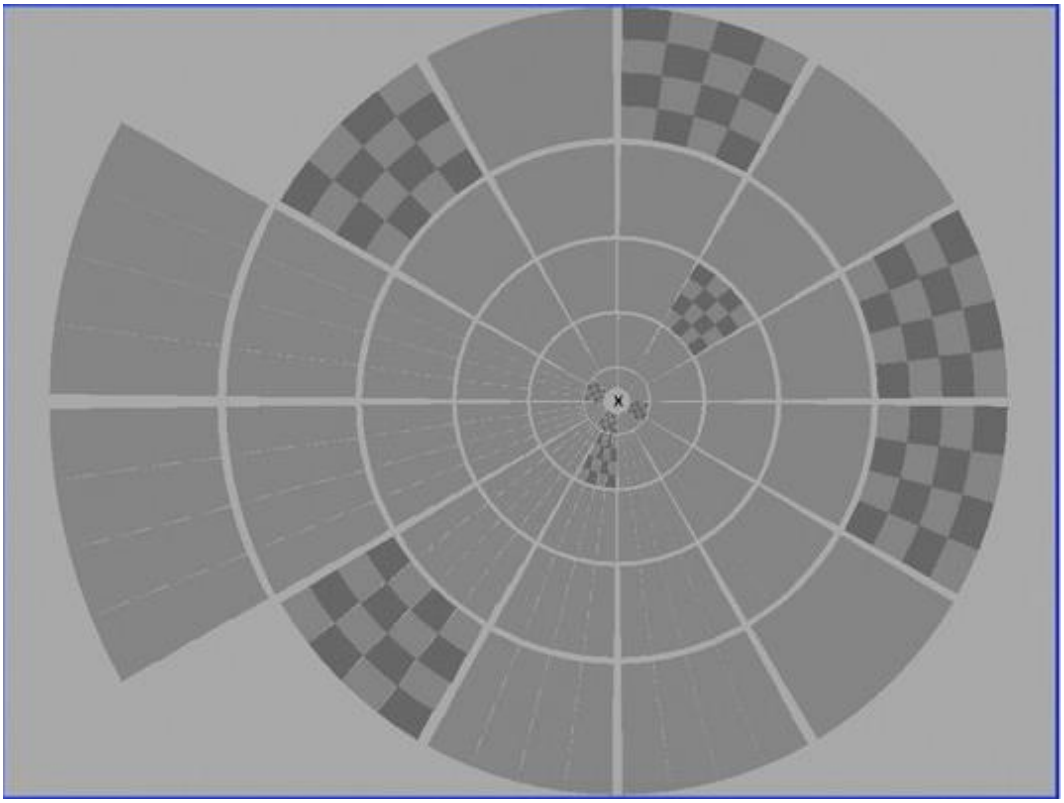

1.10 Structure and Function Models In Glaucoma

Historically, it has been generally believed that structural abnormalities of the optic nerve and retinal nerve fiber layer precede visual function loss associated with glaucoma. There is considerable evidence in support of this view for standard automated perimetry[201,202,82]. However, the development of new visual function tests that are suggested to be more sensitive than SAP opens up the possibility that some visual function deficits may be concurrent with or occur before measurable structural glaucomatous damage. The derivation of quantitative relationships that link structure and function for normal eyes or eyes with glaucomatous neuropathy is important for understanding the basic disease process.

A study by Alencar et al[203] evaluated and compared rates of change in neuroretinal rim area (RA) and retinal nerve fiber layer thickness (RNFLT) measurements in glaucomatous patients, glaucoma suspects, and normal controls followed over time. The average rate of decline for RNFLT measurements was significantly higher in the progressing group compared to the non-progressing group (-0.65μm/year vs. -0.11μm/year, respectively; $P<0.001$) The ability to discriminate eyes progressing by SAP and/or stereo photographs from stable eyes was significantly greater for RNFLT compared to RA measurements.

Garway-Heath et al[204] observed a good level of association between the strength of correlation between points in the Visual Field and relative location of those test points in the peripheral retina and in corresponding RNFL bundles at the ONH thus validating the relationship between structure and function changes in glaucoma.

In the study by Felipe et al[205] a joint multivariate mixed-effects model was implemented within a Bayesian hierarchical modeling framework to evaluate the relationship between the two longitudinal measures obtained over time (i.e., the GDx RNFL measurements and SAP VFI) Linear mixed models were used to evaluate the evolution of each response over time. Estimates of sensitivity and specificity of the Bayesian method were compared with those obtained by the conventional approach of ordinary least squares (OLS) regression. Bayesian methods allow the distribution of glaucomatous visual field progression rates in the population to constrain individual progression rate estimates. The same group also combined a structure / function approach to estimate retinal ganglion cell (RGC) counts[206] with the purpose of merging results of structural and functional tests into a single index that could be used for diagnosis, staging, and detecting glaucomatous progression.

A study by Meira-Freitas et al[207] evaluated the ability of baseline and longitudinal estimates

of retinal ganglion cell (RGC) counts in predicting progression in eyes suspected of having glaucoma. Participants had normal standard automated perimetry (SAP) at baseline. Retinal nerve fiber layer thickness assessment was performed with optical coherence tomography (OCT). Joint longitudinal survival models were used to evaluate the ability of baseline and rates of change in estimated RGC counts for predicting progression over time, adjusting for confounding variables. The study concluded that baseline and longitudinal estimates of RGC counts might be helpful in predicting progression better than conventional approaches.

Gardiner et al[208] studied 109 healthy controls with 166 subjects who either were diagnosed with glaucoma or suspected to have the disease using HRT and SAP. The HRT images were divided into 36 sectors, which were then correlated with SAP thresholds. They came up with a map relating regions of the ONH to SAP test locations particularly suitable for localized glaucomatous loss. Their results point out that the narrowing of the NRR in some areas is more significant than the others in predicting functional loss.

A linear model that relates RNFL thickness on OCT to losses in SAP sensitivity for arcuate regions of glaucomatous visual fields was postulated by Hood et al[209] in 2007. The model was applicable for all stages of the disease. The study indicated that SAP losses of more than -10dB would not yield an RNFL thickness detectably different than the baseline level and conclude that RNFL thickness is of limited use for regions of extensive damage. They suggest that progression is best observed by examining the relatively healthy regions of the same eye.

There have been several recent developments in imaging methods in the clinical assessment of the optic nerve head. It has been suggested that the Bruch's Membrane Opening (BMO) should be a consistent anatomical landmark from which NRR measurements should be made[210,69,7,211]. A comparative study was done against disc margin-based rim area using CSLT, Bruch's membrane opening-based horizontal rim width, peripapillary RNFL thickness using SD-OCT and Visual Field sensitivities to assess the structure-function relationship. This study used the Garway-Heath map[212,204] customized for various biometric parameters. The current disc margin based rim assessment showed a weak structure-function relationship but the same was enhanced using the Bruch's membrane opening based horizontal rim width and showed a higher correlation with visual field sensitivity[211].

The correlation between the circumpapillary RNFL thickness and the mean deviation of HVF varies with optic disc morphology in OAG[213] suggesting that different disc types such as focal ischemic, myopic glaucomatous, senile sclerotic and generalized enlargement should be considered in structure-function studies in glaucoma. Our study excluded all of the mentioned disc types and the different disc morphologies was not a confounding factor in the study.

1.11 Comparing electrophysiology of the visual pathway with conventional measures of visual field loss using HVF and other structural measures like OCT and HRT

For glaucoma patients, a reasonable correspondence has been demonstrated between subjective visual field perimetry and the assessment of visual field topography based on mfVEP magnitude. In a study by Goldberg et al.[147] mfVEP was performed for patients with Primary Open Angle Glaucoma (POAG). The VEP amplitude reductions correlated well with the visual field defects recorded on HVF. The topographic location of the defect was also well correlated between the functional tests. MfVEP also detected deficits in the hemifields with normal HVF results in glaucoma patients with unilateral hemifield defects[214]. Contradicting these findings was a study conducted by Bengtsson et al[215] using an early version of AccuMap where the agreement between VEP and standard perimetry was relatively poor for the glaucoma group.

Recently, Greenstein et al.[181] assessed 40 eyes of patients with open-angle glaucoma to see if the visual field defects determined with automated static perimetry and with mfVEPs correlated with the visual fields defects predicted from anatomical measures of the optic nerve head. Healthy and glaucomatous optic discs were discriminated with confocal scanning laser ophthalmoscopy (Heidelberg Retina Tomograph II, HRT II) for six different sectors of the optic nerve head. Each of these sectors was related to corresponding visual field regions. Thus, for six regions, visual fields were predicted from the state of the respective optic nerve head sectors. In 87% of the regions subjective automated static perimetry and objective mfVEP-based visual fields were in agreement. Of these regions, 85% were in agreement with the visual field defects determined from the anatomical measurements acquired with confocal scanning laser ophthalmoscopy of the optic nerve head.

The sensitivity of mfVEP, HVF and OCT in detecting visual abnormality in Multiple Sclerosis (MS) was compared by Laron et al[216]. MfVEP amplitude/latency identified more abnormality on MS-ON (Multiple sclerosis with Optic neuritis) eyes than HVF and OCT. It was concluded that MfVEP detects identifies both demyelination and neural degeneration as indicated by increased latency and reduced amplitude respectively. The test also revealed more abnormality than HVF and OCT in MS patients. A similar relationship between MfVEP

and OCT was established by Sriram et al[217] in non-optic neuritis eyes of subjects with Multiple sclerosis. Strong topographical associations between structural and functional methods of optic nerve integrity using OCT and MfVEP is also well established in subjects with optic neuritis[218].

Hood et al[181] studied the hemifields of both eyes of 50 subjects with OAG using monocular mfVEP and SAP and concluded that both tests showed a comparable number of defects. The mfVEP showed more abnormalities than HVF when the interocular test results were included.

SAP, mfVEP and HRT results of 20 subjects with open angle glaucoma were assessed in a study by Greenstein et al[219]. The optic nerve head measurements for the 6 sectors in HRT were related to the HVF locations and the 60 sectors of the mfVEP display. This study also used the map developed by Garway-Heath et al[212] to relate the test locations of the HVF and the mfVEP to sectors of the ONH measured with the HRT II. It appeared that most sectors defined as abnormal on the mfVEP but normal on the HVF were located in the center of the visual field. The study included borderline HRT results as abnormal, which in the author's opinion lead to a decrease in the number of sectors showing agreement on the two tests.

1.12 Application to clinical trials

Currently there is no specific test that can be regarded as the perfect reference standard for detection of glaucomatous structural and /or functional progression. Progression detected by functional means will not always be corroborated using structural tests and vice versa. Corroboration of glaucomatous progression through the use of more than one test may provide effective and more rapid detection of disease progression than repeated confirmation of change using a single modality. The use of visual fields as the sole endpoint in glaucoma trials is potentially limited by the need for large samples, long term follow-up, variability of results and inconsistency in the available methods to define visual field progression.

Progressive optic disc damage could be used as an endpoint in glaucoma clinical trials with a number of advantages, including faster acquisition of a sufficient number of endpoints with reduction in sample size requirements. In several studies many patients developed visual field progression despite undetectable changes in the optic disc[51,220]. Therefore, it is important to use both structural and functional endpoints in studies of glaucoma progression. Disagreement between structural and functional measures of detecting progression could be

related to the different algorithms employed to assess change, to the variability of measurements over time, or to the different scales used to assess structure and function. It is likely that a combination of structural and functional measurements would improve detection of clinically significant disease progression compared to either method used alone.

Although there are several studies that assess the structure function relationship in glaucoma comparing the disc measurements using SD-OCT and CSLO to visual field sensitivities using SAP, very little has been reported on combining this relationship to include electrophysiological measures of visual function in glaucoma.

CHAPTER 2

MATERIALS AND METHODS

2.1 Aim

The aim of this thesis is to further understand the role of specialized objective perimetric methods (BonY and LLA mfVEP) targeting specific visual pathways and comparing their ability to detect the change and likely progression of preperimetric glaucoma with conventional methods of structural and functional tests for glaucoma in clinical practice. This chapter describes in detail the study design, recruitment of participants, criteria for inclusion and exclusion, methods involved in the various structural and functional tests for glaucoma and statistical analysis involved.

2.2 Human Ethics

Human ethics approval was granted initially through University of Sydney, HREC Approval Number: 2102/ 743 and subsequently Macquarie University External ethics 05-2009/11594 was granted under the title "Optimizing the detection of early glaucoma targeting specific visual pathways in combination with structural measures".

All human experimental work was conducted under the tenets of the Helsinki agreement with written and verbal informed consent. All participation was voluntary and no coercion or incentives were offered.

2.3 Recruitment of Study Participants: Normal Controls

Subjects for inclusion in the study cohort were age matched and recruited from the general community as part of ongoing research projects undertaken at the Save Sight Institute, Sydney. All subjects underwent basic ophthalmological assessment including dilated fundus examination by a consultant ophthalmologist. Eligibility criteria included best-corrected

visual acuity of 6/9 or better; normal anterior and posterior segment examination, healthy optic disc morphology and normal and reliable visual fields on HVF. The visual field was considered reliable if the fixation losses were less than 20% and the false negative and false positive rates were less than 33% (rates of reliability fixed by the perimeter software).

2.4 Glaucoma Subjects

Fifty-one early-glaucoma subjects were recruited from a Sydney-based private glaucoma practice. Glaucoma diagnosis was made prior to the study based on the glaucomatous cupping of the optic disc, as judged by stereoscopic ophthalmoscopy. The subjects had at least one glaucomatous optic disc but still normal, reliable visual fields in that eye.

2.5 Inclusion Criteria

Glaucomatous optic discs were identified based on one or more of the following criteria: (a) Definite focal rim notching, (b) Cup-disc asymmetry ≥ 0.2 with no disc size asymmetry, plus rim irregularity, (c) markedly thinner inferior than superior rim (representing violations of the ISNT rule) of an eye with no abnormal disc configuration (e.g., tilting). Reliable and normal SITA-Standard achromatic Humphrey 24-2 visual field in at least one eye with glaucomatous disc change on at least 2 occasions was required for inclusion. The Glaucoma Hemifield Test was normal and there was no abnormal field depression on total or pattern deviation plot. The subjects had a best-corrected visual acuity of 6/9 or better. Refractive error $< \pm 3.0$ D with astigmatism < 2.0 D were included.

2.6 Exclusion Criteria

Patients with significant cataract or other media opacities and/or any other past or present history of diseases involving the cornea, lens, macula or any disease involving the retinal pathway were excluded. Optic discs with focal ischemia, myopic and tilted glaucomatous, senile sclerotic discs and optic discs with generalized enlargement were excluded from the study. We don't believe that color blindness will have any impact on SWAP or BonY perimetry. Unfortunately, we could not find any reference indicating the impact of color blindness on SWAP. Also since color vision is a rare condition, we expect the overall effect, if any, of color blindness in SWAP and BonY perimetry to be negligible.

All the glaucoma subjects had an initial baseline visit with a complete ophthalmic examination and the structural and functional tests for glaucoma. The investigations thereafter

were repeated every year for a period of 5 years. HVF testing was repeated twice for baseline recording to confirm normal visual fields and the subsequent development of a scotoma to confirm the defect in case of progression. The controls underwent the same set of investigations once at the beginning of the study and at the end of the 5-year period.

2.7 Tests and Measurement Techniques

All subjects underwent visual acuity testing, subjective refraction, standard white on white perimetry (Humphrey 24-2, SITA-Standard), short wavelength automated perimetry (SWAP, 24-2 SITA-SWAP), FDT Matrix perimetry (24-2, full threshold), Spectralis OCT, Heidelberg Retinal Tomography (HRT III) and color stereoscopic optic disc photographs. MFVEP was recorded using low luminance achromatic (LLA) stimulation and Blue on Yellow stimulation. The order of tests was randomized and the subjects received sufficient breaks between tests to avoid fatigue.

2.8 Subjective Perimetry Tests

2.8.1 White on white **Standard Automated Perimetry (SAP)** and **Short Wavelength Automated Perimetry (SWAP)** tests were performed using a Humphrey Field Analyzer using the 24-2/SITA-Standard, and SWAP programs (HFA, Zeiss Humphrey Systems, Dublin, CA). The participants were optimally corrected for near for both SAP and SWAP. While performing SWAP, all participants were allowed to adapt to the background light for at least 5 minutes before testing. Each participant was given the same instructions for the examination, regardless of their perimetric experience, to minimize the effects of operator bias. The test was repeated if the reliability indices were not within the accepted limit (Fixation loss > 20%, False positive or False negative >33%).

A defect or scotoma on the subjective visual field tests (both SAP and SWAP) is defined as a cluster of three or more abnormal points in the same hemifield with P<5%, with at least two points at P < 2% on the pattern standard deviation(PSD) plot. Points immediately above and below the blind spot did not qualify as part of the scotoma. Peripheral rim points qualified as part of the overall scotoma only if two or more of the points qualifying as the scotoma nucleus had to be nonrim. The defect should be repeatable on subsequent visit[221]. For the purposes of this study we used the same criteria for abnormality in SAP and SWAP

Guidelines for Progression:

Any new defect should be confirmed with subsequent visit. In a previously normal region of the field, on two or more reliable tests, the existence of a new isolated defect, defined as a cluster of three points worsening by 5dB each, one of which has worsened by 10dB could be taken as evidence for progression.

Disease progression is defined by the Early Manifest Glaucoma Trial (EMGT)[36] criteria as a statistically significant loss of sensitivity at three or more test points in the same location on three consecutive visual field evaluations. Deviations from baseline are presented numerically as well as symbolically, with an open triangle demonstrating progression on one field, a half-dark triangle indicating progression on two fields, and a fully dark triangle signifying progression on three consecutive fields. Based on this, suspected progression on GPA has ≥ 3 open triangles. Possible progression is noted when there is ≥ 2 half-open triangles and ≥ 2 black triangles indicates likely progression on GPA[96, 222].

HVF mean deviation values were recorded and used as a means to classify glaucoma into those with early glaucoma (MD>7dB), moderate (MD 7-13dB) and advanced (MD>14dB).

The criteria used for glaucomatous visual field defect in SWAP vary across studies[223,224,103]. The prevalence of abnormal SWAP defects strongly depends on the applied criteria. The clinical criteria that are significant are poorly defined. Several studies therefore apply the same criteria for conversion in SWAP as in SAP[111,102, 196].

2.8.2 Frequency doubling perimetry was performed with the FDT Humphrey Matrix (Carl Zeiss Meditec) using the 24-2 full-threshold strategy with 5° stimuli and a spatial frequency of 0.5 cycles per degree, counter phase flickered at 18Hz. Reliability and abnormality criteria was similar to the other perimetry tests.

2.9 Structural Tests

2.9.1 RNFL Imaging with the Spectralis Spectral Domain-OCT (software-v. 5.3.3.0) was used to obtain RNFL thickness measurements. Images with quality score > 25dB (range 0-40

dB) were considered acceptable. Ideally all images should have signal strength of 6 or more. For each sector of RNFL (superonasal, superotemporal, inferonasal, inferotemporal, nasal and temporal), the software provided a GPA classification of thickness (within normal limits, borderline, and outside normal limits) based on the comparison with an internal normative database.

The GPA (guided progression analysis) was classified as within normal limits if its value fell within the 95% confidence interval (CI) of the healthy, age-matched population. A 'borderline' result indicated that the value was between the 99% and 95% CI, and 'outside normal limits' result indicated that the value was lesser than the 99% CI. Abnormality in this study was defined as any sector with RNFL thickness < 99% CI. Progression rates on OCT are defined as a reproducible mean RNFL thinning of >20μm in the given sector[72,225]. The GPA evaluates and compares scans acquired longitudinally and gives a summary analysis after considering the expected test-retest variability. The corresponding rate of change and a p value is given. Evaluating GPA is considered better than ONH and macular thickness parameters in detecting change over time. At least 4 visits are needed to get a GPA report. The GPA overlays serial RNFL thickness profiles and performs linear regression analysis of average RNFL thickness against the duration of follow-up. Progression is defined when a significant negative slope in the linear regression analysis between RNFL thickness at any clock hour and age[63, 206].

The instrument also provides a "RNFL Change Report" that includes individual baseline and follow-up scans for the overall and sectorial RNFL measurements and classifications. In this study, all borderline values were considered as normal for analysis.

2.9.2 The Heidelberg Retinal Tomograph III (HRT-III) (Heidelberg Explorer Software v. 1.5.10.0, Heidelberg Engineering) was used to acquire CSLO images in the study. Good images required a focused reflectance image with a standard deviation not greater than 50 μm.

Glaucoma Probability Score (GPS) and Moorfields regression analysis (MRA) are the two classification systems available in HRT. The GPS is an operator-independent algorithm with respect to defining the disc margin. In addition to the numeric GPS score, a graphical representation of the GPS is generated with red crosses that indicate an 'outside normal limits' disc sector, a yellow exclamation mark indicating a 'borderline' disc sector and green check marks indicating a 'within normal limits' disc sector. If the GPS classification changes

between repeated tests in the absence of glaucomatous progression, the information provided would be unreliable.

The Moorefield's Regression Analysis (MRA) provides a classification for each disc sector (similar to Spectralis OCT) and classifies the sectors as within normal limits, borderline, and outside normal limits. MRA uses an algorithm to compare the NRR area globally and in six sectors (temporal, superotemporal, inferotemporal, nasal, superonasal and inferonasal) with fixed values from a normative database. Only MRA was used for analysis in this study.

2.9.3 Stereo photographs of the optic disc: 20^0 sequential stereo-photographs (centered on the optic disc) were taken under dilation with a digital fundus camera (Zeiss VISUPAC 450) at the baseline visit and annually thereafter. Two glaucoma specialists, who were masked to clinical information and to each other's findings, graded the optic disc photographs.

Both examiners confirmed a) eligibility based on definition, b) identified the location of glaucomatous rim changes as right superior, right inferior, left superior and/or left inferior and c) identified the location of the worst rim. The disc photos were used only for the diagnosis of glaucoma and inclusion of the study participants. Progression of the disease was identified with a combination of repeatable visual field defect on HVF and OCT progression.

2.10 Multifocal Visual Evoked Potentials

The mfVEP was performed using Accumap version 2.0 (ObjectiVision Pty. Ltd., Sydney, Australia). Two different pattern onset stimulus presentations were used. Both the Low Luminance contrast Achromatic (LLA) stimulus and the Blue-on-Yellow (BonY) consisted of a cortically scaled dartboard pattern of 58 segments (eccentricity to 24°, nasally to 32°). 56 of these segments were arranged in five concentric rings (eccentricities 1-2.5°, 2.5-5°, 5-10 °, 10-16° and 16-24°) and two segments straddled the horizontal meridian nasally (24-32°). The fixation target occupied the central 1°.

(i) For the **BonY mfVEP**, each segment contained a 4×4 grid of grey checks scaled proportional to segment size (luminance, 20 cd/m^2), which appeared briefly on a lighter grey background (luminance, 125 cd/m^2) according to a pseudorandom binary sequence. Briefly, the pseudorandom sequence had a total length of 440 elements and consisted of 2 types of elements (element 0 and element 1) distributed pseudo-randomly. Element 1 of the binary

sequence was represented by 2 consecutive states: a pattern-on (checker-board blue-and-yellow pattern) state, which lasted 2 frames, and a pattern-off (diffuse, bright yellow illumination of the entire segment) state, which lasted 7 frames. For the element 0 of stimulating sequence, the pattern-off state (diffuse yellow illumination) was active for all 9 frames of the element.

(ii) The **LLA mfVEP** stimulus was similar to the BonY stimulus, but its equivalent in gray scale. The yellow background was replaced by light gray of the same luminance as the yellow, and the blue color of the checkerboard was replaced by a darker gray of the same luminance as the blue.

The visual stimulus was generated on a 21-inch high-resolution display (Hitachi Ltd., Tokyo, Japan) with a refresh rate of 75 Hz.

MfVEP Recording: Four gold-cup electrodes (Grass- Telefactor, Warwick, RI) placed in a custom-built electrode holder were used for bipolar recording with two electrodes positioned 4 cm on either side of the inion, 1 electrode in the midline 2.5 cm above the inion, and 1 electrode 4-5 cm below the inion. The electrodes are secured with a Velcro tape firmly around the forehead of the subject. Electrical signals were recorded along 4 channels, as the difference between superior and inferior, left and right, and obliquely between left and inferior and between right and inferior electrodes. The ground electrode was placed on the ear lobe.

The subjects were seated comfortably with their chin elevated to relax the neck muscles. All subjects were refracted optimally for near and seated 30 cm from the display using full aperture lenses. All recordings were conducted monocularly, with an undilated pupil starting right eye first. All glaucoma subjects and controls were alternately assigned to start with either LLA mfVEP or BonY mfVEP.

The visual evoked responses were amplified 100,000 times (sampling rate, 512 Hz) and bandpass filtered (1–20 Hz). Recording of each eye lasted 5 to 7 minutes depending on the number of runs required to maximize signal-to-noise ratio (SNR). 6-8 runs will typically provide the accepted SNR. All recordings were performed monocularly. The custom designed software correlated the electrical responses with the stimulus appearance and assigned signals to the corresponding segments. This software also scaled the responses to the

background electroencephalogram to reduce the inter-individual variability. A noise artefact algorithm identifies any noise contamination.

Analysis of the raw data is essentially the same for BonY and LLA mfVEP. Raw trace data are analyzed using the OPERA (Objective Perimetry Evoked Response Analysis) custom designed software. Maximal peak-to-trough amplitudes for each wave within the interval of 60-180 m sec are determined and compared among channels for every stimulated segment of the visual field. The software selects the wave of maximal amplitude from each zone in the field and creates a combined topographic map. The amplitude values from the Trace array are compared to the normative database and probability of abnormality plots is constructed.

Defining a scotoma on BonY and LLA mfVEP is defined as a cluster of three abnormal zones on the amplitude deviation plot with at least two of those zone with a P value < 0.02 and at least 1 segment of P< 0.01 b) a cluster of 3 or more abnormal segments on intereye asymmetry deviation plot with P<0.01, c) 2 or more zones with P<0.005 and d) Accumap Severity index > 30. In the asymmetry plot, at least two of the zones should qualify as nucleus, non-rim zones.

The AccuMap Severity Index (ASI) is designed to give an overall score based on the number of abnormal zones on both amplitude plot and the asymmetry plot, with relative weighting for severity and to score zones for clusters in certain locations within the field. This provides an overall index of whether the AccuMap result is within normal limits (score less than 11, P>5%), borderline (score in 11-19 range, 5%>P>1%) or outside normal (score >20, P<1%). The Noise artefact provides an indication of the quality of the recording should be within acceptable limits.

Due to the extensive number of investigations involved in the study, the tests were done over two days. The subjective visual field tests, and optic disc imaging was done on the same day with adequate rest period between tests to avoid fatigue. BonY and LLA mfVEP recordings were done on a different day within the same week.

2.11 Statistical analysis

Comparison of the performance of the subjective and objective tests on was done using contingency tables. P value was calculated using McNemar's test on IBM SPSS Statistics

Version 24, IBM Corp. Chi squared and Odd's Ratio values were also calculated using Prism 7 for Mac OS X, Graphpad Software, Inc.

The baseline parameters of the subjective and objective tests between the progressive and non-progressive groups were compared and P values were calculated using the Mann-Whitney- Wilcoxon (Wilcoxon rank sum) Test on Prism 7 for Mac OS X, Graphpad Software, Inc. The change between the baseline and follow up parameters for the various tests within the progressive and non-progressive groups were calculated using the Paired T tests on Prism 7 for Mac OS X, Graphpad Software, Inc. Change over time (baseline Vs. final visits) for the parameters between the progressors and non-progressors were analyzed using the Kruscal-Wallis test of repeated measures one-way ANOVA, Prism 7 for Mac OS X, Graphpad Software, Inc. Correlation between the parameters was measured using Excel on Mac, MS office 2011, Microsoft Inc. P values for the correlation was performed using StatPlus:max, AnalystSoft Inc. add on for Excel 2011.

Sensitivity, specificity, Positive PV and NPV were all calculated using the contingency table analyses on Prism 7, Graphpad Inc. using Wilson/Brown method (CI 95%) and P value calculated using Fisher's exact test.

2.12 Major technical issue affecting scope of thesis

The baseline investigations for all the recruited subjects and control volunteers were completed using an original AccuMap amplifier. This was later replaced with a grass amplifier during the course of the study. The mfVEP recordings for both the BonY and LLA mfVEP were tested with the replaced amplifier before resuming follow-up recording for the study participants and it seemed to be performing adequately. However, when the final analysis of the mfVEP amplitude and latency data for the follow up years was completed, the generated results did not fit into any predictable pattern. The polarities of the recordings were noted to be reversed in several of the follow up recordings compared to the baseline recordings.

The recording device facilitates recalculating each run for all the visits. Using this, all runs were recalculated for both BonY and LLA mfVEP for both controls and subjects for the entire follow-up period was done over several weeks to isolate the cause for such a discrepancy. By reviewing each of the recordings, I was able to establish that all these changes occurred after a certain timeline associated with the change of the grass amplifier. Application of correctional

factors unfortunately did not rectify the error. There appeared to a new variable performance introduced by the newer amplifier shortly after it was implemented that was not detected. After extensive review of these findings the decision had to made to exclude all follow up BonY and LLA mfVEP recordings and data for both subjects and controls which was a **major setback for this study** as it removed the longitudinal mfVEP data. The baseline recordings done with the original amplifier and the data generated remained unaffected so this was used as an initial cross-sectional study (Chapter 3) and then as a baseline predictor for future glaucomatous change using the data from all the other test protocols (Chapters 4 and 5). Unfortunately, the ability to examine for longitudinal changes in mfVEP responses was lost because of this technical problem, and a large amount of data had to be disregarded.

It must be emphasized that mfVEP is an evolving technology and there will be major advances in future. Along with advances in novel stimulus presentations like those addressed in this thesis, improving SNR of the records, reduction in testing time, improved analysis using new algorithms, the need for making these technologies clinically viable and more robust for general use becomes essential and the technical challenges we have faced will take us a step closer to achieving that.

CHAPTER 3

IDENTIFICATION OF FUNCTIONAL VISUAL LOSS IN GLAUCOMA - COMPARING THE PERFORMANCE OF OBJECTIVE AND SUBJECTIVE PERIMETRY TESTS BASED ON MAGNOCELLULAR AND KONIOCELLULAR PATHWAYS

3.1 Introduction

It has been established that visual information processing happens along three major retino-geniculo-cortical pathways namely Parvocellular, Koniocellular and Magnocellular pathways[226,227,228,229,230]. The role of the parvocellular pathway is well established in the processing of high contrast, high spatial frequency information and is responsible for about 80% of the information processing from ganglion cells. However, The magnocellular and Koniocellular pathways contribute for only 10% respectively for information processing. The magnocellular pathway conveys information about low contrast and low spatial frequency achromatic images and the Koniocellular pathway conveys a blue-on/ yellow-off color signal to the brain.

In glaucomatous optic neuropathy, a substantial number of retinal ganglion cells are lost prior to the development of an achromatic visual field deficit and this has been established in both human and primate models[231,232,31]. Standard Automated Perimetry (SAP) is relatively insensitive to early structural damage from glaucoma, which led to the development of various psychophysical tests aimed at detecting early functional loss.

Newer subjective perimetry tests have been developed based on the pathways that stimulate the ganglion cells with less redundancy. These include SWAP (targeting the Koniocellular pathway) and FDT (targeting the Magnocellular pathway). Several studies have assessed the ability of the FDT and SWAP to detect glaucomatous visual field defects, even at early stages of the disease[233,103, 234,235]. A study by Ferreras et al [196] assessing the ability of FDT and SWAP to detect glaucomatous change in preperimetric glaucoma subjects, established that at least 20% of the patients with preperimetric glaucoma demonstrated functional losses in FDT and SWAP. A study by Spry et al [236] FDT exhibited the highest repeatability(47%) followed

closely by SWAP (42%). The more severe the structural damage, the greater the sensitivity for detecting glaucomatous visual field losses.

Similar studies on the role of objective perimetry using multifocal VEP Blue-on-yellow stimulus (koniocellular) and Low luminance achromatic stimulus (magnocellular) have been done[169, 193, 199, 200]. These have been described in chapter 1.

However, a head to head comparison between these subjective and objective tests targeting the two pathways has not been previously undertaken.

3.2Aim

To compare the performance of the subjective and objective perimetry tests based on the Magnocellular pathway namely the Frequency Doubling Perimetry (FDP) and the Low Luminance Achromatic Perimetry and the performance of the tests based on the Koniocellular pathway namely Short Wavelength Automated Perimetry (SWAP) and Blue on Yellow multifocal VEP. The aim is to further determine if one pathway is superior to the other at detecting glaucomatous damage on both objective and subjective measures.

3.3 Methods

Participants: One hundred and two eyes from fifty-one early-glaucoma subjects (23 Female and 28 male) were recruited from a Sydney-based private glaucoma practice. Glaucoma diagnosis was made prior to the study based on the glaucomatous cupping of the optic disc, as judged by stereoscopic ophthalmoscopy. The subjects had at least one glaucomatous optic disc but still maintaining a normal, reliable visual field in that eye (i.e. pre-perimetric). Approval was obtained from the University's review board. 30 healthy eyes of 15 controls and underwent a complete ophthalmic examination along with BonY and LLA VEP recordings, HVF and OCT. Written informed consent was obtained from all the participants and controls and the study was conducted in accordance with the tenets of the Declaration of Helinski[237].

Inclusion and Exclusion criteria, measurement and recording techniques of subjective and objective perimetry tests involved in this study, defining abnormalities for the relevant tests have been explained in detail in the Methods section in Chapter 2. Stereo disc photographs

were used for the diagnosis of glaucoma and inclusion into the study but progression was identified with a combination of repeatable visual field defect on HVF and OCT changes.

Abnormality criteria of subjective and objective perimetry tests have also been explained in the Methods chapter. The AccuMap Severity Index (ASI) for LLA and BonY mfVEP is designed to give an overall index the AccuMap result and classifies the results as, within normal limits (score less than 11, P>5%), borderline (score in 11-19 range, 5%>P>1%) or outside normal (score >20, P<1%).

The order in which the tests were performed was randomized using the Random number generator on Microsoft Excel. Based on this, each subject underwent either subjective or objective perimetry tests to start with. The same process was used to determine which subjective (SAP/ SWAP/ FDT) or objective (LLA mfVEP/ BonY mfVEP) perimetry test was done first All visual field defects on FDT and SWAP were repeatable with excellent reliability indices. LLA mfVEP and BonY mfVEP recordings were done monocularly.. Recording of each eye lasted 6-8 minutes. Each eye had a minimum of 6 runs to maximize the signal-to-noise ratio. Each run was then assessed for the recording quality and noise artifacts. Noisy runs were discarded and repeated. The Opera software correlates the electrical responses with the stimulus appearance and assigned signals to the respective segments.

3.4 Analysis

Comparison of the performance of the subjective and objective VEP tests on Magno and Koniocellular pathways was done using contingency tables. P value was calculated using McNemar's test on IBM SPSS Statistics Version 24, IBM Corp. Chi squared and Odd's Ratio values were also calculated using Prism 7 for Mac OS X, Graphpad Software, Inc.

3.5 Results

Demographics:

Of the 102 eyes, 60 eyes of 42 patients had preperimetric glaucoma and 42 eyes of 34 patients had early glaucoma. The mean age of the patients was 62.92 ± 6.4 years. The median Mean Deviation at baseline for the 60 eyes was -0.93. All the subjects had investigations done at baseline, 6 months after baseline and yearly thereafter. The mean follow-up period for the

cohort was 4.03 ± 1.03 years. Only the baseline visits of the BonY and LLA mfVEP results were considered for this study.

For the purposes of this study, only the 60 eyes of 42 pre perimetric subjects were included as we were interested in detection of very early glaucoma. They had a clinical diagnosis of glaucoma based on glaucomatous disc changes and were under the care of a glaucoma specialist. The white on white SAP was normal with reliable performance and confirmed on subsequent testing. The average baseline HFA Mean Deviation of the included eyes was 0.12 ± 1.27 dB and MD of SWAP and FDP were -0.44 ± 2.85 dB and -0.34 ± 3.74 dB respectively.

Analysis of the performance of subjective perimetry (FDP) versus the objective perimetry (LLA mfVEP) tests both based on the Magnocellular pathway and subjective (SWAP) and objective perimetry (BonY) tests based on the Koniocellular pathway was performed.

3.6 Comparing subjective and objective perimetry tests based on the MAGNOCELLULAR PATHWAY

Sixteen eyes out of sixty (26.6%) were abnormal on FDP at baseline and 37.5% (6/16) eyes eventually developed scotoma on HVF over the course of the study (2-5 years). The scotoma that developed on HVF matched topographically with that on FDT in 5 out of 6 instances (83.3%).

Thirty four of sixty eyes (56.6%) presented with scotoma on LLA mfVEP at baseline of which 11 (32.35%) subsequently developed defects on HVF. 81.8% of those defects matched topographically with the baseline defect on LLA mfVEP. Only 8/60 (13.33%) eyes had defects on both FDP and LLA mfVEP. 6 (75%) of those 8 eyes had FDP defects corresponding to the hemifield defect on LLA. 2 eyes presented with defects in the opposite hemifield. Table 3.1 shows the number of eyes showing abnormality for each test at baseline for the 60 preperimetric eyes that subsequently developed scotoma on HVF. Functional loss on HVF appeared 30 (median) months after the defect was detected on LLA mfVEP at baseline (Mean 17.2 months ± 15.35).

Table 3.1: Performance of the subjective and objective perimetry tests in Progressors and topographic correlation of the defect. **OCT: Borderline defect was considered normal.*

	Eyes with defect at baseline (%)	Eyes that developed subsequent HVF defect (%)	Eyes that had a positive defect on OCT* (%)	Topographic correspon-dence with HVF defect developed (%)	Topographic correspon-dence with OCT defect final visit (%)
FDP	16/60 (26.6%)	6/16 (37.5%)	10/16 (62.5%)	5/6 (83.3%)	6/6 (100%)
LLA mfVEP	34/60 (56.6%)	11/34 (32.3%)	21/34 (61.7%)	9/11 (81.8%)	7/11 (63.6%)
SWAP	15/60 (25%)	5/15 (33.3%)	9/15 (60%)	5/5 (100%)	4/5 (80%)
BonY mfVEP	20/60 (33.3%)	7/20 (35%)	12/20 (60%)	4/7 (57.1%)	4/7 (57.1%)

Table 3.1: Comparison of FDT perimetry and LLA mfVEP (magnocellular pathway) at baseline using McNemar's test

		FDT perimetry defects at baseline		
LLA mfVEP defects at baseline		DEFECT	NO DEFECT	TOTAL
	DEFECT	8 (23.5%)	26 (76.4%)	34
	NO DEFECT	8 (30.7%)	18 (69.2%)	26
	TOTAL	16	44	60

Comparing the eyes with defect at baseline on FDT perimetry and LLA mfVEP, the positivity rate of LLA mfVEP test was significantly better than the FDT (P = 0.0036) using McNemar's test with continuity correction. (Chi squared value was 8.5 with 1° of freedom. Odd's Ratio was 3.25 with a 95% CI extending from 1.429 to 8.306).

The sensitivity of the LLA mfVEP was noted to be higher than the FDP; and the identification of abnormalities associated with a functional visual loss in eyes that progressed on SAP were quite similar in both the subjective and objective perimetry tests based on the Magnocellular pathway.

3.7 Comparing the subjective and objective perimetry tests based on the KONIOCELLULAR PATHWAY

15 out of 60 pre-perimetric eyes (25%) had an abnormal SWAP at baseline and 20 out of 60 (33.33%) had baseline defects on BonY mfVEP. 6 eyes had defects on both SWAP and BonY. The defects on all 6 eyes corresponded topographically on both the tests. Out of the 15 eyes that developed scotoma on HVF eventually, 5 out of 15 eyes (33.3%) presented with baseline SWAP defects and 7 (46.6%) on BonY mfVEP.

Table 3.3 Comparison of SWAP and BonY mfVEP (koniocellular pathway) at baseline using McNemar's test

BonY mfVEP defects at baseline	SWAP defects at baseline: DEFECT	SWAP defects at baseline: NO DEFECT	TOTAL
DEFECT	6 (30%)	14 (70%)	20
NO DEFECT	9 (22.5%)	31 (77.5%)	40
TOTAL	15	45	60

Comparing the eyes with defect at baseline on SWAP and BonY mfVEP, there was no significant difference between the positivity rates of the tests (P = 0.4042) (McNemar's test with continuity correction. Chi squared value was 0.696 with 1° of freedom. Odd's Ratio was 1.556 with a 95% CI extending from 0.627 to 4.074). Both the tests performed equally in detecting abnormalities.

The results suggest that both SWAP and BonY mfVEP which are based on testing the Koniocellular pathway may have the ability to identify functional visual loss in glaucoma earlier that the standard white on white SAP. While the performance of the BonY has been marginally better in this particular study, SWAP was almost as effective.

3.8 Comparing the performance of the BonY mfVEP and LLA mfVEP tests based on the Koniocellular and Magnocellular pathway

Table 3.4 shows the contingency table comparing the baseline BonY defects and Baseline LLA defects. (P value calculated using McNemar's test with continuity correction was 0.0056. The Chi squared value was 7.682 with 1° of freedom. Odd's ratio was 0.222 with a 95% CI extending from 0.055 to 0.675).

LLA mfVEP test based on the Magnocellular pathway had a significantly higher positivity rate compared to the BonY mfVEP.

Table 3.4: Comparison of BonY mfVEP (koniocellular pathway) and LLA mfVEP (Magnocellular Pathway) at baseline

Baseline defects on BonY Mf VEP

Baseline defects on LLA Mf VEP

	DEFECT	NO DEFECT	TOTAL
DEFECT	16 (47.06%)	18 (52.94%)	34
NO DEFECT	4 (15.38%)	22 (84.62%)	26
TOTAL	20	40	60

To further look at the association between the subjective and objective perimetry tests, Pearson's correlation coefficient was calculated between the baseline mean deviation (MD) of Frequency Doubling Perimetry (FDP) and the baseline AccuMap Severity Index (ASI) (Page 77 in the Method's chapter) of LLA mfVEP and between MD of SWAP and ASI of BonY mfVEP.

There was a negative correlation between the mean deviation of the FDP and the ASI of the low luminance achromatic mfVEP as expected (correlation coefficient r = -0.3624; P=0.004. In other words, the severity index of LLA increased with decrease in the mean deviation of the FDP (Fig 3.1).

As with FDP and LLA mfVEP, there was a negative correlation between the SWAP MD and ASI of BonY mfVEP (correlation coefficient r = -0.3147; P=0.015). In both instances, the severity index of the mfVEP technique increases with decrease in MD of the subjective perimetry test and the correlation coefficient of both groups are similar. The correlation between the tests of the Magnocellular pathway is marginally stronger (Fig 3.2).

Fig 3.1: Correlation between the MD of FDT and ASI of LLA mfVEP at baseline

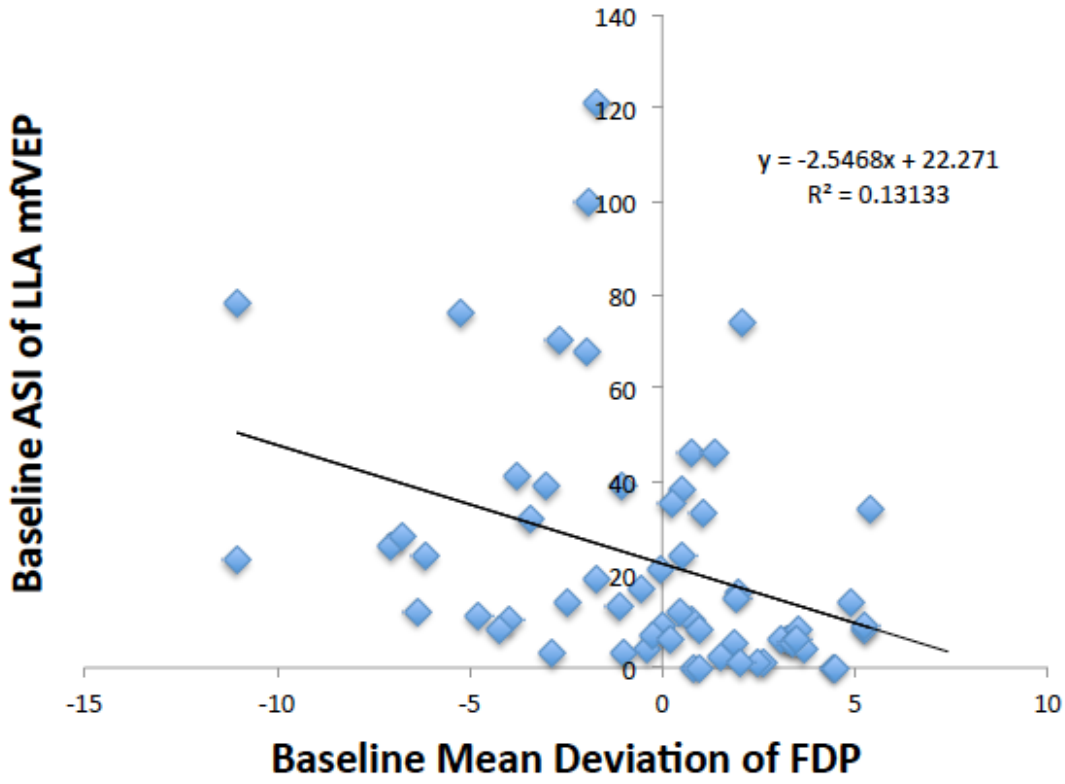

Fig 3.2: Correlation between the MD of SWAP and ASI of BonY mfVEP at baseline

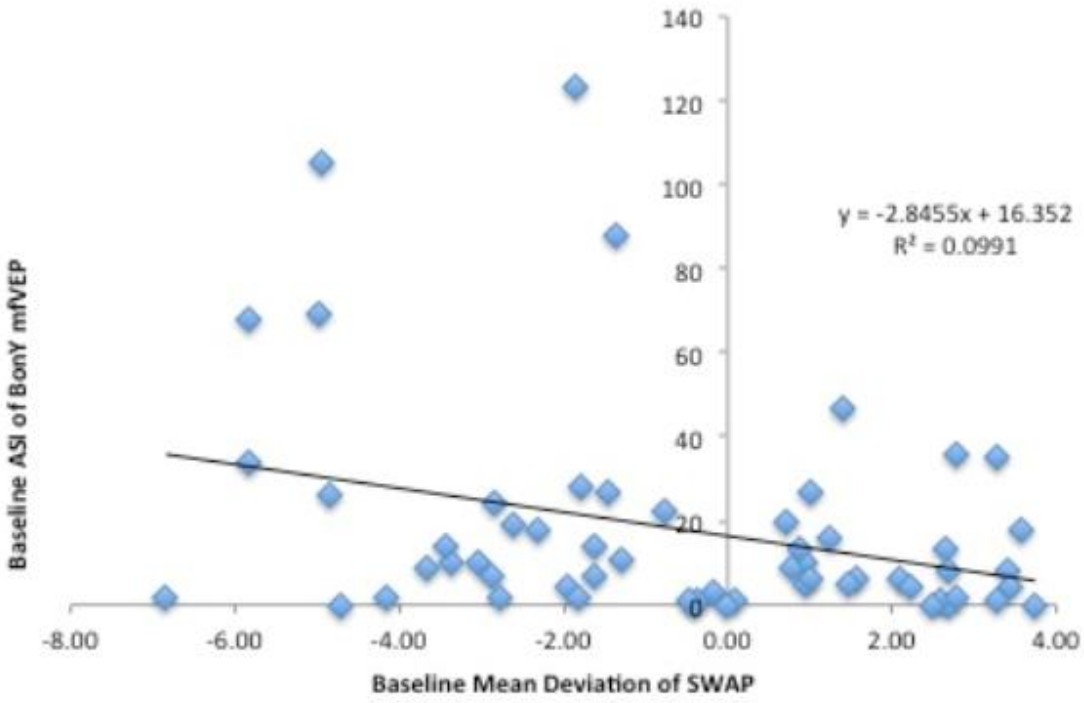

The outliers in both instances have been verified and found to be a true value. Comparing the performance of both the objective perimetry tests reveals that the LLA mfVEP based on the Magnocellular pathway revealed that 16 out of 60 eyes had baseline defects on both LLA and BonY tests out of which only 6 eyes eventually developed defects on HVF (37.5%) and 4 out of 6 (66.6%) times the scotoma corresponded topographically both between the two mfVEP tests and with the HVF defect (Fig 3.4 b). The defect was considered to be topographically corresponding if the hemifield location of the baseline mfVEP defect matched the location of the new HVF defect in subsequent visit. Development of a new defect on HVF has been described in Page 69 of 'Methods' in Chapter 2.

AccuMap Severity Index (ASI described in page 77, Methods Chapter) was also compared between the baseline LLA mfVEP and BonY mfVEP for the 60 pre-perimetric eyes. The average ASI (± SD) of LLA mfVEP was 23.15 ± 26.30 and that of BonY was 19.46 ± 28.38. Although the ASI of LLA is marginally higher than the BonY, (paired T test) revealed a P value of 0.1603 (95% CI -8.866 to 1.499; R^2 0.03314). The difference between the ASI of both tests was not statistically significant (Fig 3.3).

Fig 3.3: Bar graph demonstrating the comparison between ASI of BonY mfVEP and LLA mfVEP at baseline

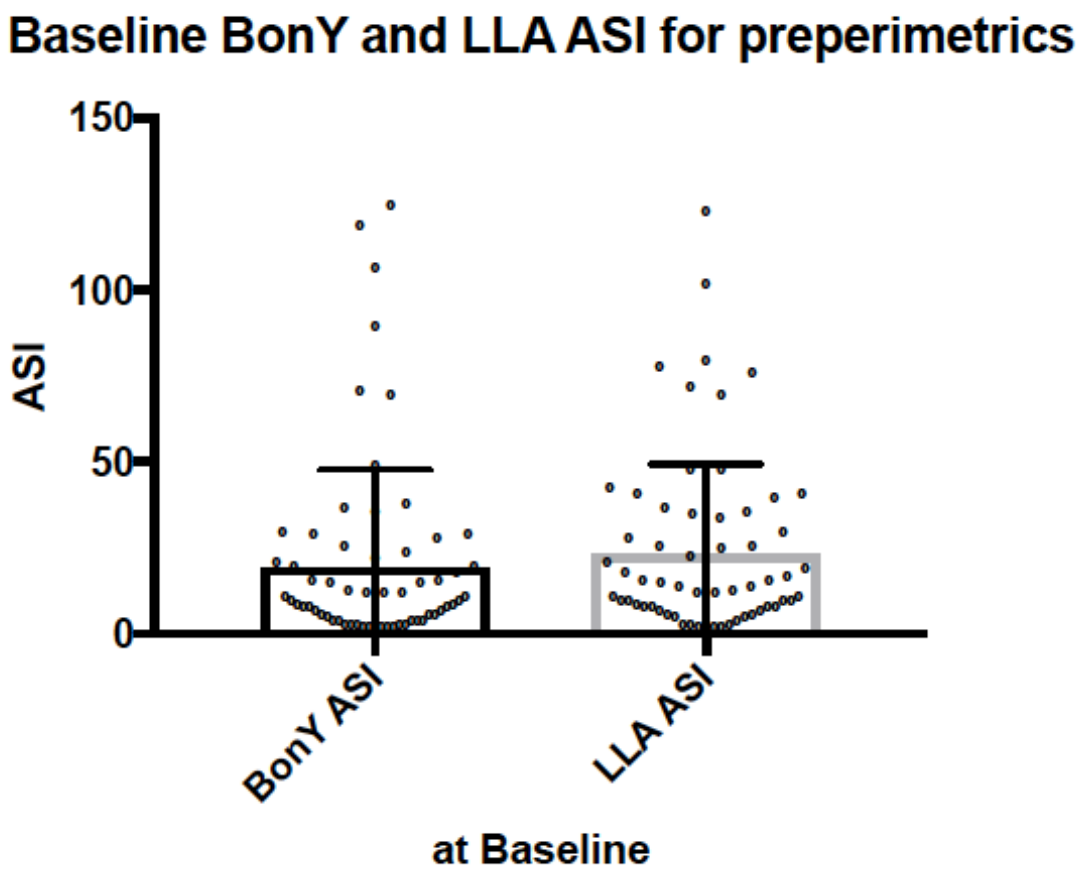

Fig 3.4 a: Subject 25 showing normal HVF at baseline and abnormalities on SWAP and FDT

Baseline HVF Mar 2011

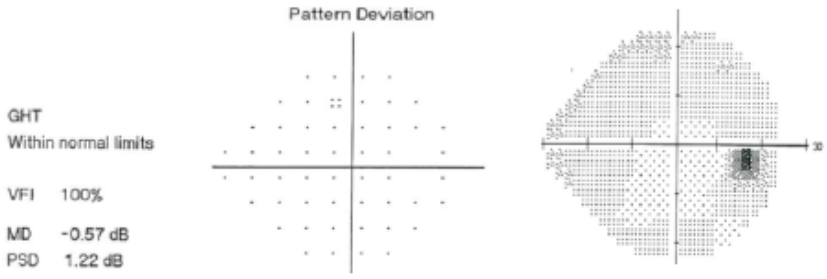

Baseline HVF Mar 2011

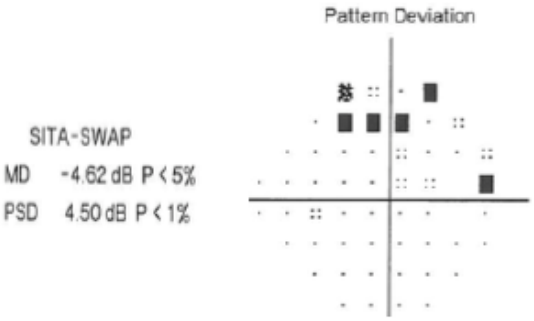

Baseline FDP Mar 2011

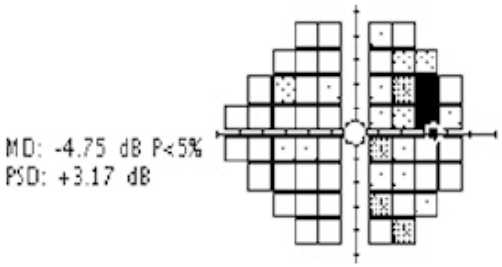

Fig 3.4 b: Subject 25 showing abnormal LLA mfVEP and BonY mfVEP at baseline, abnormal HVF at 4th year follow-up.

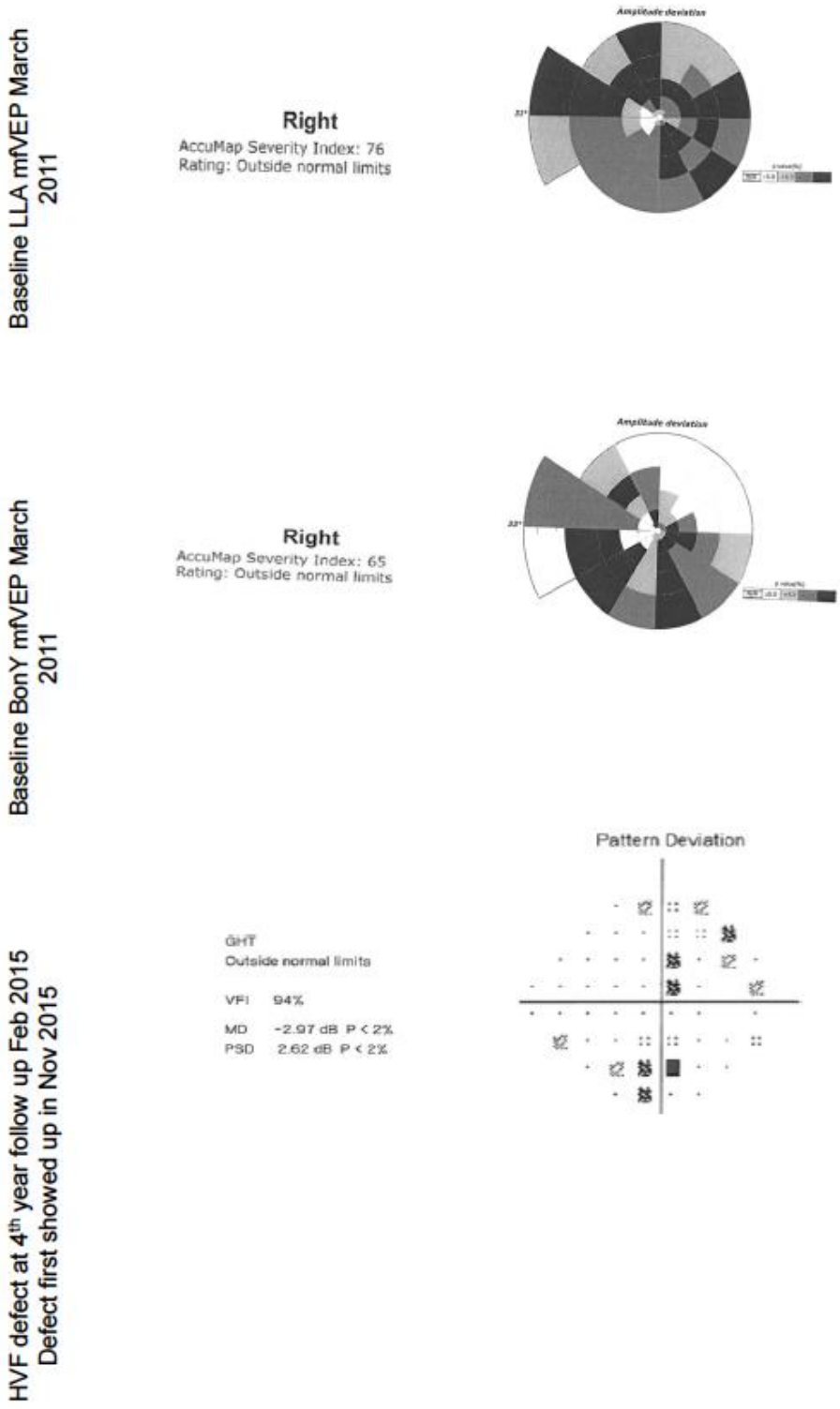

3.9 Discussion

In this study, among the four tests compared (FDT, SWAP, LLA mfVEP and BonY mfVEP) baseline abnormality in pre-perimetric glaucoma was always detected on more than one test. The primary criteria for inclusion of glaucoma subjects included were normal repeatable HVF despite the presence of glaucomatous optic disc. LLA mfVEP showed the highest sensitivity at baseline, which is in agreement with a previous study[200]. However, that advantage was reduced when subjects subsequently developed a scotoma on HVF a few years into the follow up.

In terms of comparison within specific pathway types, LLA mfVEP was more sensitive to changes in early pre-perimetric glaucoma than FDT. But the sensitivities of the objective (BonY mfVEP) and subjective (SWAP) perimetry tests targeting the koniocellular pathway were comparable. There was a negative correlation between the Severity Index of both the objective perimetry tests and Mean deviation of the subjective perimetry tests. The baseline severity indices of BonY and LLA mfVEP were also analogous.

The results indicated that only 32.35% of those flagged as abnormal in baseline LLA mfVEP eventually develop HVF defects. There was a high range in the follow up period for the subjects ranging from 2 years to 5 years and there is a possibility that some of these eyes will develop a visual field defect later. Out of the 15 eyes that progressed, there was only one subject with a 3-year follow-up and 9 eyes had over 5 years of follow-up data. The time frame of the appearance of the defect on HVF was varied and there was no difference in the progression rates in those with less or more than 4 years of follow-up. To examine if the LLA mfVEP defects indicate true defects or false positive, concordance of the defects with OCT was analyzed. Approximately 60% of all eyes showing abnormality on the four tests have abnormal OCT supporting associated structural damage. Eyes with anatomical variations of the optic nerve were ruled out and the number represents only those with true glaucomatous changes. This suggests the presence of a true abnormality on the functional tests rather than a false positive. All the 11 eyes out of the 34 abnormal eyes on LLA had abnormality on OCT and an additional 10 eyes (29%) indicated abnormality where the HVF was still normal. There exists a clear possibility for eyes showing abnormality on LLA mfVEP to develop a visual field defect on future HVF testing. Ideally this study would have reported on longitudinal changes in mfVEP parameters, but although testing was performed this data was unusable due to the change in amplifier used (see section 2.11).

The mean age of our study population was (± SD) 63.76 ± 6.2 years. Although all clinical evaluations were done for the subjects in every follow up visit, subjects with early cataract were not excluded from the study if their best-corrected (refractive error within the acceptable limits as mentioned in the Inclusion criteria) visual acuity was better than 6/9. Several studies confirm that image degradations can induce changes in mfVEP responses. Image blur can impact the response topographies of mfVEPs leading to mainly central response reduction[168,238].Since media opacities can impact all perimetry, impact of image blur is not a unique disadvantage[239,240,238]. However, none of the study participants had media opacities that could potentially compromise the mfVEP recordings. Care was also taken to correct the refractive error appropriately to avoid retinal blur. Decreasing pupil size can also contribute to reduced retinal illumination and thereby affect the mfVEP recording[175,159, 241,168,] but all subjects had normal pupil diameters, with no patients using pilocarpine.

Multifocal VEP responses to achromatic stimulation saturate at approximately 40% to 50% luminance contrast[164, 197, 242] similar to levels used in this study for LLA mfVEP. The contrast response function of parvocellular neurons is linear, while magnocellular neurons demonstrate saturation at low levels of luminance contrast[243, 194]. The low luminance achromatic stimulus seems to have an advantage over Blue on yellow stimulus and the subjective perimetry tests, being more sensitive to the smallest decline in ganglion cells. These results also concur with previous reports that suggest that magnocellular responses change early in the course of glaucoma[198,244] but this remains a controversial observation.

In conclusion, we observed in pre-perimetric glaucomas a slightly higher detection rate of abnormality on objective (mfVEP) compared to subjective tests (SWAP/FDT), and this applied to both koniocellular or magnocellular based testing. There was a negative correlation between LLA mfVEP severity index and MD of the FDT and between the BonY mfVEP severity indexes with MD of SWAP but the correlation of the subjective and objective tests of the magnocellular pathway was statistically significant.

CHAPTER 4

BLUE-ON-YELLOW AND LOW LUMINANCE ACHROMATIC MULTIFOCAL VEP LATENCIES: ARE THEY EARLY INDICATORS FOR FUTURE GLAUCOMA PROGRESSION?

4.1 Introduction

In glaucoma, damage to the ganglion cells and/or their axons produce characteristic visual field defects. The latency of the responses can possibly indicate the health of these retinal ganglion cells. Several studies indicate that latency can be used as a measure of early glaucomatous damage before retinal ganglion cell death. In glaucoma patients, large latency delays of over 20ms has been detected using conventional VEP (cVEP) technique[184, 245, 185]. Parisi et al[186] reported that all their patients with POAG had on an average 27.8ms longer latencies than the control group. In a study by Rodarte et al[158] about 40% of their study participants showed modest mfVEP latency delays.

The Blue on Yellow mfVEP and Low luminance mfVEP has been described by Klistorner et al[169] and Arvind et al[199] respectively. The studies revealed a negative correlation between age and average amplitude of blue on yellow mfVEP and a positive correlation between age and latency. The team also observed a loss of amplitude and an increase in latency with age more than 60 years. A normative database was also established for the tests with amplitude corrected for age based on best fitting of data. The inherent latency change with age was not incorporated in the normative database. Several studies have been published by this group indicating that both BonY and LLA mfVEP is significantly better than the conventional mfVEP in identifying early glaucoma.

A multifocal VEP recording in normal subjects varies between eyes, across individuals and across the visual field. For subjects without visual field defects, mfVEP recorded from monocular stimulation of each eye should essentially be identical. But a small amplitude asymmetry along the horizontal meridian and inter-ocular latency difference across the midline (about 4-5 ms) with right eye leading in the right visual field and vice versa common. There is also a wide variation in mfVEP recordings of normal individuals because of the

location of the calcarine fissure in relation to the electrode placement or external landmarks and differences in the cortical convolutions in the V1 region[246,247,248]. Within the visual field, the mfVEP responses vary in amplitude from regions at the same eccentricity; the average responses are smaller below the horizontal meridian than above and responses along the vertical meridian differs from the waveform of other responses indicating more than one source of the generated mfVEP signals. A latency difference of about 5ms can be found between the eyes along the midline due to the conduction time of the unmyelinated ganglion cell axons on the retinal surface[161, 167,249]

Since previous reports in the literature on VEP latency delays in glaucoma had been quite variable as mentioned above, with the conventional understanding that latency delay would more likely reflect demyelination while amplitude would reflect axonal loss, we studied the mfVEP latency delay for both LLVEP and BonY VEP to determine if there were any subtle changes that might be identified and useful clinically in glaucoma.

4.2 Aim

To compare the baseline latencies of BonY mfVEP and LLA mfVEP between the preperimetric glaucoma subjects that had a worsening visual field defect over time and those that remained stable with no field progression and to assess if this parameter can be an early indicator of future progression. This chapter will also aim to establish the relationship between the baseline latencies and amplitudes of BonY and LLA mfVEP tests with other functional and structural measures of glaucoma (Mean Deviation of the SAP and the RNFL thickness measured with OCT). Correlation between the hemifield latencies of the mfVEPs and hemifield SAP and OCT parameters will be assessed to establish defect correspondence between the tests.

4.3 Methods

Participants: One hundred and two eyes from fifty-one early-glaucoma subjects (23 Female and 28 male) were recruited from a Sydney-based private glaucoma practice. Glaucoma diagnosis was made prior to the study based on the glaucomatous cupping of the optic disc, as judged by stereoscopic ophthalmoscopy. The subjects had at least one glaucomatous optic disc and normal, reliable visual fields in that eye. Approval was obtained from the University's review board. 30 healthy eyes of 15 controls and underwent a complete

ophthalmic examination along with BonY and LLA VEP recordings, HVF and OCT. Written informed consent was obtained from all the participants and controls and the study was conducted in accordance with the tenets of the Declaration of Helinski[237].

Inclusion and Exclusion criteria, measurement and recording techniques of subjective and objective perimetry tests involved in this study, defining abnormalities for the relevant tests have been explained in detail in the Methods section in Chapter 2. Stereo disc photographs were used for the diagnosis of glaucoma and inclusion into the study but progression was identified with a combination of repeatable visual field defect on HVF and OCT changes.

Abnormality criteria of subjective and objective perimetry tests have also been explained in the Methods chapter. All visual field defects on FDT and SWAP were repeatable with excellent reliability indices. LLA mfVEP and BonY mfVEP recordings were done monocularly. The order in which the tests were performed was randomized. Recording of each eye lasted 6-8 minutes. Each eye had a minimum of 6 runs to maximize the signal-to-noise ratio. Each run was then assessed for the recording quality and noise artifacts. Noisy runs were discarded and repeated. The Opera software correlates the electrical responses with the stimulus appearance and assigned signals to the respective segments. Both BonY and LLA mfVEP recordings on the Accumap™ (Objectivision Pty Ltd, Sydney) use a 58-segment dartboard configuration. The segments are cortically scaled with eccentricity to stimulate approximately equal areas of the striate surface. The Objectivision system generates the latency and amplitude values for each of the 58 segments, which are imported as excel files. The average amplitude and latency for the eye as well as the hemifield averages were then obtained from the excel sheet. Maximal peak to trough amplitudes for each wave were determined and compared among channels from each segment in the field. The hemifield mean deviation values for HVF were calculated manually for each subject.

4.4 Analysis

The baseline parameters of both the mfVEP tests were compared and P values were calculated using the Mann-Whitney- Wilcoxon (Wilcoxon rank sum) Test on Prism 7 for Mac OS X, Graphpad Software, Inc. Comparison of the means of various parameters of the subjective and objective tests for both the groups were also calculated using the same. The change between the baseline and follow up parameters for the various tests within the progressive and non-progressive groups were calculated using the Paired T tests on Prism 7 for Mac OS X, Graphpad Software, Inc. Change over time (baseline Vs. final visits) for the various structural

and functional parameters between the progressors and non-progressors were analyzed using the Kruscal-Wallis test of repeated measures one-way ANOVA, Prism 7 for Mac OS X, Graphpad Software, Inc. Correlation between the baseline BonY and LLA mfVEP latencies, MD of HVF and global RNFLT of OCT were done using Excel on Mac, MS office 2011, Microsoft Inc.

4.5 Results

60 eyes of 42 pre-perimetric subjects were included for the analysis. 15 eyes 13 subjects (9male, 4 female) showed development of a visual field defect during the course of the study. The mean age of the progressive group was 63.7 ± 5.9 years. The visual field defects were confirmed with subsequent testing. Criteria for a new defect include a cluster of three points worsening by 5dB each, one of which has worsened by 10dB. Disease progression is defined as a statistically significant loss of sensitivity at three or more test points in the same location on two or more consecutive visual field evaluations[36]. The average Mean Deviation of HVF in progressives was -0.58 ± 0.98dB.

45 eyes of 33 subjects (18 male, 15 female) had stable normal visual fields throughout the course of the study. The mean age of the group was 62.3 ± 6.1 years. The average Mean Deviation of HVF in the non-progressive group was 0.35 ± 1.27 dB.

Table 4.1 shows the comparison of different parameters of structural and functional tests between the progressive and non-progressive groups at baseline and final visits.

Table 4.1: Comparing the structural and functional parameters between the Progressive and Non-progressive groups at Baseline. *P Value calculated using Mann-Whitney-Wilcoxon test*

	Baseline Visit		
Test Parameter	Progressive (n=15)	Non-progressive (n=45)	P Value
MD HVF	-0.58 ± 1.02	0.35 ± 1.27	0.004**
MD SWAP	-1.70 ± 2.45	-0.02 ± 2.88	0.037*
MD FDP	-1.25 ± 3.21	-0.03 ± 3.91	0.101(ns)
OCT RNFLT Global	77.33 ± 10.86	85.33 ± 7.08	0.007**
OCT RNFLT Inferior	98.33 ± 17.49	109.2 ± 15.90	0.008**
OCT RNFLT Superior	92.53 ± 12.39	107.4 ± 10.71	0.005**
HRT mean RNFLT	0.20 ± 0.06	0.22 ± 0.072	0.55 (ns)

The structural parameters between the progressive and non-progressive groups were compared using the Mann-Whitney- Wilcoxon (Wilcoxon rank sum) test. The average baseline Mean Deviation of HVF, SWAP was significantly worse in the progressive eyes (P Value 0.004, 0.037 respectively). Although the average MD of FDT was marginally lower in the progressives, the same was not statistically significant.

The global RNFLT in OCT showed a significant difference between the two groups (P= 0.007) and the average RNFL thickness was considerably smaller in the progressives. The average superior and inferior RNFLT in OCT were also significantly reduced in the progressive eyes (P = 0.008 and P = 0.005 respectively). There was no difference in the mean RNFLT of HRT in both groups.

Table 4.2a: Change in structural and functional parameters over time in the Progressive and non-progressive groups (*Paired T test)*

	PROGRESSIVE n= 15			NON PROGRESSIVE n= 45		
Test Parameter	Baseline	Final	P Value	Baseline	Final	P Value
MD HVF	-0.58 ± 1.02	-1.57 ± 2.03	0.019*	0.35 ± 1.27	0.17 ± 1.14	0.313 (ns)
MD SWAP	-1.70 ± 2.45	-0.53 ± 3.83	0.047*	-0.02 ± 2.88	0.69 ± 3.20	0.010**
MD FDP	-1.25 ± 3.21	-2.40 ± 3.73	0.027*	-0.03 ± 3.91	-0.40 ± 3.61	0.205 (ns)
OCT RNFLT Global	77.33 ± 10.86	74.93 ± 11.06	0.163 (ns)	85.33 ± 7.08	82.46 ± 9.75	<0.0001**
OCT RNFLT Inferior	98.33 ± 17.49	94.66 ± 19.70	0.105 (ns)	109.2 ± 15.90	105.93 ± 15.19	<0.0001**
OCT RNFLT Superior	98.33 ± 17.49	87.4 ± 12.95	0.037*	107.4 ± 10.71	100.73 ± 16.19	0.0052*
HRT mean RNFLT	0.20 ± 0.06	0.18 ± 0.09	0.163 (ns)	0.22 ± 0.072	0.21 ± 0.08	0.334 (ns)

Table 4.2b: Comparing the change in parameters over time between the Progressive and non-progressive groups (*Kruskal-Wallis test of RM one-way ANOVA).*

Kruskal-Wallis test of Repeated Measures one-way ANOVA

Test Parameter	P Value
MD HVF	0.0005**
MD SWAP	0.0740 (ns)
MD FDP	0.0798 (ns)
OCT RNFLT Global	0.0021**
OCT RNFLT Inferior	0.0022**
OCT RNFLT Superior	<0.0001**
HRT mean RNFLT	0.7009 (ns)

Change in the structural and functional parameters over time was also calculated for both groups using the Paired T test on Prism7 for Mac (Table 4.2a). There was a significant change in the MD of HVF, SWAP and FDT (P value 0.019, 0.047 and 0.027 respectively) over the study duration in the progressive group as expected and no significant change was noted in MD of HVF and FDT in the stable eyes. Interestingly, the difference in the MD of SWAP was highly significant (P value 0.010) in the non-progressive eyes as well. The MD of SWAP in both progressive and non-progressive eyes improved from the baseline to the final visit and is contrary to what is expected in a progressive disease emphasizing the variability associated with SWAP and its role in detecting progression.

While the difference in the global and inferior RNFLT of OCT between visits in progressive eyes was insignificant, the superior RNFLT had a significant (P = 0.037) change over time. The average global, superior and inferior RNFLT had a significant difference between visits in the non-progressive eyes. Change in the mean RNFLT of HRT between visits was not significant in both groups.

Comparison of change in parameters over time between the progressive and non-progressive eyes was analyzed using the Kruscal-Wallis test of repeated measures one-way ANOVA (Table 4.2b). The change in MD of HVF, global, superior and inferior RNFLT of OCT over the study duration between the two groups was very significant (P value 0.0005, 0.002, <0.0001 and 0.002 respectively) The change over time was not significant for MD of SWAP, MD of FDT and mean RNFLT of HRT between groups.

Table 4.3: Comparison of baseline parameters of BonY mfVEP and LLA mfVEP (*Mann-Whitney-Wilcoxon test)*

Test Parameter	Progressive Eyes (n=15) (Mean ± SD)	Non-progressive Eyes (n=45) Mean ± SD)	P Value
BonY mfVEP ASI	30.73 ± 32.38	15.71 ± 26.25	0.060 (ns)
BonY mfVEP Amplitude (nV)	567 ± 161	644 ± 175	0.040*
BonY mfVEP Latency (ms)	149 ± 14	141 ± 13	0.080 (ns)
LLA mfVEP ASI	35.33 ± 34.16	19.08 ± 22.11	0.011**
LLA mfVEP Amplitude (nV)	484 ± 144	591 ± 172	0.007 **
LLA mfVEP Latency (ms)	161 ± 11	158 ± 13	0.315 (ns)

Table 4.4: Comparison of baseline parameters between BonY mfVEP and LLA mfVEP in progressive eyes *(Independent T test)*

	BonY mfVEP	LLA mfVEP	P Value
ASI	30.73 ± 32.38	35.33 ± 34.16	0.4079 (ns)
Amplitude	567 ± 161	484 ± 144	0.0098**
Latency	149 ± 14	161 ± 11	0.0014**

Baseline BonY and LLA mfVEP parameters were compared between the groups using the using the Mann-Whitney- Wilcoxon (Wilcoxon rank sum) test. The average severity index for BonY mfVEP was higher (nearly twice) in the progressive eyes but the difference was not statistically significant. The BonY amplitudes were significantly reduced in the progressive eyes (P value 0.040). The difference in the average amplitudes between the groups was ~ 75 nV. The LLA mfVEP ASI was significantly higher and LLA amplitudes were significantly reduced in the progressives (P value 0.011 and 0.007 respectively). The difference in the average amplitudes of LLA mfVEP between the two groups was ~ 105 nV.

The average BonY latency in the progressive eyes was 8ms longer but this difference was not statistically significant. The latency delay between the groups was 3ms in LLA mfVEP (P not significant) (Table 4.3). Independent T test was performed between the average ASI, amplitude and latency values between BonY and LLA mfVEP in the progressive eyes. The baseline severity index was higher in the LLA than BonY but the difference was not statistically significant. The average baseline amplitude was over 80 nV lower and the average latency was 12 ms longer in LLA mfVEP compared to BonY mfVEP (P = 0.009 and P = 0.001 respectively) shown in Table 4.4.

Figure 4.1: Comparison of baseline BonY mfVEP and LLA mfVEP Latencies for the 60-pre perimetric eyes.

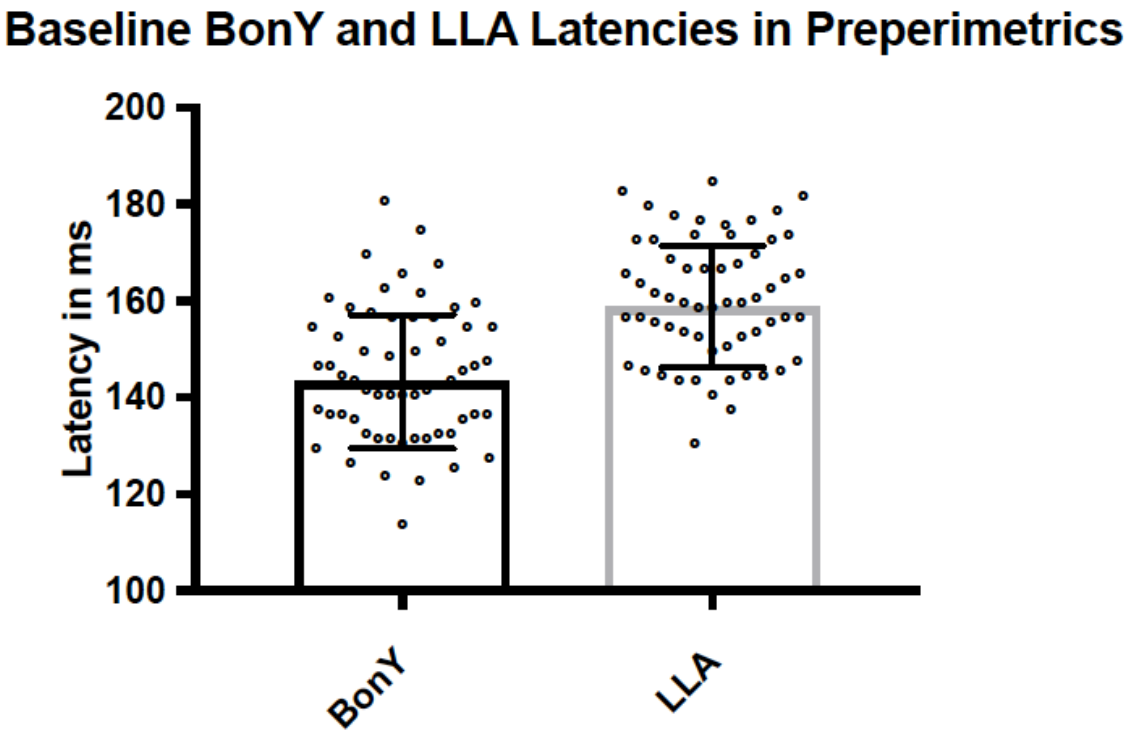

Figure 4.2: Comparison of baseline BonY mfVEP and LLA mfVEP Amplitudes for the 60 pre-perimetric eyes.

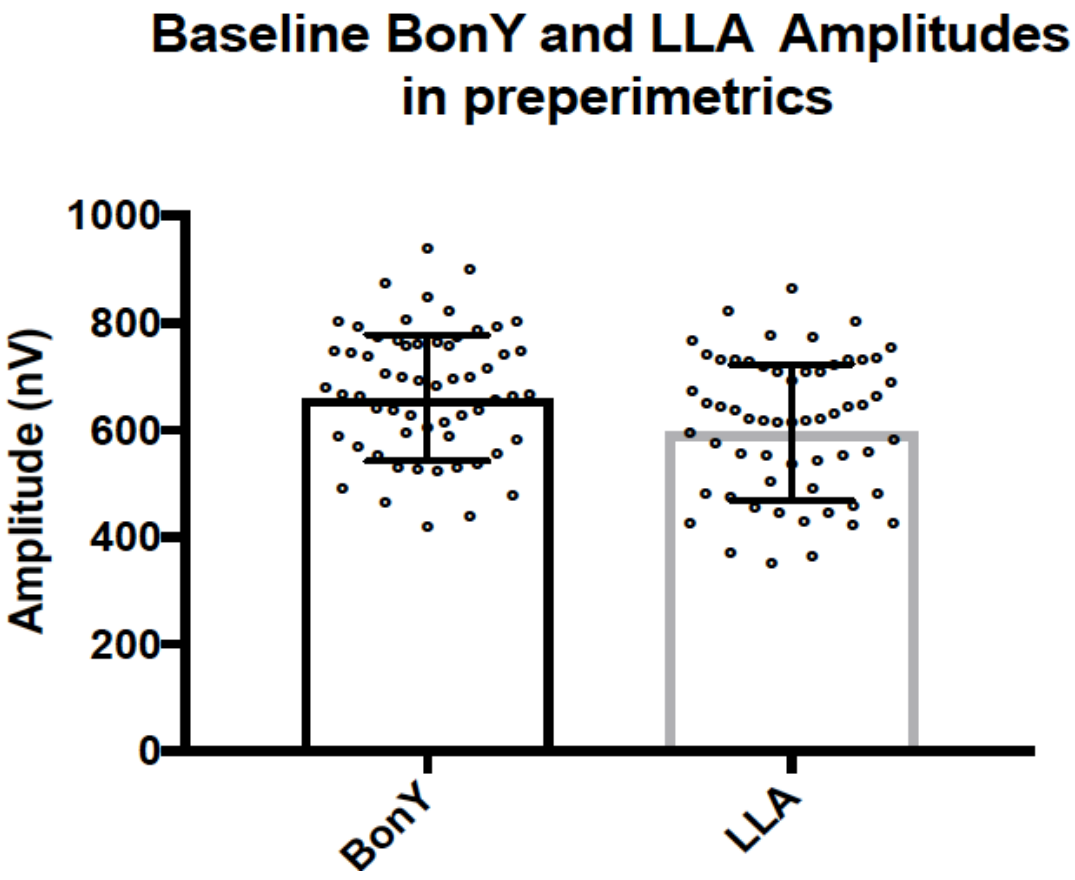

Figures 4.1 and 4.2 show the comparison between the baseline latencies and amplitudes of BonY and LLA mfVEP in the 60 pre-perimetric eyes. The error bars represent the 95% CI of the mean latencies (Fig 4.1) and amplitudes (Fig 4.2) in LLA and BonY mfVEP at baseline in the pre-perimetric group. The average baseline latencies of LLA mfVEP were significantly longer and the average amplitudes were smaller in the pre-perimetric eyes ($P < 0.0001$ in both instances).

Correlation between the baseline latencies of BonY and LLA mfVEP with baseline MD of HVF and global RNFLT of OCT have been shown in Figures 4.3 and 4.4 respectively. There was a significant negative correlation between the BonY mfVEP and MD HVF ($P = 0.007$) but the correlation between LLA mfVEP and MD HVF was poor. The association between global RNFLT of OCT and both mfVEPs was weak.

Figure 4.3: Correlation of BonY and LLA latencies with MD HVF at baseline for preperimetric eyes.

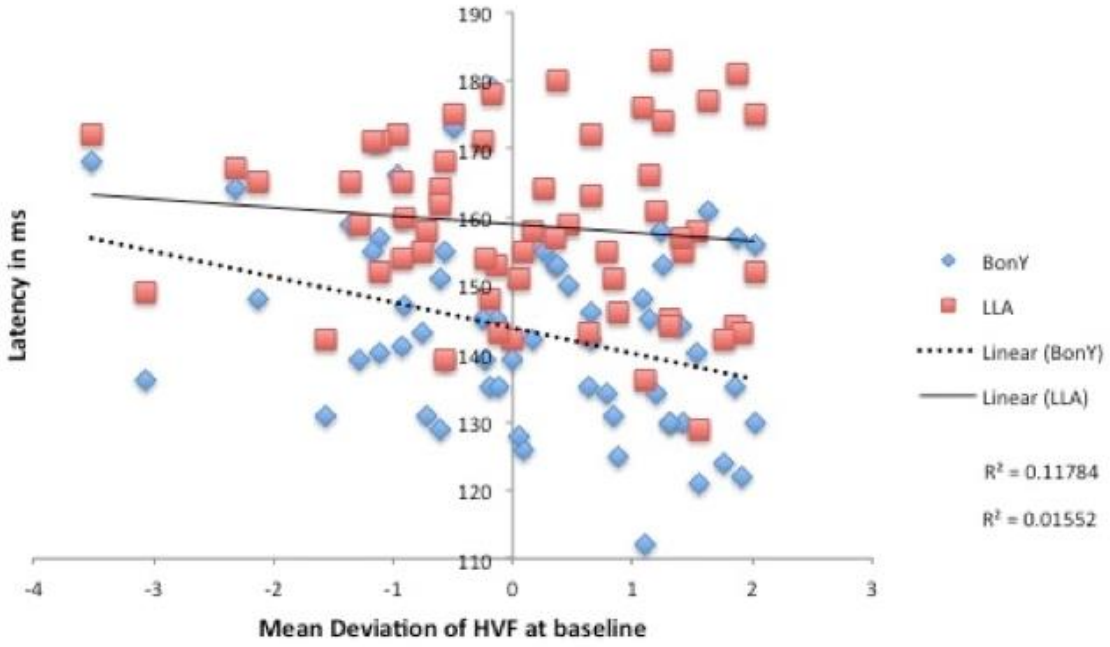

Figure 4.4: Correlation of BonY and LLA latencies with global RNFLT of OCT at baseline for preperimetric eyes.

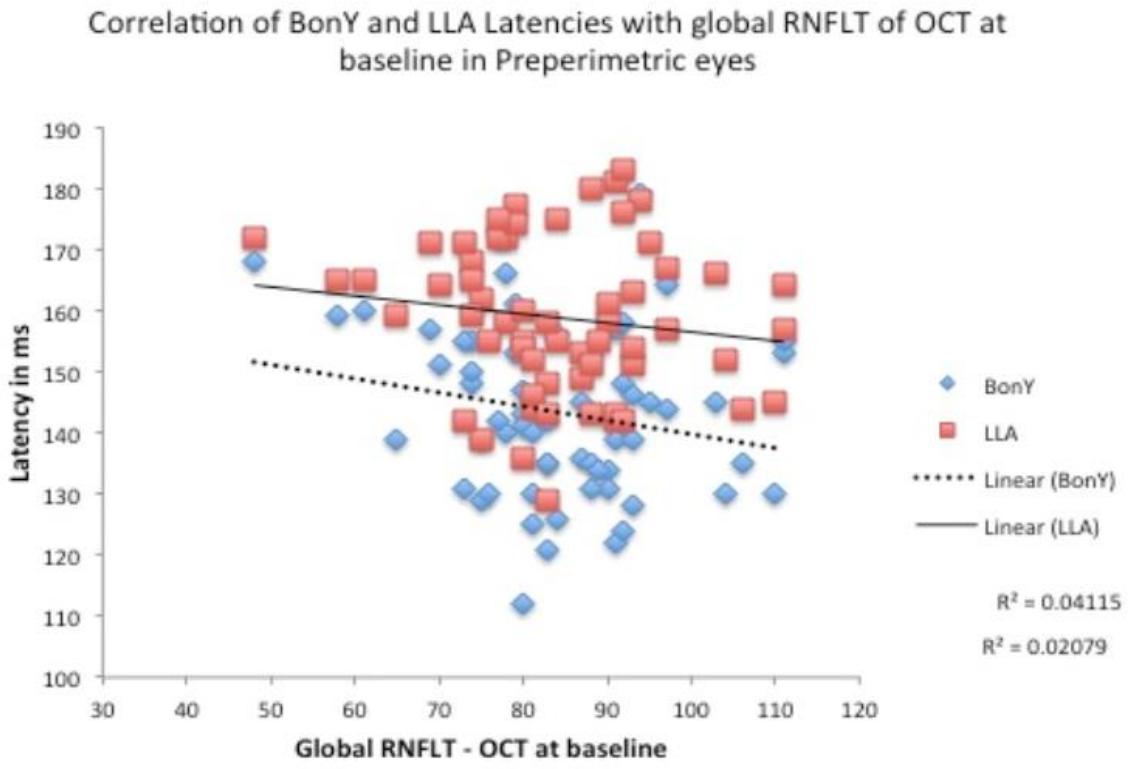

Figure 4.5: Correlation of BonY and LLA amplitudes with MD HVF at baseline for preperimetric eyes.

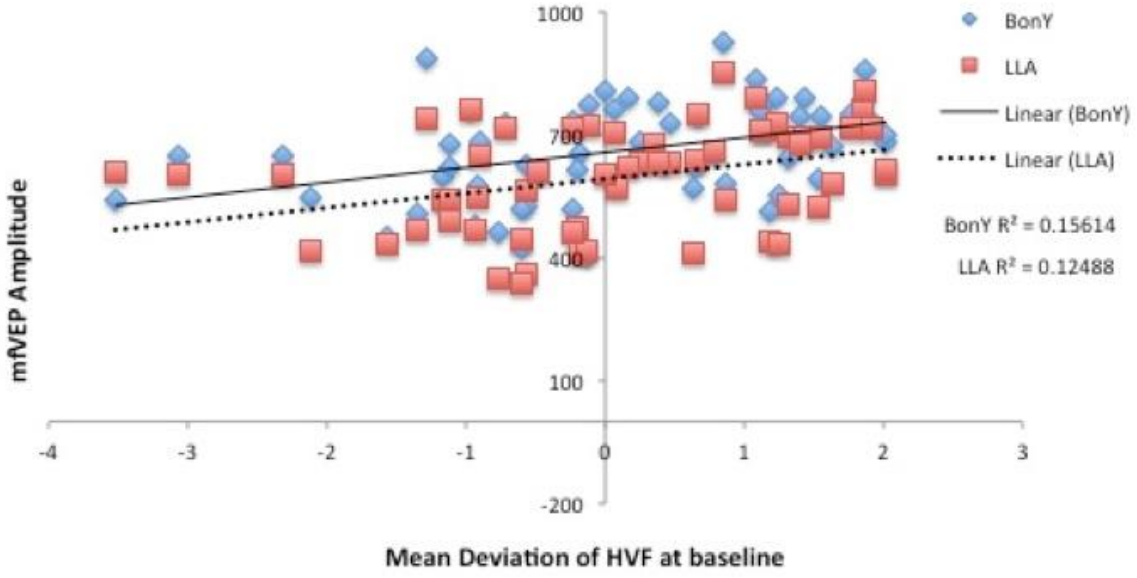

Figure 4.6: Correlation of BonY and LLA amplitudes with global RNFLT of OCT at baseline for preperimetric eyes.

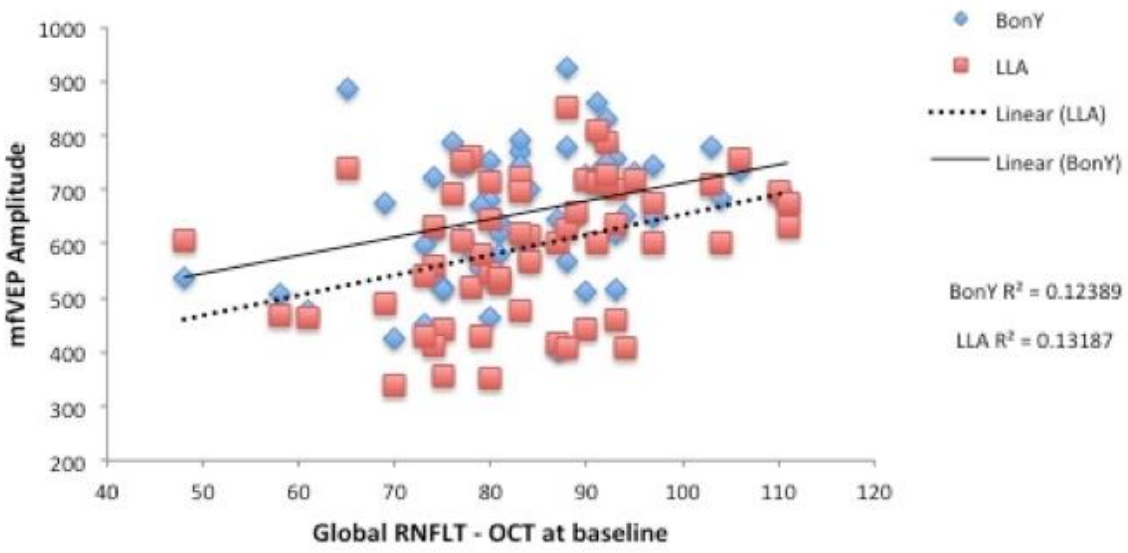

Figures 4.5 and 4.6 show the correlation between BonY and LLA baseline amplitudes and MD HVF and global RNFLT of OCT respectively. Both the MD HVF and RNFLT OCT showed a positive relationship with the amplitudes of BonY and LLA. The correlation and P values are listed in Table 4.5.

Table 4.5: Correlation of BonY and LLA latencies with global RNFLT of OCT and MD HVF at baseline for preperimetric eyes.

Table 4.5: Correlation of BonY and LLA latencies with global RNFLT of OCT and MD HVF at baseline for preperimetric eyes.

	LLA Latency	BonY Latency	LLA Amplitude	BonY Amplitude
MD of HVF	$R^2 = 0.015$ P = 0.342	$R^2 = 0.117$ P = 0.007	$R^2 = 0.124$ P = 0.005	$R^2 = 0.156$ P = 0.001
Global RNFLT of OCT	$R^2 = 0.020$ P = 0.120	$R^2 = 0.041$ P = 0.271	$R^2 = 0.131$ P = 0.004	$R^2 = 0.123$ P = 0.005

Figure 4.7: Correlation of superior mfVEP latencies with superior MD of HVF.

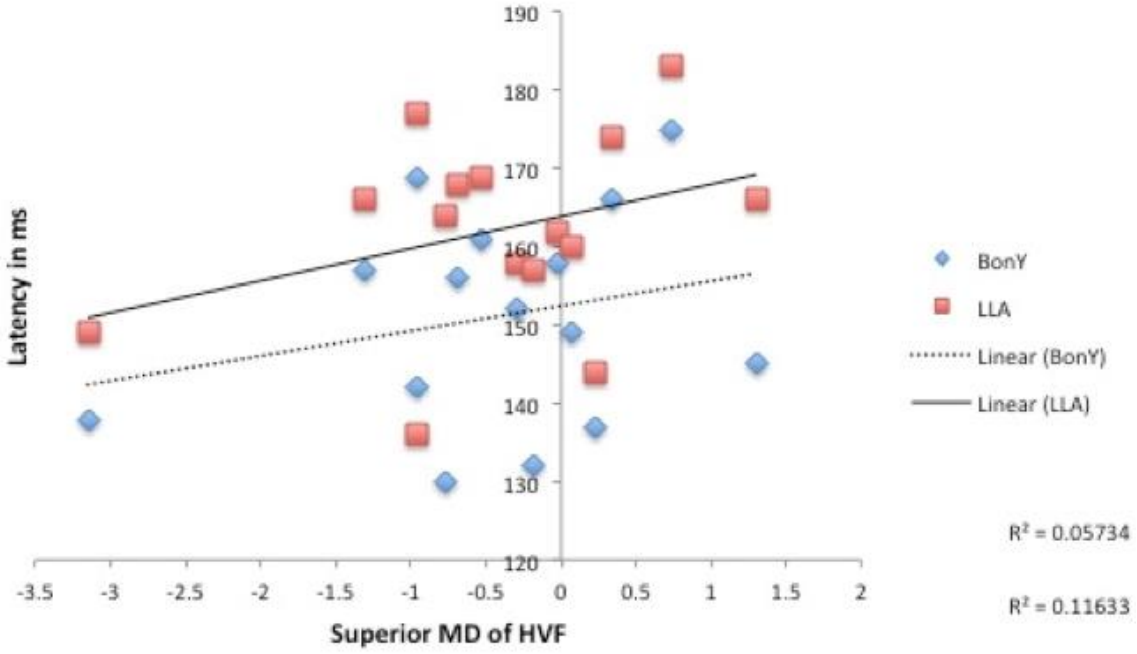

Figure 4.8: Correlation of inferior mfVEP latencies with inferior MD of HVF.

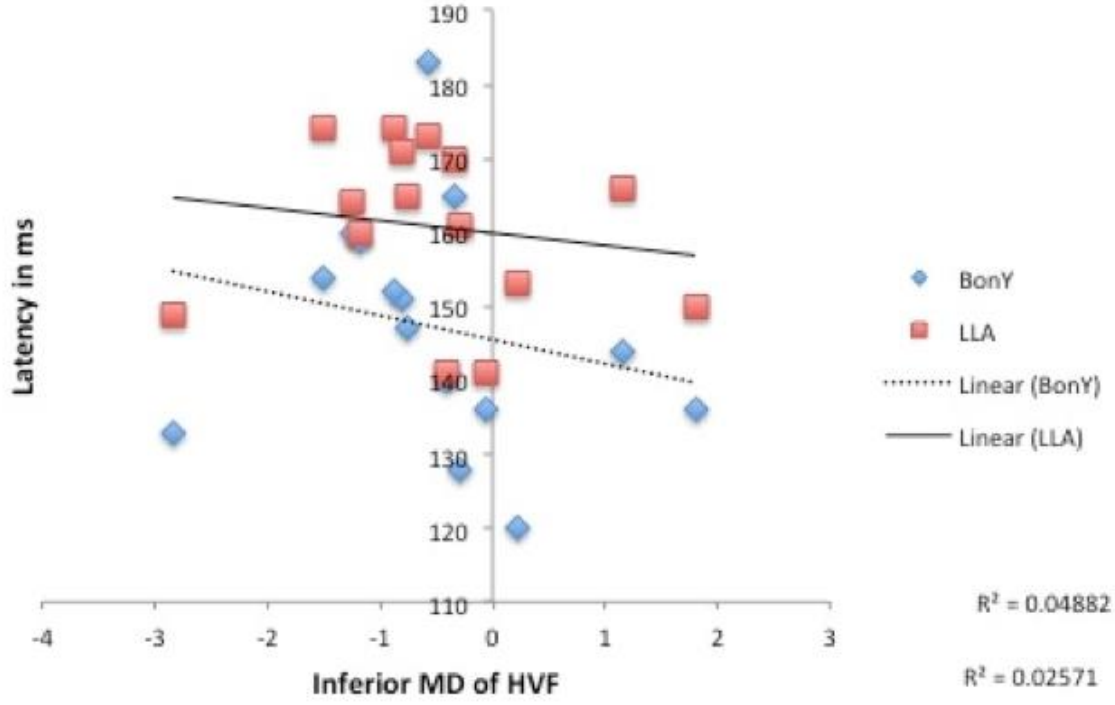

Figure 4.9: Correlation of superior mfVEP latencies with superior RNFLT of OCT.

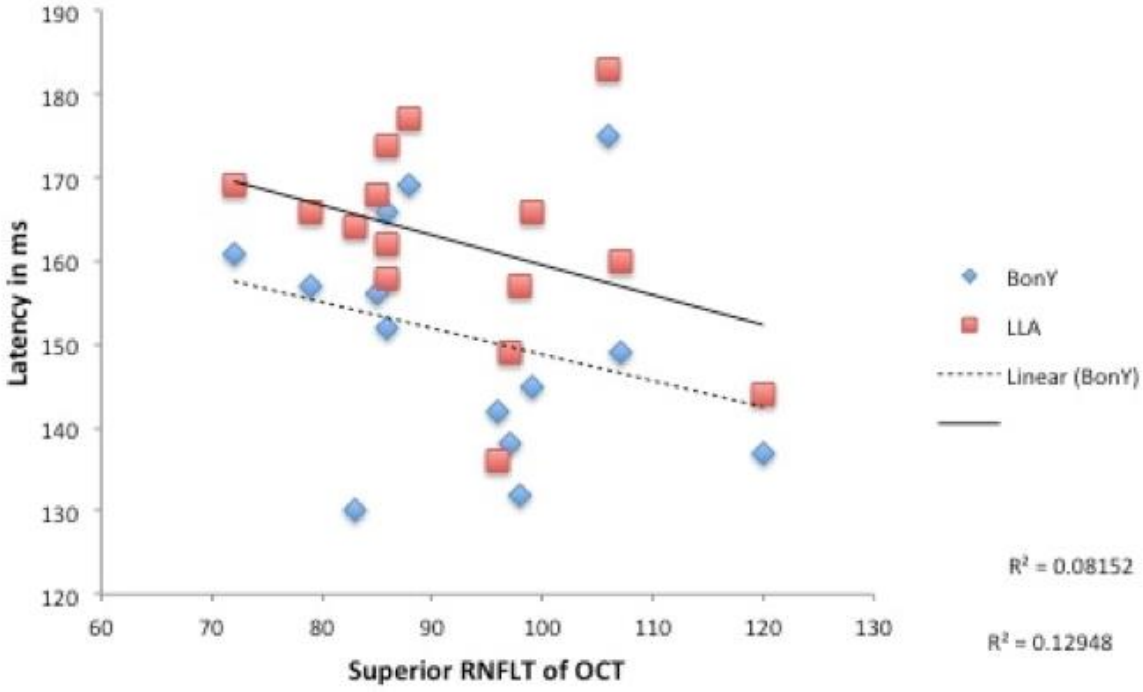

Figure 4.10: Correlation of inferior mfVEP latencies with inferior RNFLT of OCT.

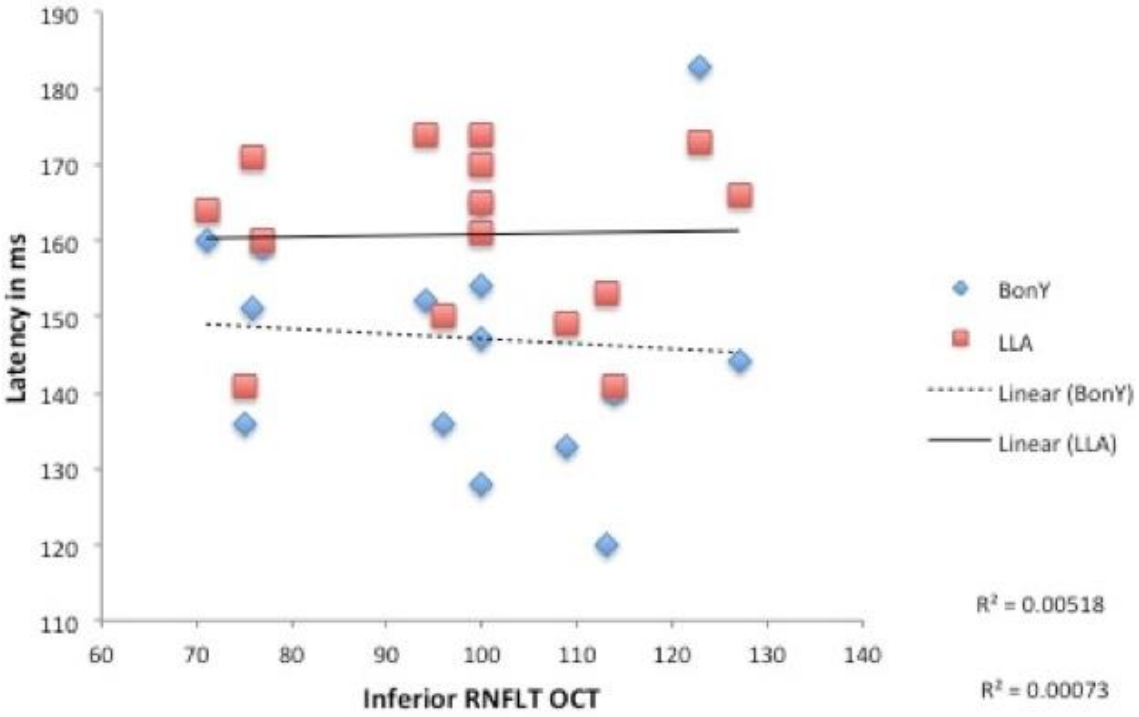

The association between BonY and LLA latencies with MD HVF and RNFLT OCT for superior and inferior hemifields were studied separately. Only the superior RNFLT of OCT showed a moderate negative correlation with the superior latencies of LLA mfVEP. All other hemifield correlations between the mfVEPs with HVF and OCT were weak.

4.6 Discussion

In this study, we investigated the possibility of baseline latencies of BonY and LLA mfVEP in detecting preperimetric glaucoma and predicting future progression of preperimetric glaucoma. Previous reports on VEP latency delays in glaucoma had been quite variable, with the usual understanding that latency delay would more likely reflect demyelination, while amplitude reduction reflects axonal loss. The study also set out to investigate the long-term changes in associated factors for structural and functional progression in patients with preperimetric glaucoma. The relationship between BonY and LLA mfVEP parameters with subjective perimetry tests and structural measures of glaucoma in progressors and non-progressors were also assessed.

4.6.1 Perimetric changes at baseline and progression rates:

There was a clear difference in the baseline indices of SAP, FDT and SWAP between the progressors and non-progressors. The MD of HVF and SWAP were significantly higher in the progressors but the MD of FDT did not show a significant difference. Long term changes in the mean deviation of HVF, FDT and SWAP were all significant in the progressive eyes. The change in the MD of HVF over the study duration (4.03 ± 1.03 years) was less than the average loss of about -2dB found in the EMGT study[250] but this change was statistically significant and agrees with the reasonable expectation for the MD to decrease in the progressive eyes. The end point for this study on preperimetric eyes was the subsequent development of a new scotoma on HVF as described in the Methods chapter. Mean deviation change in SWAP from baseline to the final visit was also interestingly significant in the non-progressive eyes. Studies indicate that SWAP defects progress faster than defects on SAP[96]. It is possible that these preperimetric eyes may develop subsequent visual field defects on SAP in the future. Similar to SWAP, FDT has also shown high sensitivity in the detection of early glaucoma[105,113,251] and has been reported to be a strong predictor of future glaucomatous damage for SAP[252,112,253]. Several studies indicate that there is a high diagnostic utility of FDP for glaucoma screening[254]. Patients with abnormal baseline FDT perimetry were approximately 9 times more likely to develop VF loss on SAP, consistent with previous

studies[111,252] and some longitudinal studies in glaucoma progression indicating that FDT can detect progression earlier than SAP[255]. Conflicting evidence was given by Sponsel et al.[256] who found that neither mean Deviation nor pattern deviation of FDT could categorize visual fields consistently. A study by Spry et al[257] suggested that FDT cannot be used confidently to monitor glaucoma progression. An earlier study by Kim et al. [258] showed no significant differences between SAP and FDT indices (MD and PSD) at baseline between progressors and non progressors.

4.6.2 Structural changes:

Average global, superior and inferior OCT RNFLT parameters were also significantly reduced in the progressive eyes at baseline. Although the progressive eyes had a further decline in the RNFLT over time, only the superior RNFLT had a significant (loss of over 9μm) between visits. Interestingly, the statistical significance of the difference in RNFLT between visits was higher in the non-progressive eyes conflicting with an earlier study by Medeiros et al[70] that showed that the mean rates of change in average RNFL thickness were significantly faster for eyes with progressive disease compared to non-progressors. This is possibly because of greater number of eyes (progressive eyes n=15, non-progressive eyes n=45) even though the actual difference in thickness was similar or lower than progressors. These results concur with earlier studies[33,68] that indicate that thinner OCT RNFLT measurements at baseline are associated with development of visual field defects in preperimetric eyes and that RNFL is an ideal independent predictor of glaucomatous change and progression. There was no difference in the mean RNFL values of HRT between progressors and non-progressors or over time between the two groups indicating that OCT RNFLT had a higher sensitivity than HRT measurements and in agreement with an earlier study by Leung et al[259].

4.6.3 mfVEP changes:

The Blue on yellow mfVEP technique has previously been described as having significantly better sensitivity in identifying glaucomatous field loss[169,193]. A later report indicated that the sensitivities of BonY and LLA mfVEP in early glaucoma were comparable and the ASI of both the mfVEP tests were also similar[199]. No comparison has yet been made between the

amplitude and latency of these two tests and in different subgroup of subjects. This is the first study to compare the parameters between these two mfVEP techniques.

The average baseline BonY and LLA mfVEP parameters were compared between the progressive and non-progressive eyes. The average baseline BonY amplitude was significantly reduced in the progressors (~70nV) and the LLA amplitude was ~ 100nV smaller in the same group. Both the decrease in local visual field sensitivity and local mfVEP signal amplitude is proportional to local ganglion cell loss[159, 260]. MfVEP amplitude reductions in preperimetric eyes has been reported and differences between amplitudes of eyes with asymmetric disease has also been previously noted[156]. Our study results were in agreement with the earlier study. Comparison of the baseline amplitudes between BonY and LLA mfVEP that the LLA mfVEP amplitudes were significantly lower than that of BonY (P = 0.0034).

The baseline latencies were compared between the two groups. Although there was a difference of 8ms between the average latency of BonY between the progressors and non-progressors (the progressors had a longer latency), this difference was statistically insignificant. The difference between the LLA mfVEP latency of both groups was only 3ms. The LLA mfVEP had much longer latencies compared to BonY mfVEP in each group (P = 0.0002). Latency delay of BonY mfVEP in glaucoma has been reported[138, 139]. The better performance of LLA mfVEP may be due to the fact that the low luminance contrast rather than its chromatic counterparts stimulating the koniocellular pathway stimulated magnocellular neurons.

Results indicate that even though the latency of mfVEP was delayed significantly in preperimetric glaucoma[193], the mfVEP latency cannot be used as an early indicator for functional visual loss or determining progression of glaucoma as hypothesized earlier. Furthermore, the relationship between the MD HVF and OCT RNFLT and the mfVEP latencies for BonY and LLA stimuli were weak. The BonY and LLA amplitudes had a significant association with both MD HVF and MD OCT in the 60 preperimetric eyes in line with earlier studies that have established the linear relationship between mfVEP amplitude and subjective perimetry[260]. The hemifield latencies and amplitudes had a poor correlation with MD HVF and OCT RNFLT in the progressive eyes indicating that there was no relationship between the hemifield with delayed latency and the topography of the defect location on HVF based on MD.

The study was unfortunately limited by the lack of follow up data for both the mfVEP amplitudes and latencies. The ability to examine for longitudinal changes in mfVEP responses

was lost because of the technical problem stated in the Methods chapter, and a large amount of follow-up mfVEP data had to be disregarded. The long-term changes in the amplitudes and latencies of BonY and LLA mfVEP could not be established in controls due to the same reason. In the analysis only peak to trough amplitudes were considered. Signal to Noise ratios (SNR) have been shown to be a useful criteria for evaluating mfVEP records of poor quality[163] but were not considered in this as they do not provide a latency value.

To conclude, the latencies of BonY and LLA mfVEP cannot be used as indicators for prediction future progression of glaucoma and its associated functional visual loss. However, amplitudes are true indicators of glaucomatous functional loss with a linear relationship with subjective visual field testing. The LLA mfVEP seems to be a better and stronger indicator of early glaucomatous loss both in terms of functional visual loss and its association with other structural parameters and subjective perimetry.

CHAPTER 5

STRUCTURAL AND FUNCTIONAL CORRELATES IN PRE-PERIMETRIC GLAUCOMA: APPLICATION TO EARLY DETECTION

5.1 Introduction

Early detection is one of the most important and challenging aspects of glaucoma management. Documenting progression is also extremely important as it may signal the need for modification of treatment strategies to prevent visual field loss. Glaucoma progression can be assessed both structurally and functionally. Structural tests are more objective and not dependent on patient responses. But establishing a functional loss corresponding to the structural changes strengthens the diagnosis. Objective perimetry using multifocal VEP is reported as a reliable method to assess functional visual loss in glaucoma[180, 147]. The use of novel stimulus presentations using the Blue-on-yellow stimulus (targeting the koniocellular pathway based on sparse stimulus presentation) and the Low Luminance Achromatic stimulus (targeting the magnocellular pathway) have been previously reported [193, 199]. Sriram et al[200] established that LLA mfVEP identified preperimetric glaucoma than other perimetric methods and a combination of LLA mfVEP and HRT was found to have a very high sensitivity for preperimetric glaucoma.

5.2 Aim

The aim of this part of the study is to evaluate the combination of structural and functional parameters, which will optimally detect early glaucoma effectively thereby facilitating early intervention to prevent loss of vision. Calculating the Positive Predictive Values (PPV) and Negative Predictive Values for combination of structural and functional tests will help in predicting the future glaucomatous defects from baseline structural and functional tests.

5.3 Methods

Early glaucoma patients with normal visual fields were recruited for this study from a private eye clinic in Sydney. Glaucoma diagnosis was made prior to the study based on the glaucomatous cupping of the optic disc, as judged by stereoscopic ophthalmoscopy. The subjects had at least one glaucomatous optic disc and normal, reliable visual fields in that eye. Inclusion and exclusion criteria, abnormality criteria of subjective and objective perimetry tests, benchmarks for determining progression for the structural and functional tests in glaucoma have all been detailed in the Methods chapter 2.

The mean follow up period for the cohort was 4.03 ± 1.03 years. At the end of the follow-up period the eyes that had progression was determined on the basis of the appearance of a repeatable visual field defect on HVF. Any new defect was confirmed with testing on a subsequent visit. In a previously normal region of the field, on two or more reliable tests, the existence of a new isolated defect could be taken as evidence for progression. Criteria for a new defect include a cluster of three points worsening by 5dB each, one of which has worsened by 10dB. The non-progressives continued to have a normal HVF throughout the study period despite changes to other structural and functional parameters.

The criteria for all abnormal structural and functional test parameters have been outlined in the Methods Chapter. For the progressive and non-progressive groups, the number of eyes that showed abnormality at baseline for each individual test and combination of tests were identified. Baseline defects in progressive and non-progressive eyes for each test was done. Topographic correspondence of the baseline defects was matched with the final RNFL changes on OCT and HVF.

5.4 Analysis

Performance metrics was determined for the structural (OCT) test, objective perimetry tests (BonY and LLA mfVEP) and subjective perimetry tests (SWAP, FDT). Performance metrics composed of true positive (TP) which indicate an abnormal baseline test that correctly identified defect (progressed), false positive (FP) in which negative instances (no progression) incorrectly flagged as abnormal, true negative (TN) which are negative instances correctly identified as negative (baseline test normal with no progression at the end of the study period)

and finally false negative (FN) which are normal baseline tests but the eye developed a visual field defect (progressive) at the end of the study period. Sensitivity and specificity were determined for each test or combination of tests based on the performance metrics.

Sensitivity (True Positive rate) is defined as the ratio of TPs and the total number of positives. Sensitivity = TP / TP + FN. Specificity (True Negative rate) is defined as the ratio of TNs and the total number of negatives. Specificity = TN / TN + FP. The sensitivity and specificity rates were then used to calculate the Positive Predictive Value (PPV) and Negative Predictive Value (NPV) for individual tests as well as combinations. Assuming that the prevalence of early glaucoma among referrals for suspect discs is roughly two of five or 40%, PPV and NPV were calculated for that prevalence. Sensitivity, specificity, PPV and NPV were all calculated using the contingency table analyses on Prism 7, Graphpad Inc. using Wilson/Brown method (CI 95%) and P value calculated using Fisher's exact test.

5.5 Results

Of the 60 preperimetric eyes recruited in the analysis, 15 (25%) eyes of 13 subjects progressed to develop a repeatable defect on HVF at the end of the study period. The mean age of those that progressed was 63.76 ± 5.96 years (9 male and 4 female). The average HFA MD of the progressive eyes in the final visit was -1.57 ± 2.03dB, average MD on SWAP was 0.53 ± 3.82 dB, and on FDT it was -2.40 ± 3.73 dB.

45 eyes (75%) of 33 subjects remained preperimetric for the entire duration of the study. The mean age of those that had a normal and stable HVF was 62.33 ± 6.22 years (18 male and 15 female). The average HFA MD of the non-progressive eyes in the final visit was 0.17 ± 1.14 dB, average MD on SWAP was 0.69 ± 3.20 dB, and on FDT it was -0.40 ± 3.61 dB. There was no significant difference in age between the progressive and the non-progressive patients (P = 0.599).

Table 5.1 summarizes the sensitivities of all the diagnostic tests. LLA mfVEP exhibited the best sensitivity in identifying patients with progression. P value compared to LLA mfVEP was calculated using McNemar's test.

Table 5.1: Sensitivity of tests in progressive eyes (n=15). *P value* compared to LLA using McNemar's test (95% CI)*

Test	Sensitivity, n (%)	P Value*	Topographic Correspondence with final HVF defect
LLA mfVEP	12 (80%)	-	83%
BonY mfVEP	9 (60%)	0.371	56%
SWAP	5 (33.3%)	0.023	80%
FDT	6 (40%)	0.0412	100%
OCT	6 (40%)	0.013	80%

Both LLA mfVEP and BonY mfVEP are more sensitive to glaucomatous progression compared to the subjective perimetry tests and the structural test of OCT. SWAP had the lowest sensitivity while both FDT and OCT were comparable. The baseline defects identified by FDT corresponded 100% with those that developed on HVF over the course of the study. BonY had the lowest topographic correspondence at 56%. LLA, SWAP and OCT were comparable at 83%, 80% and 80% respectively.

Table 5.2a and 5.2b show the sensitivities, specificities, positive and negative predictive values for individual tests and combination of tests with a CI of 95%. While the sensitivity of LLA was the highest, it also had the lowest specificity. Both FDT and SWAP had a high specificity and was also comparable. Of the 15 eyes that progressed, 8 (53.3%) eyes were positive on LLA, BonY and OCT. This was the maximum number of eyes that were identified for any combination of functional tests with OCT (positive on any one or more tests).

Combination of one structural test with one functional test was assessed in an effort to increase the diagnostic performance to predict progression of glaucomatous damage. The combination of tests was considered positive if any one of the tests yields a positive result. When combining two tests, a combination of OCT and LLA mfVEP gave the highest percentage of eyes identified as progressive (73%) but the specificity of this combination was the lowest among all individual tests and test combinations.

Table 5.2 a: Sensitivity, Specificity, Positive and Negative Predictive Values of individual tests (95% CI). **PPV and NPV calculated for prevalence of 40% and 25%*

Test	Sensitivity n (%)	Specificity %	PPV*	NPV*	PPV (25%prevalence)	NPV (25%prevalence)
OCT	6 (40%)	71.1	0.42	0.68	0.33	0.55
LLA mfVEP	12 (80%)	51.1	0.47	0.82	0.36	0.68
BonY mfVEP	9 (60%)	71.1	0.35	0.64	0.27	0.52
FDT	6 (40%)	77.7	0.49	0.70	0.40	0.59
SWAP	5 (33.3%)	77.7	0.45	0.70	0.35	0.58

Table 5.2b: Sensitivity, Specificity, Positive and Negative Predictive Values for combination of tests (95% CI). **PPV and NPV calculated for prevalence of 40%*

Test	Sensitivity n (%)	Specificity %	PPV*	NPV*
OCT+LLA	11(73%)	31.1	0.56	0.86
OCT+BonY	10 (66.6%)	42.2	0.30	0.70
OCT+FDT	9 (60%)	48.8	0.58	0.75
OCT+SWAP	9 (60%)	53.3	0.54	0.73
OCT+LLA+FDT	12 (80%)	42.2	0.71	0.87
OCT+BonY+SWAP	10 (66.6%)	46.6	0.37	0.72
OCT+FDT+SWAP	9 (60%)	55.5	0.63	0.85
OCT+LLA+FDT+SWAP	12 (80%)	40	0.69	0.87
OCT+BonY+FDT=SWAP	10 (66.6%)	40	0.38	0.74

Positive and negative predictive values were calculated for the individual tests as well as combinations. PPV and NPV were calculated for the prevalence of 40% assuming that the prevalence of preperimetric glaucoma among referrals for suspect discs is roughly two of five. Among individual tests, FDT had the highest PPV (49.4%) while LLA (47%) and OCT (42.9%) were close enough. Positive and Negative predictive values have also been calculated for 25%. The best Positive Predictive Value (71%) and the best Negative Predictive value (87%) was seen for the combination of OCT + LLA + FDT Matrix. For a combination of one structural and one functional test, the best NPV (86%) was for LLA and OCT.

Figures 5.1 and 5.2 show the Venn diagram combinations of positivity for all the tests for progressive and non-progressive groups.

Figure 5.1: Comparison of the positive tests in eyes that progressed on SAP

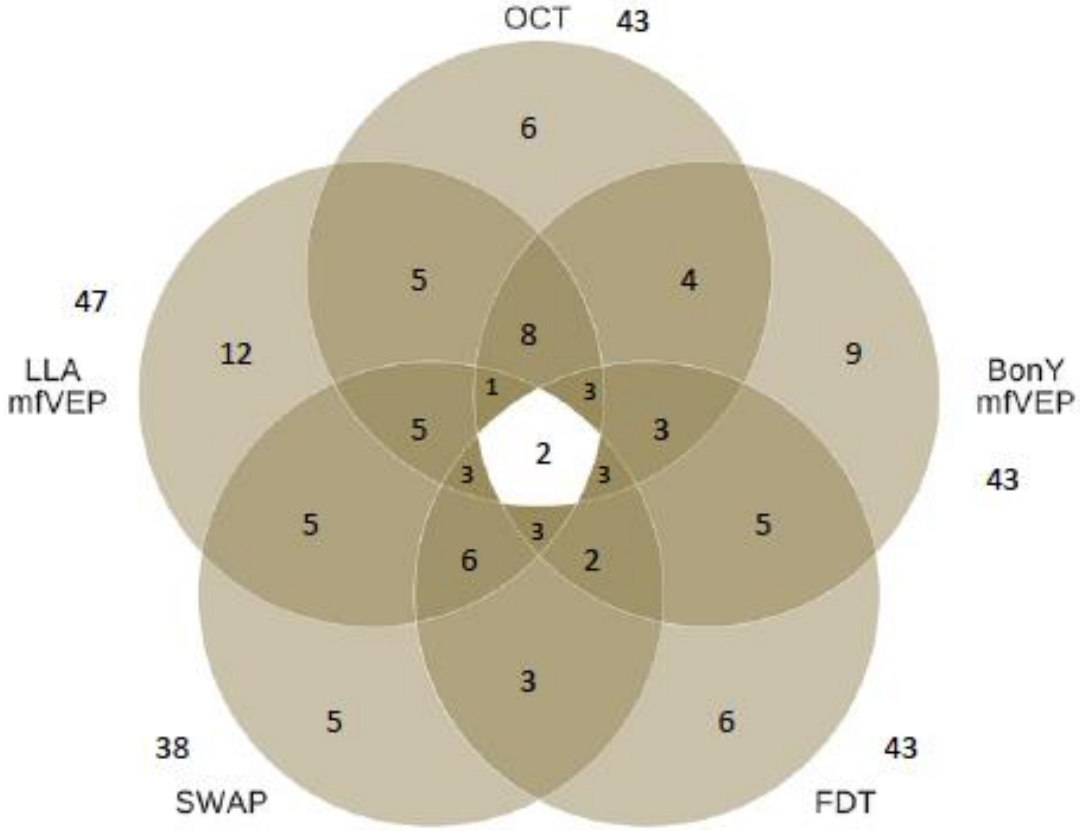

Figure 5.2: Comparison of the positive tests in non-progressive eyes

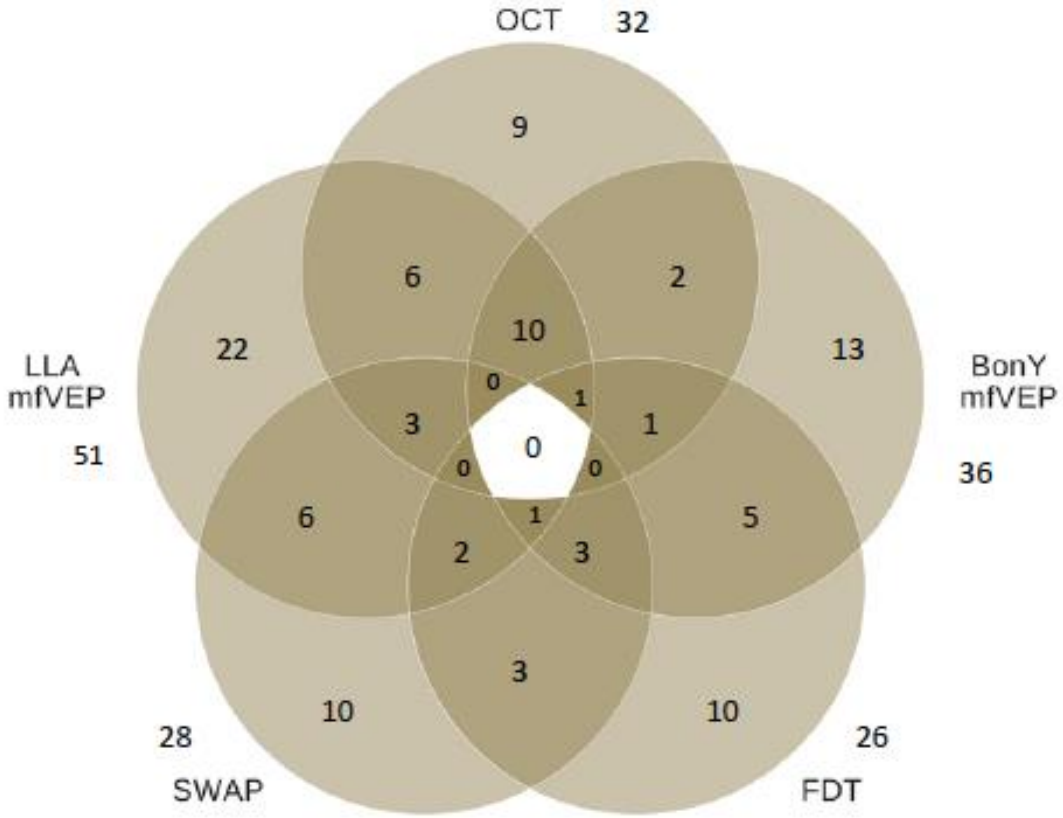

Fig 5.3 Example of progression on HVF as shown by the overview report

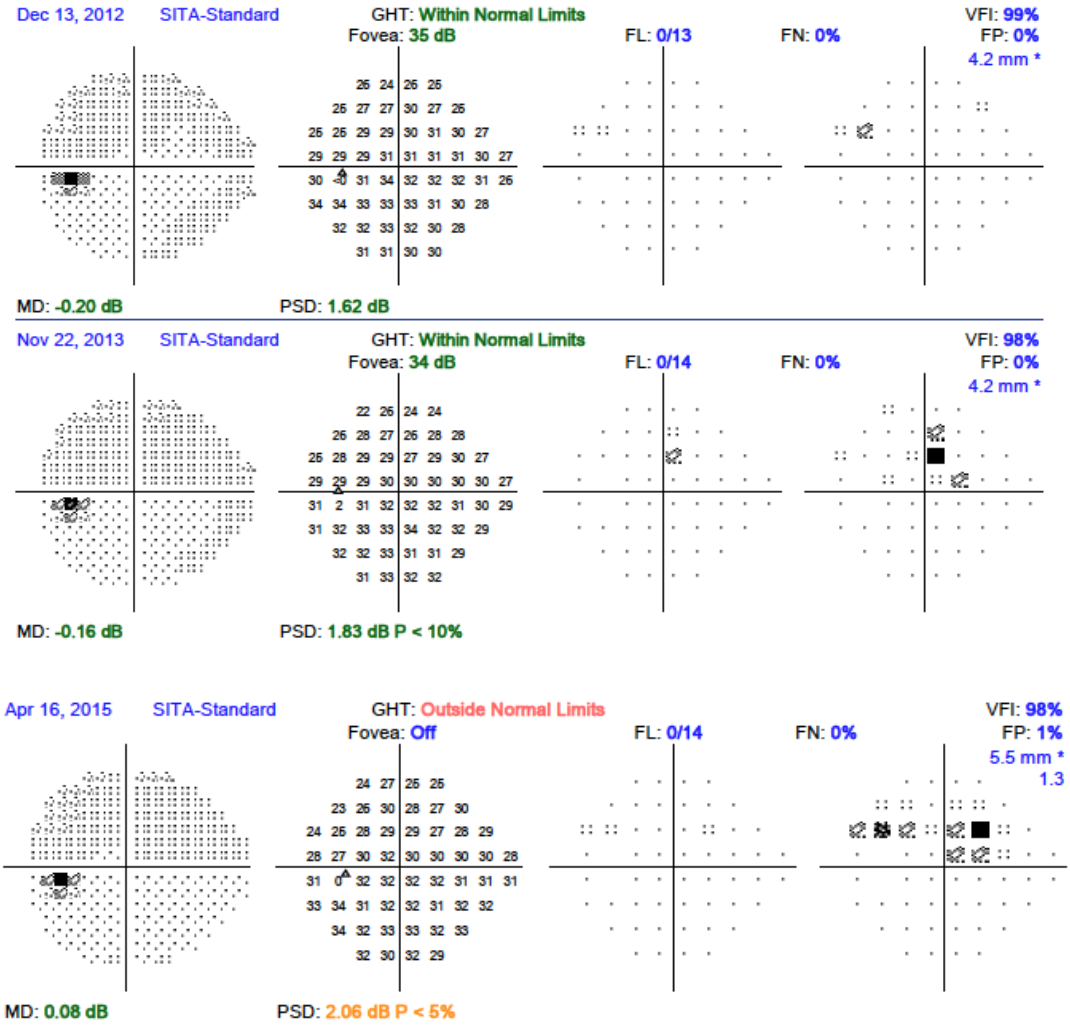

Fig 5.4: Example of subject with baseline abnormality showing progression on FDT

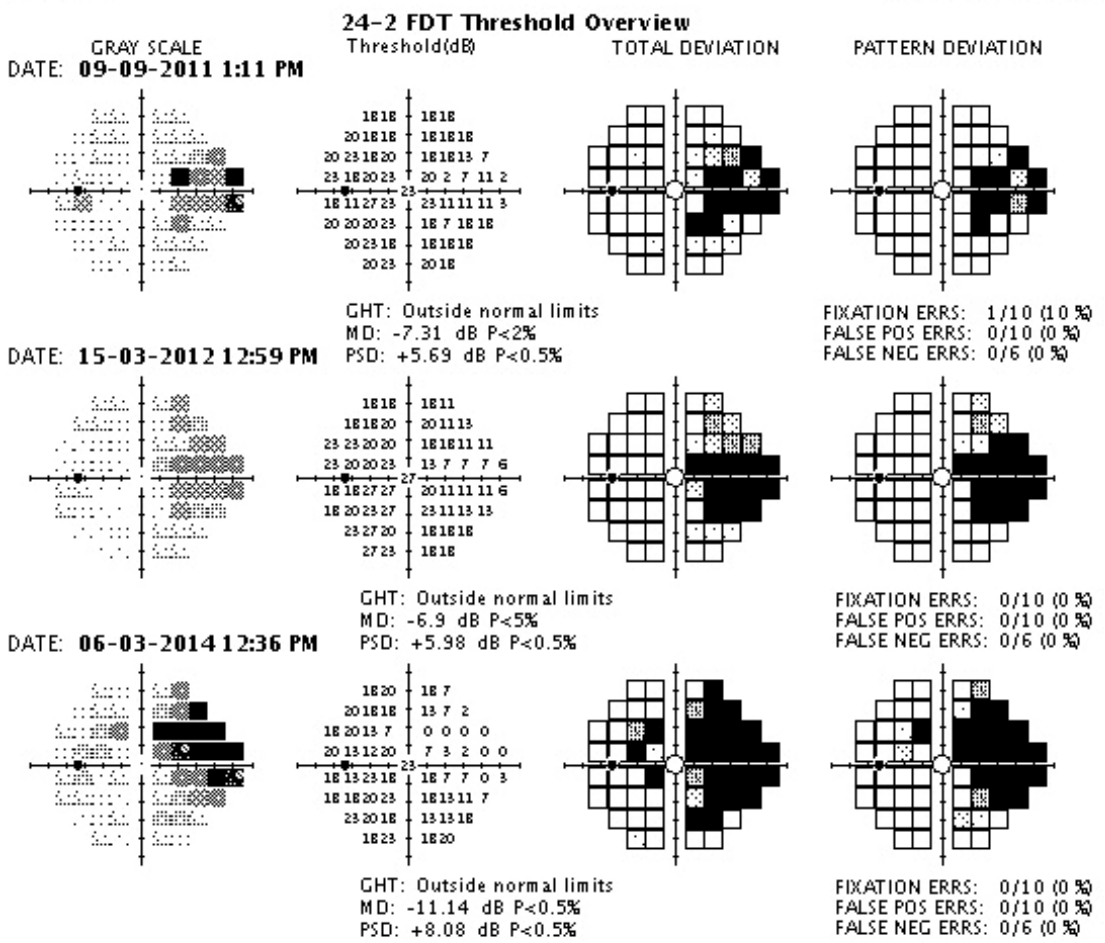

Fig 5.5: Example of subject with baseline abnormality showing progression on SWAP

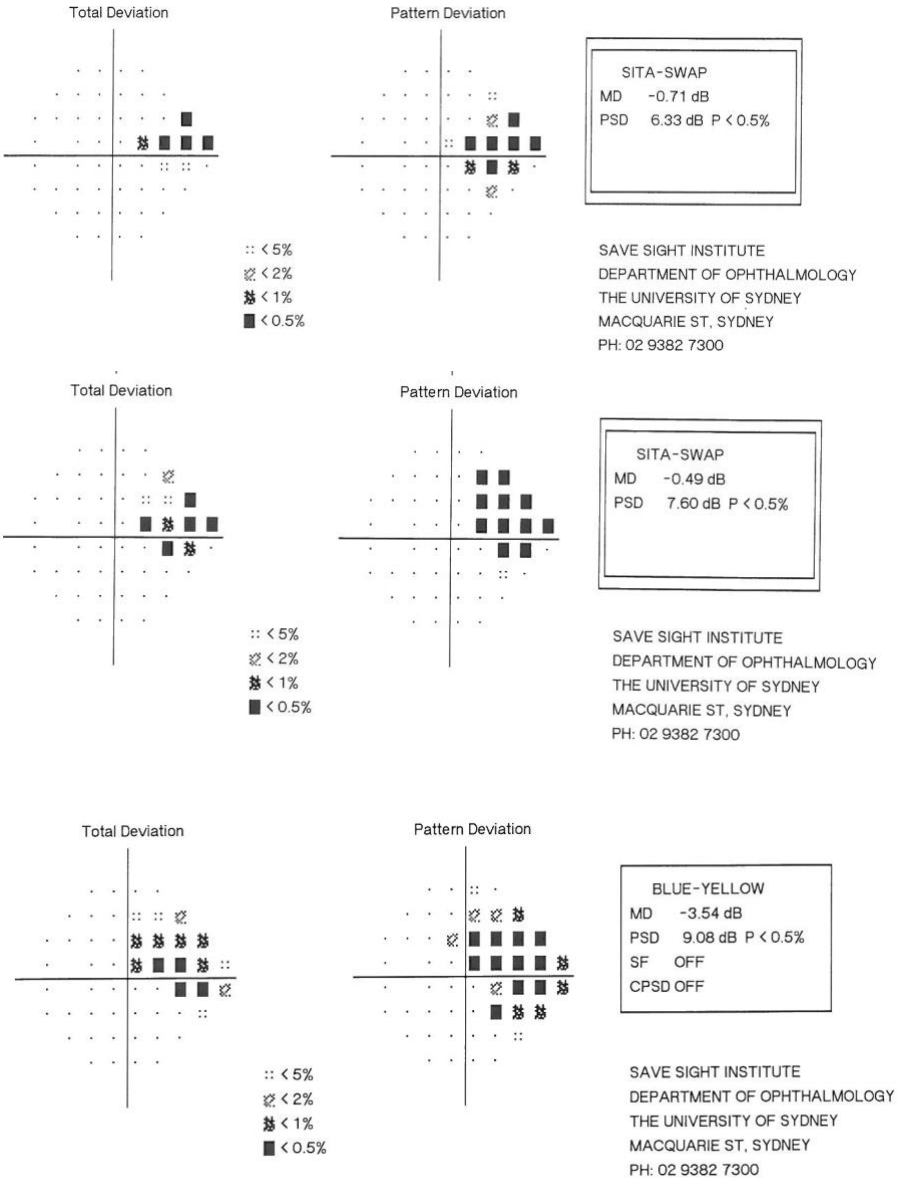

Figure 5.3 shows progression of visual field defects from preperimetric at baseline. Figures 5.4 and 5.5 show progression of visual field loss on FDT and SWAP respectively for subjects who had baseline defects in these two tests.

5.6 Discussion

Many studies have examined the association of structural and functional measures of glaucoma to understand better the nature of the disease and to evaluate and compare different clinical measures. Documented progression of glaucoma may require modification of treatment strategies to prevent loss of vision. However, determining progression is one of the most important and challenging aspects of management. Progression of glaucoma can be assessed with both structural and functional tests. This chapter compares the performance of LLA mfVEP and BonY mfVEP amplitudes in predicting subsequent progression in isolation and in combination of other structural and functional tests. The previous chapter showed no significant changes in latency so this was not considered as part of this analysis.

Our research group previously investigated LLA mfVEP[200] and BonY mfVEP[193] in preperimetric glaucoma. LLA was abnormal in 43% and BonY in 50% of preperimetric glaucoma cases. The advance of the current longitudinal study indicates that LLA mfVEP also has a very high sensitivity in flagging eyes that have the potential to progress over time. Recent advancements in OCT have resulted in increased reproducibility and accuracy in the assessment of progressive damage to RNFL and ONH and macula affected by glaucomatous damage[261, 262]. A study by Wollstein et al.[65] concluded that there was a greater likelihood of detecting glaucomatous progression with OCT compared to standard HVF. Mean rates of change in RNFL thickness measurements of OCT were significantly faster for progressive disease compared to non-progressors[263,264,265]. OCT is also more likely to detect progression in the preperimetric settings far greater than identifying disease worsening at advanced stages[71]. In this study, the sensitivity of LLA in progressors was even higher than that of OCT as a baseline predictor. This result agrees with earlier studies that indicate that structural measures like OCT may not be more sensitive than a functional test, depending on the underlying relationship between structure and function and the relative variability of each test[266]. Unfortunately, due to the change in amplifiers, this study was not able to compare longitudinal mfVEP results with OCT or VF progression rates, which had been part of the original study design.

. LLA mfVEP also outperformed BonY mfVEP in sensitivity. The preferential stimulation of the magnocellular pathway compared to the koniocellular pathway may support the performance of using an LLA stimulus[197, 242, 164, 267, 21].

Among non-progressors, LLA mfVEP also shows the highest rate of test positives. While these could represent false positives, it is possible that these patients may develop defects indicating progression on HVF over time. Chauhan et al.[268] estimated that even with 3 tests per year, a -4dB loss would be needed for detection in 2 years assuming a moderate amount of variability. Certainly many of these subjects showed some possible changes but these did not reach our criteria for progression.

Several studies indicate that OCT is an excellent test to measure structural change and progression associated with glaucoma, but also the device outperforms HRT II in this aspect. A study by Suda et al.[269] indicates that longitudinally detectable progressive glaucoma changes were detectable with VF testing and SD-OCT but not with HRT II. The test-retest variability also is known to inhibit the ability to detect glaucoma progression[268] which may explain why HRT II indices had a lower ability to detect glaucoma progression. Sensitivity of RNFL damage detection using HRT II is found to be lower than OCT and OCT had a much lower measurement error than HRT with less variability of measurements[270,271].

For these reasons, we considered OCT as the gold standard for assessing RNFL change associated with progression in preperimetric glaucoma and all combination of functional tests were done in combination with OCT as the structural parameter. The combination of one structural and one functional test is common practice in glaucoma clinics around the world and is realistic in most clinical situations. For this reason, combination of functional tests with OCT as the structural parameter was used to maximize sensitivity.

The combination of OCT and LLA yields the highest sensitivity (73%) for one structural and one functional parameter and OCT + LLA + FDT had the highest sensitivity (80%) for the combination of one structural, one subjective and one objective perimetry test. This combination also had the highest PPV and NPV amongst all combination of tests. In addition, FDT had the highest (100%) percentage of topographic correlation with the final HFV defect. LLA mfVEP and OCT were not far behind at 83% and 80% respectively. Abnormal defects on global, superior or inferior hemifields were considered as a defect on OCT. This could have significantly increased the sensitivity of the OCT test. For both LLA and BonY mfVEP, a defect on either amplitude deviation or asymmetry deviation was considered as an abnormality. Adding a fourth study to the combination of tests did not increase the sensitivity. Adding SWAP to the combination of OCT + FDT + LLA increases the PPV to

85.7%. PPV and NPV are important because identifying those who will remain stable is as important as recognizing progressors.

Stereo photographs of the optic disc were not used as a measure for assessing progression. A recent study, even when three glaucoma specialists agreed, there was a 40% false-positive rate indicating that stereo photographs are not a good standard for assessing progression[272].

The major limitation of this study was the lack of longitudinal data for the mfVEP to determine if functional change was in fact correctly identified objectively, and further progressed in those showing subjective progression. Subsequent studies will have to address this. The study does have longitudinal data on the other perimetric and structural measures, and has been able to confirm the utility of these tests.

In conclusion, the objective perimetry test of LLA mfVEP combined with OCT represented the best combination of tests both to identify preperimetric glaucoma as indicated earlier [200] and to predict subsequent progression of glaucoma. The clinician has to also consider the tradeoffs between sensitivity and specificity while combining tests. Sensitivity will increase and specificity will decrease because of greater probability of results being outside the normal limits for the combination compared with individual tests.

CHAPTER 6

CONCLUSIONS AND FUTURE DIRECTIONS

This thesis sought to address the hypothesis that both BonY mfVEP and LLA mfVEP show the potential to detect functional visual loss associated with early glaucoma prior to changes on SAP, and further establish that scotomas detected by BonY and LLA mfVEP reflect local structural and functional glaucomatous defects as detected by visual field testing and imaging techniques. In addition to this, the thesis proposed that a combination of specialized mfVEP technique and structural imaging was beneficial in identifying early glaucomatous changes and detecting progression thereby enabling a confident treatment plan to prevent irreversible vision loss.

Chapter 3 aimed at addressing the research questions related to the performance of the subjective and objective perimetry tests based on the magnocellular pathway: Frequency Doubling Perimetry (FDP) and the Low Luminance Achromatic multifocal VEP (LLVEP), and the performance of tests based on the koniocellular pathway: Short Wavelength Automated Perimetry (SWAP) and Blue on Yellow multifocal VEP (BonY mfVEP). The aim was to further determine if one pathway is superior to the other at detecting glaucomatous damage on both objective and subjective measures. The study demonstrated that objective perimetry tests (LLA and BonY) had a marginally higher detection rate of abnormality compared to subjective perimetry tests (SWAP and FDT). This applied to both koniocellular and magnocellular based testing. The correlation of the subjective and objective tests based on the magnocellular pathway namely LLA mfVEP and FDT was significantly better compared to those of the koniocellular pathway (BonY and SWAP).

Chapter 4 intended to assess if latency delay of LLA and BonY mfVEP can be an early indicator of future glaucoma progression and to establish a relationship between the baseline latencies and amplitudes of BonY and LLA mfVEP tests with other functional and structural measures of glaucoma (Mean Deviation of the SAP and the RNFL thickness measured with OCT).

The plan was also to establish the relationship between the baseline latencies and amplitudes of BonY and LLA mfVEP tests with other functional and structural measures of glaucoma (Mean Deviation of the SAP and the RNFL thickness measured with OCT). The results indicate that latencies of BonY and LLA mfVEP cannot be used as ideal indicators for prediction of future progression of glaucoma and its associated functional visual loss. The amplitudes as indicated in earlier studies are true indicators of glaucomatous functional loss with a more linear relationship with subjective visual field testing. The LLA mfVEP seems to be a better and stronger indicator of early glaucomatous loss both in terms of functional visual loss and its association with other structural parameters and subjective perimetry.

Chapter 5 examined the combination of structural and functional parameters, which will optimally detect early glaucoma and also monitor progression effectively. The study looked at predicting future glaucomatous defects from baseline structural and functional tests by calculating the Positive Predictive Values (PPV) and Negative Predictive Values for combination of structural and functional tests. The objective perimetry test of LLA mfVEP combined with OCT emerged as an ideal combination of tests both to identify preperimetric glaucoma and to predict progression of glaucoma much earlier than other structural or functional tests. This combination could also be a clinically relevant and feasible option to monitor glaucoma progression.

The main limitation of the study was the lack of follow-up data for both LLA mfVEP and BonY mfVEP both in controls and in glaucoma subjects. A major technical issue with the mfVEP recording device rendered all the collected follow-up data unusable. This was a major setback for this study and it removed the longitudinal mfVEP data from all analyses.

Future work following on from this thesis involves long term prospective studies for LLA mfVEP in both normal controls and in early glaucoma with a newer and faster mfVEP system. This would help us determine the long-term changes in the mfVEP and how these correlate with the structural changes on high resolution OCT. The recent development of OCT angiography means it will also be possible to study localize vascular changes at the optic nerve head and macular regions to see if these correlate with functional and structural losses. .

While it is still controversial that any particular pathway is preferentially affected early in glaucoma, this study seemed to favor a magnocellular test strategy. The clinician is currently faced with a wide variety of tests, and it is not practical to apply all tests to individual patients. It is however easy to apply a single specialized mfVEP strategy in addition to conventional VF testing, and when combined with OCT imaging in glaucoma clinics this could help identify and prevent glaucomatous damage and subsequent vision loss.

Bibliography

1. Ng JS. Adler's Physiology of the Eye (11th ed.). *Optom Vis Sci*. 2012;89(4):E513. doi:10.1097/OPX.0b013e318253c8a6.

2. Reese BE. Development of the Retina and Optic Pathway. *Vision Res*. 2010;51(7):613-632. doi:10.1016/j.visres.2010.07.010.

3. Weale R a. *The Vertebrate Retina. Principles of Structure and Function*. Vol 58. 1974. doi:10.1136/bjo.58.11.948-c.

4. Solomon SG, Lee BB, White AJR, et al. The retinal pigment epithelium in visual function. *Physiol Rev*. 2005;85(1):85-98. doi:10.1152/physrev.00021.2004.

5. Radius RL, Anderson DR. The histology of retinal nerve fiber layer bundles and bundle defects. *Arch Ophthalmol*. 1979;97(5):948-950. doi:10.1001/archopht.1979.01020010506027.

6. Minckler DS. The organization of nerve fiber bundles in the primate optic nerve head. *Arch Ophthalmol*. 1980;98(9):1630-1636. doi:10.1001/archopht.1980.01020040482019.

7. Reis ASC, Sharpe GP, Yang H, Nicolela MT, Burgoyne CF, Chauhan BC. Optic disc margin anatomy in patients with glaucoma and normal controls with spectral domain optical coherence tomography. *Ophthalmology*. 2012;119(4):738-747. doi:10.1016/j.ophtha.2011.09.054.

8. Garway-Heath DF, Hitchings R a. Quantitative evaluation of the optic nerve head in early glaucoma. *Br J Ophthalmol*. 1998;82:352-361. doi:10.1136/bjo.82.4.352.

9. Jonas JB, Fernández MC, Stürmer J. Pattern of glaucomatous neuroretinal rim loss. *Ophthalmology*. 1993;100(1):63-68. doi:10.1016/S0161-6420(13)31694-7.

10. Field GD, Chichilnisky EJ. Information processing in the primate retina: circuitry and coding. *Annu Rev Neurosci*. 2007;30:1-30. doi:10.1146/annurev.neuro.30.051606.094252.

11. Weber AJ, Harman CD. Structure-function relations of parasol cells in the normal and

glaucomatous primate retina. *Investig Ophthalmol Vis Sci*. 2005;46(9):3197-3207. doi:10.1167/iovs.04-0834.

12. Watanabe M, Rodieck RW. Parasol and midget ganglion cells of the primate retina. *J Comp Neurol*. 1989;289:434–454. doi:10.1002/cne.902890308.

13. Kaplan E. The P, M and K Streams of the Primate Visual System: What Do They Do for Vision? In: *The Senses: A Comprehensive Reference*. Vol 1. ; 2010:369-381. doi:10.1016/B978-012370880-9.00274-7.

14. Jacoby R, Stafford D, Kouyama N, Marshak D. Synaptic inputs to ON parasol ganglion cells in the primate retina. *J Neurosci*. 1996;16(24):8041-8056.

15. Schiller PH, Colby CL. The responses of single cells in the lateral geniculate nucleus of the rhesus monkey to color and luminance contrast. *Vision Res*. 1983;23(12):1631-1641. doi:10.1016/0042-6989(83)90177-3.

16. Lee BB, Pokorny J, Smith VC, Martin PR, Valberg A. Luminance and chromatic modulation sensitivity of macaque ganglion cells and human observers. *J Opt Soc Am A*. 1990;7(12):2223-2236. doi:10.1364/JOSAA.7.002223.

17. Livingstone MS, Hubel DH. Psychophysical evidence for separate channels for the perception of form, color, movement, and depth. *J Neurosci*. 1987;7(11):3416-3468.

18. Lynch JJ, Silveira LC, Perry VH, Merigan WH. Visual effects of damage to P ganglion cells in macaques. *Vis Neurosci*. 1992;8(6):575-583. doi:10.1017/S0952523800005678.

19. Merigan WH. Chromatic and achromatic vision of macaques: role of the P pathway. *J Neurosci*. 1989;9(3):776-783.

20. Schiller PH, Logothetis NK, Charles ER. Parallel pathways in the visual system: Their role in perception at isoluminance. *Neuropsychologia*. 1991;29(6):433-441. doi:10.1016/0028-3932(91)90003-Q.

21. Hendry S, Reid C. The Koniocellular Pathway in Primate Vision. *Annu Rev Neurosci*. 2000;23:127-153. doi:10.1146/annurev.physiol.66.032102.111604.

22. Shostak Y, Ding Y, Casagrande VA. Neurochemical comparison of synaptic arrangements of parvocellular, magnocellular, and koniocellular geniculate pathways in owl monkey (Aotus trivirgatus) visual cortex. *J Comp Neurol*. 2003;456(1):12-28.

doi:10.1002/cne.10436.

23. Xu X, Ichida JM, Allison JD, Boyd JD, Bonds AB, Casagrande VA. A comparison of koniocellular, magnocellular and parvocellular receptive field properties in the lateral geniculate nucleus of the owl monkey (Aotus trivirgatus). *J Physiol*. 2001;531(1):203-218. doi:10.1111/j.1469-7793.2001.0203j.x.

24. Szmajda BA, Gr??nert U, Martin PR. Retinal ganglion cell inputs to the koniocellular pathway. *J Comp Neurol*. 2008;510(3):251-268. doi:10.1002/cne.21783.

25. Telkes I, Lee SCS, Jusuf PR, Gr??nert U. The midget-parvocellular pathway of marmoset retina: A quantitative light microscopic study. *J Comp Neurol*. 2008;510(5):539-549. doi:10.1002/cne.21813.

26. Jusuf PR, Martin PR, Gr??nert U. Synaptic connectivity in the midget-parvocellular pathway of primate central retina. *J Comp Neurol*. 2006;494(2):260-274. doi:10.1002/cne.20804.

27. De Monasterio FM, Gouras P. Functional properties of ganglion cells of the rhesus monkey retina. *J Physiol*. 1975;251(1):167-195. doi:10.1113/jphysiol.1975.sp011086.

28. Schiller PH, Malpeli JG. Functional specificity of lateral geniculate nucleus laminae of the rhesus monkey. *J Neurophysiol*. 1978;41(3):788-797.

29. Nassi JJ, Callaway EM. Parallel processing strategies of the primate visual system. *Nat Rev Neurosci*. 2009;10(5):360-372. doi:10.1038/nrn2619.

30. Mitchell P, Smith W, Attebo K, Healey PR. Prevalence of Open-angle Glaucoma in Australia. *Ophthalmology*. 1996;103(10):1661-1669. doi:10.1016/S0161-6420(96)30449-1.

31. Kerrigan-Baumrind LA, Quigley HA, Pease ME, Kerrigan DF, Mitchell RS. Number of ganglion cells in glaucoma eyes compared with threshold visual field tests in the same persons. *Investig Ophthalmol Vis Sci*. 2000;41(3):741-748.

32. Quigley HA, Dunkelberger GR, Green WR. Retinal ganglion cell atrophy correlated with automated perimetry in human eyes with glaucoma. *Am J Ophthalmol*. 1989;107(5):453-464. doi:10.1016/0002-9394(89)90488-1.

33. Lalezary M, Medeiros FA, Weinreb RN, et al. Baseline Optical Coherence Tomography Predicts the Development of Glaucomatous Change in Glaucoma

Suspects. *Am J Ophthalmol*. 2006;142(4). doi:10.1016/j.ajo.2006.05.004.

34. Kass MA, Heuer DK, Higginbotham EJ, et al. The Ocular Hypertension Treatment Study: a randomized trial determines that topical ocular hypotensive medication delays or prevents the onset of primary open-angle glaucoma. *Arch Ophthalmol*. 2002;120(6):701-713-830. doi:10.1001/archopht.120.6.701.

35. Sample PA, Madrid ME, Weinreb RN. Evidence for a variety of functional defects in glaucoma-suspect eyes. *J Glaucoma*. 1994;3 Suppl 1:S5-S18. doi:10.1097/00061198-199400321-00003.

36. Leske MC, Heijl A, Hyman L, Bengtsson B. Early manifest glaucoma trial. *Ophthalmology*. 1999;106(11):2144-2153. doi:10.1016/S0161-6420(99)90497-9.

37. Heron G, Adams a J, Husted R. Central visual fields for short wavelength sensitive pathways in glaucoma and ocular hypertension. *Invest Ophthalmol Vis Sci*. 1988;29(1):64-72. http://www.ncbi.nlm.nih.gov/pubmed/3335434.

38. Sample PA, Bosworth CF, Weinreb RN. Short-wavelength automated perimetry and motion automated perimetry in patients with glaucoma. *Arch Ophthalmol*. 1997;115(9):1129-1133. http://search.proquest.com/docview/231948351?accountid=15533.

39. Anderson DR. Collaborative normal tension glaucoma study. *Curr Opin Ophthalmol*. 2003;14(2):86-90. doi:10.1097/00055735-200304000-00006.

40. Medeiros F a., Zangwill LM, Bowd C, Sample P a., Weinreb RN. Use of progressive glaucomatous optic disk change as the reference standard for evaluation of diagnostic tests in glaucoma. *Am J Ophthalmol*. 2005;139(6). doi:10.1016/j.ajo.2005.01.003.

41. Fingeret M, Medeiros F a., Susanna R, Weinreb RN. Five rules to evaluate the optic disc and retinal nerve fiber layer for glaucoma. *Optometry*. 2005;76(11):661-668. doi:10.1016/j.optm.2005.08.029.

42. Feuer WJ, Parrish RK, Schiffman JC, et al. The Ocular Hypertension Treatment Study: Reproducibility of cup/disk ratio measurements over time at an Optic Disc Reading Center. *Am J Ophthalmol*. 2002;133(1):19-28. doi:10.1016/S0002-9394(01)01338-1.

43. Parrish RK. The European Glaucoma Prevention Study and the Ocular Hypertension Treatment Study: why do two studies have different results? *Curr Opin Ophthalmol*.

2006;17(2):138-141. doi:10.1097/01.icu.0000193079.55240.18.

44. Ederer F, VanVeldhuisen PC, Dally LG, et al. The advanced glaucoma intervention study (AGIS): 9. Comparison of glaucoma outcomes in black and white patients within treatment groups. *Am J Ophthalmol*. 2001;132(3):311-320. doi:10.1016/S0002-9394(01)01028-5.

45. Parrish RK, Schiffman JC, Feuer WJ, et al. Test-retest reproducibility of optic disk deterioration detected from stereophotographs by masked graders. *Am J Ophthalmol*. 2005;140(4):762-764. doi:10.1016/j.ajo.2005.04.044.

46. Kim M, Kim TW, Weinreb RN, Lee EJ. Differentiation of parapapillary atrophy using spectral-domain optical coherence tomography. *Ophthalmology*. 2013;120(9):1790-1797. doi:10.1016/j.ophtha.2013.02.011.

47. Dai Y, Jonas JB, Huang H, Wang M, Sun X. Microstructure of parapapillary atrophy: Beta zone and gamma zone. *Investig Ophthalmol Vis Sci*. 2013;54(3):2013-2018. doi:10.1167/iovs.12-11255.

48. Lee EJ, Kim T-W, Weinreb RN, Park KH, Kim SH, Kim DM. beta-Zone Parapapillary Atrophy and the Rate of Retinal Nerve Fiber Layer Thinning in Glaucoma. *Invest Ophthalmol Vis Sci*. 2011;52(7):4422-4427. doi:10.1167/iovs.10-6818.

49. Chauhan BC, Blanchard JW, Hamilton DC, Leblanc RP. Technique for Detecting Serial Topographic Changes in the Optic Disc and Peripapillary Retina Using Scanning Laser Tomography. 2016:775-782.

50. Chauhan BC, Hutchison DM, Artes PH, et al. Optic disc progression in glaucoma: Comparison of confocal scanning laser tomography to optic disc photographs in a prospective study. *Investig Ophthalmol Vis Sci*. 2009;50(4):1682-1691. doi:10.1167/iovs.08-2457.

51. Chauhan BC, McCormick T a, Nicolela MT, LeBlanc RP. Optic disc and visual field changes in a prospective longitudinal study of patients with glaucoma: comparison of scanning laser tomography with conventional perimetry and optic disc photography. *Arch Ophthalmol*. 2001;119:1492-1499.

52. DeLeón Ortega JE, Sakata LM, Kakati B, et al. Effect of glaucomatous damage on repeatability of confocal scanning laser ophthalmoscope, scanning laser polarimetry, and optical coherence tomography. *Investig Ophthalmol Vis Sci*. 2007;48(3):1156-

1163. doi:10.1167/iovs.06-0921.

53. Strouthidis NG, White ET, Owen VMF, Ho T a, Garway-Heath DF. Improving the repeatability of Heidelberg retina tomograph and Heidelberg retina tomograph II rim area measurements. *Br J Ophthalmol*. 2005;89:1433-1437. doi:10.1136/bjo.2005.067306.

54. Strouthidis NG, White ET, Owen VMF, Ho T a, Hammond CJ, Garway-Heath DF. Factors affecting the test-retest variability of Heidelberg retina tomograph and Heidelberg retina tomograph II measurements. *Br J Ophthalmol*. 2005;89:1427-1432. doi:10.1136/bjo.2005.067298.

55. Zangwill L, Irak I, Berry CC, Garden V, de Souza Lima M, Weinreb RN. *Effect of Cataract and Pupil Size on Image Quality with Confocal Scanning Laser Ophthalmoscopy.* Archives of ophthalmology 115, 983-990 (1997). doi:10.1001/archopht.1997.01100160153003.

56. Miglior S, Albé E, Guareschi M, Rossetti L, Orzalesi N. Intraobserver and interobserver reproducibility in the evaluation of optic disc stereometric parameters by Heidelberg Retina Tomograph. *Ophthalmology*. 2002;109(6):1072-1077. doi:10.1016/S0161-6420(02)01032-1.

57. Verdonck N, Zeyen T, Van Malderen L, Spileers W. Short-term intra-individual variability in heidelberg retina tomograph II. *Bull Soc Belge Ophtalmol*. 2002;(286):51-57. http://www.ncbi.nlm.nih.gov/pubmed/12564317.

58. Strouthidis NG, Garway-Heath DF. New developments in Heidelberg retina tomograph for glaucoma. *Curr Opin Ophthalmol*. 2008;19(2):141-148. doi:10.1097/ICU.0b013e3282f4450b.

59. Artes PH, Chauhan BC. Longitudinal changes in the visual field and optic disc in glaucoma. *Prog Retin Eye Res*. 2005;24(3):333-354. doi:10.1016/j.preteyeres.2004.10.002.

60. Zeimer R, Asrani S, Zou S, Quigley H, Jampel H. Quantitative detection of glaucomatous damage at the posterior pole by retinal thickness mapping: A pilot study. *Ophthalmology*. 1998;105(2):224-231. doi:10.1016/S0161-6420(98)92743-9.

61. Zeimer R, Shahidi M, Mori M, Zou S, Asrani S. A new method for rapid mapping of the retinal thickness at the posterior pole. *Investig Ophthalmol Vis Sci*.

1996;37(10):1994-2001.

62. Vizzeri G, Balasubramanian M, Bowd C, Weinreb RN, Medeiros F, Zangwill LM. Spectral domain-optical coherence tomography to detect localized retinal nerve fiber layer defects in glaucomatous eyes. *Opt Express*. 2009;17(5):4004-4018. doi:10.1364/OE.17.004004.

63. Abe RY, Gracitelli CPB, Medeiros FA. The Use of Spectral-Domain Optical Coherence Tomography to Detect Glaucoma Progression. *Open Ophthalmol J*. 2015;9:78-88. doi:10.2174/1874364101509010078.

64. Vizzeri G, Kjaergaard SM, Rao HL, Zangwill LM. Role of imaging in glaucoma diagnosis and follow-up. *Indian J Ophthalmol*. 2011;59 Suppl:S59-68. doi:10.4103/0301-4738.73696.

65. Wollstein G, Schuman JS, Price LL, et al. Optical coherence tomography longitudinal evaluation of retinal nerve fiber layer thickness in glaucoma. *Arch Ophthalmol*. 2005;123:464-470. doi:10.1001/archopht.123.4.464.

66. Leung CKS, Chiu V, Weinreb RN, et al. Evaluation of retinal nerve fiber layer progression in glaucoma: A comparison between spectral-domain and time-domain optical coherence tomography. *Ophthalmology*. 2011;118(8):1558-1562. doi:10.1016/j.ophtha.2011.01.026.

67. Leung CK, Yu M, Weinreb RN, et al. Retinal nerve fiber layer imaging with spectral-domain optical coherence tomography: a prospective analysis of age-related loss. *Ophthalmology*. 2012;119(4):731-737. doi:10.1016/j.ophtha.2011.10.010.

68. Leung CKS, Yu M, Weinreb RN, Lai G, Xu G, Lam DSC. Retinal nerve fiber layer imaging with spectral-domain optical coherence tomography: Patterns of retinal nerve fiber layer progression. *Ophthalmology*. 2012;119(9):1858-1866. doi:10.1016/j.ophtha.2012.03.044.

69. Chauhan BC, Burgoyne CF. From clinical examination of the optic disc to clinical assessment of the optic nerve head: A paradigm change. *Am J Ophthalmol*. 2013;156(2). doi:10.1016/j.ajo.2013.04.016.

70. Medeiros FA, Zangwill LM, Alencar LM, et al. Detection of glaucoma progression with stratus OCT retinal nerve fiber layer, optic nerve head, and macular thickness measurements. *Investig Ophthalmol Vis Sci*. 2009;50(12):5741-5748.

doi:10.1167/iovs.09-3715.

71. Banegas S, Anton A, MD P, et al. Evaluation of the Retinal Nerve Fiber Layer Thickness, the Mean Deviation, and the Visual Field Index in Progressive Glaucoma. *J Glaucoma*. 2015;25(3):229-235. doi:10.1097/IJG.0000000000000280.

72. Wessel JM, Horn FK, Tornow RP, et al. Longitudinal analysis of progression in glaucoma using spectral-domain optical coherence tomography. *Invest Ophthalmol Vis Sci*. 2013;54(5):3613-3620. doi:10.1167/iovs.12-9786.

73. Medeiros F a, Alencar LM, Zangwill LM, Bowd C, Sample P a, Weinreb RN. Prediction of functional loss in glaucoma from progressive optic disc damage. *Arch Ophthalmol*. 2009;127(10):1250-1256. doi:10.1016/S0084-392X(10)79321-7.

74. Leung CKS, Cheung CYL, Weinreb RN, et al. Evaluation of retinal nerve fiber layer progression in glaucoma: A study on optical coherence tomography guided progression analysis. *Investig Ophthalmol Vis Sci*. 2010;51(1):217-222. doi:10.1167/iovs.09-3468.

75. Caprioli J. Automated perimetry in glaucoma. *Am J Ophthalmol*. 1991;111(2):235-239.

76. Artes PH, Iwase A, Ohno Y, Kitazawa Y, Chauhan BC. Properties of perimetric threshold estimates from full threshold, SITA standard, and SITA fast strategies. *Investig Ophthalmol Vis Sci*. 2002;43(8):2654-2659.

77. Johnson CA. Selective versus nonselective losses in glaucoma. *J Glaucoma*. 1994;3 Suppl 1:S32-S44. doi:10.1097/00061198-199400321-00005.

78. Johnson CA, Cioffi GA, Liebmann JR, Sample PA, Zangwill LM, Weinreb RN. The relationship between structural and functional alterations in glaucoma: a review. *Semin Ophthalmol*. 2000;15(4):221-233. doi:10.3109/08820530009037873.

79. Bengtsson B, Heijl A. Normal Intersubject Threshold Variability and Normal Limits of the SITA SWAP and Full Threshold SWAP Perimetric Programs. *Investig Ophthalmol Vis Sci*. 2003;44(11):5029-5034. doi:10.1167/iovs.02-1220.

80. Heijl A, Lindgren G, Olsson J. Normal variability of static perimetric threshold values across the central visual field. *Arch Ophthalmol*. 1987;105(11):1544-1549. doi:10.1001/archopht.1987.01060110090039.

81. Heijl a, Lindgren a, Lindgren G. Test-retest variability in glaucomatous visual fields. *Am J Ophthalmol*. 1989;108(2):130-135. doi:10.1016/0002-9394(89)90006-8.

82. Heijl A, Bengtsson B, Chauhan BC, et al. A Comparison of Visual Field Progression Criteria of 3 Major Glaucoma Trials in Early Manifest Glaucoma Trial Patients. *Ophthalmology*. 2008;115(9):1557-1565. doi:10.1016/j.ophtha.2008.02.005.

83. Vessani RM, Moritz R, Batis L, Zagui RB, Bernardoni S, Susanna R. Comparison of quantitative imaging devices and subjective optic nerve head assessment by general ophthalmologists to differentiate normal from glaucomatous eyes. *J Glaucoma*. 2009;18(3):253-261. doi:10.1097/IJG.0b013e31818153da.

84. Birch MK, Wishart PK, O'Donnell NP. Determining progressive visual field loss in serial Humphrey visual fields. *Ophthalmology*. 1995;102(8):1227-1234-1235. doi:10.1016/S0161-6420(95)30885-8.

85. Musch DC, Lichter PR, Guire KE, Standardi CL. The Collaborative Initial Glaucoma Treatment Study. *Ophthalmology*. 1998;106:653-662. doi:10.1016/S0161-6420(99)90147-1.

86. Wild JM. Short wavelength automated perimetry. *Acta Ophthalmol Scand*. 2001;79(6):546-559. doi:10.1034/j.1600-0420.2001.790602.x.

87. Dacey DM, Lee BB. The "blue-on" opponent pathway in primate retina originates from a distinct bistratified ganglion cell type. *Nature*. 1994;367(6465):731-735. doi:10.1038/367731a0.

88. Adams AJ, Rodic R, Husted R, Stamper R. Spectral sensitivity and color discrimination changes in glaucoma and glaucoma-suspect patients. *Investig Ophthalmol Vis Sci*. 1982;23(4):516-524.

89. Westheimer G. Directional sensitivity of the retina: 75 years of Stiles-Crawford effect. *Proc Biol Sci*. 2008;275(1653):2777-2786. doi:10.1098/rspb.2008.0712.

90. Havvas I, Papaconstantinou D, Moschos MM, et al. Comparison of SWAP and SAP on the point of glaucoma conversion. *Clin Ophthalmol*. 2013;7:1805-1810. doi:10.2147/OPTH.S50231.

91. Bengtsson B, Heijl A. Diagnostic Sensitivity of Fast Blue-Yellow and Standard Automated Perimetry in Early Glaucoma. A Comparison between Different Test Programs. *Ophthalmology*. 2006;113(7):1092-1097. doi:10.1016/j.ophtha.2005.12.028.

92. van der Schoot J, Reus NJ, Colen TP, Lemij HG. The Ability of Short-Wavelength

Automated Perimetry to Predict Conversion to Glaucoma. *Ophthalmology*. 2010;117(1):30-34. doi:10.1016/j.ophtha.2009.06.046.

93. Johnson C a, Adams a J, Casson EJ, Brandt JD. Blue-on-yellow perimetry can predict the development of glaucomatous visual field loss. *Arch Ophthalmol*. 1993;111:645-650. doi:10.1001/archopht.1993.01090050079034.

94. Demirel S, Johnson CA. Incidence and prevalence of short wavelength automated perimetry deficits in ocular hypertensive patients. *Am J Ophthalmol*. 2001;131(6):709-715. doi:10.1016/S0002-9394(00)00946-6.

95. Sample PA, Medeiros FA, Racette L, et al. Identifying glaucomatous vision loss with visual-function-specific perimetry in the diagnostic innovations in glaucoma study. *Investig Ophthalmol Vis Sci*. 2006;47(8):3381-3389. doi:10.1167/iovs.05-1546.

96. Johnson C a, Adams a J, Casson EJ, Brandt JD. Progression of early glaucomatous visual field loss as detected by blue-on-yellow and standard white-on-white automated perimetry. *Arch Ophthalmol*. 1993;111:651-656. doi:10.1001/archopht.1993.01090050085035.

97. Sample PA, Taylor JD, Martinez GA, Lusky M, Weinreb RN. *Short-Wavelength Color Visual Fields in Glaucoma Suspects at Risk.* American journal of ophthalmology 115, 225-233 (1993).

98. Johnson C, Brandt JD, Khong AM, Adams AJ. Short-wavelength automated perimetry in low-, medium-, and high-risk ocular hypertensive eyes: initial baseline results. *Arch Ophthalmol*. 1995;113(1):70-76. doi:10.1001/archopht.1995.01100010072023.

99. Teesalu P, Vihanninjoki K, Airaksinen PJ, Tuulonen A, Läärä E. Correlation of blue-on-yellow visual fields with scanning confocal laser optic disc measurements. *Investig Ophthalmol Vis Sci*. 1997;38(12):2452-2459.

100. Sánchez-Galeana CA, Bowd C, Zangwill LM, Sample PA, Weinreb RN. Short-wavelength automated perimetry results are correlated with optical coherence tomography retinal nerve fiber layer thickness measurements in glaucomatous eyes. *Ophthalmology*. 2004;111(10):1866-1872. doi:10.1016/j.ophtha.2004.04.017.

101. Liu S, Lam S, Weinreb RN, et al. Comparison of standard automated perimetry, frequency-doubling technology perimetry, and short-wavelength automated perimetry for detection of glaucoma. *Investig Ophthalmol Vis Sci*. 2011;52(10):7325-7331.

doi:10.1167/iovs.11-7795.

102. Girkin C a, Emdadi a, Sample P a, et al. Short-wavelength automated perimetry and standard perimetry in the detection of progressive optic disc cupping. *Arch Ophthalmol*. 2000;118:1231-1236. doi:10.1001/archopht.118.9.1231.

103. Polo V, Larrosa JM, Pinilla I, Perez S, Gonzalvo F, Honrubia FM. Predictive value of short-wavelength automated perimetry: a 3-year follow-up study. *Ophthalmology*. 2002;109(4):761-765.

104. Kelly DH. Frequency Doubling in Visual Responses. *J Opt Soc Am*. 1966;56(11):1628-1632. doi:10.1364/JOSA.56.001628.

105. Cello KE, Nelson-Quigg JM, Johnson CA. Frequency doubling technology perimetry for detection of glaucomatous visual field loss. *Am J Ophthalmol*. 2000;129(3):314-322. doi:10.1016/S0002-9394(99)00414-6.

106. Wang YX, Xu L, Zhang RX, Jonas JB. Frequency-doubling threshold perimetry in predicting glaucoma in a population-based study: The Beijing Eye Study. *Arch Ophthalmol*. 2007;125(10):1402-1406. doi:10.1016/S0084-392X(08)79161-5.

107. Sample PA, Bosworth CF, Blumenthal EZ, Girkin C, Weinreb RN. Visual function-specific perimetry for indirect comparison of different ganglion cell populations in glaucoma. *Investig Ophthalmol Vis Sci*. 2000;41(7):1783-1790.

108. Quigley HA. Identification of glaucoma-related visual field abnormality with the screening protocol of frequency doubling technology. *Am J Ophthalmol*. 1998;125(6):819-829. doi:10.1016/S0002-9394(98)00046-4.

109. Xin D, Greenstein VC, Ritch R, Liebmann JM, de Moraes CG, Hood DC. A comparison of functional and structural measures for identifying progression of glaucoma. *Investig Ophthalmol Vis Sci*. 2011;52(1):519-526. doi:10.1167/iovs.10-5174.

110. Haymes SA, Hutchison DM, McCormick TA, et al. Glaucomatous visual field progression with frequency-doubling technology and standard automated perimetry in a longitudinal prospective study. *Investig Ophthalmol Vis Sci*. 2005;46(2):547-554. doi:10.1167/iovs.04-0973.

111. Bayer AU, Erb C. Short wavelength automated perimetry, frequency doubling

technology perimetry, and pattern electroretinography for prediction of progressive glaucomatous standard visual field defects. *Ophthalmology*. 2002;109(5):1009-1017. doi:10.1016/S0161-6420(02)01015-1.

112. Clement CI, Goldberg I, Healey PR, Graham S. Humphrey matrix frequency doubling perimetry for detection of visual-field defects in open-angle glaucoma. *Br J Ophthalmol*. 2009;93(5):582-588. doi:10.1136/bjo.2007.119909.

113. Brusini P, Salvetat ML, Zeppieri M, Parisi L. Frequency doubling technology perimetry with the Humphrey Matrix 30-2 test. *J Glaucoma*. 2006;15(2):77-83. doi:10.1097/00061198-200604000-00001.

114. Vaegan, Graham SL, Goldberg I, Buckland L, Hollows FC. Flash and pattern electroretinogram changes with optic atrophy and glaucoma. *Exp Eye Res*. 1995;60(6):697-706. doi:10.1016/S0014-4835(05)80011-9.

115. Hood DC, Greenstein VC, Holopigian K, et al. An attempt to detect glaucomatous damage to the inner retina with the multifocal ERG. *Investig Ophthalmol Vis Sci*. 2000;41(6):1570-1579.

116. Machida S, Gotoh Y, Toba Y, Ohtaki A, Kaneko M, Kurosaka D. Correlation between photopic negative response and retinal nerve fiber layer thickness and optic disc topography in glaucomatous eyes. *Investig Ophthalmol Vis Sci*. 2008;49(5):2201-2207. doi:10.1167/iovs.07-0887.

117. Viswanathan S, Frishman LJ, Robson JG, Harwerth RS, Smith EL. The photopic negative response of the macaque electroretinogram: Reduction by experimental glaucoma. *Investig Ophthalmol Vis Sci*. 1999;40(6):1124-1136.

118. Viswanathan S, Frishman LJ, Robson JG, Walters JW. The photopic negative response of the flash electroretinogram in primary open angle glaucoma. *Investig Ophthalmol Vis Sci*. 2001;42(2):514-522.

119. Luo X, Frishman LJ. Retinal pathway origins of the pattern electroretinogram (PERG). *Investig Ophthalmol Vis Sci*. 2011;52(12):8571-8584. doi:10.1167/iovs.11-8376.

120. Ventura LM, Porciatti V, Ishida K, Feuer WJ, Parrish RK. Pattern electroretinogram abnormality and glaucoma. *Ophthalmology*. 2005;112(1):10-19. doi:10.1016/j.ophtha.2004.07.018.

121. Bach M, Unsoeld AS, Philippin H, et al. Pattern ERG as an early glaucoma indicator in ocular hypertension: A long-term, prospective study. *Investig Ophthalmol Vis Sci*. 2006;47(11):4881-4887. doi:10.1167/iovs.05-0875.

122. Ventura LM, Sorokac N, De Los Santos R, Feuer WJ, Porciatti V. The relationship between retinal ganglion cell function and retinal nerve fiber thickness in early glaucoma. *Investig Ophthalmol Vis Sci*. 2006;47(9):3904-3911. doi:10.1167/iovs.06-0161.

123. Bode SFN, Jehle T, Bach M. Pattern electroretinogram in glaucoma suspects: New findings from a longitudinal study. *Investig Ophthalmol Vis Sci*. 2011;52(7):4300-4306. doi:10.1167/iovs.10-6381.

124. Banitt MR, Ventura LM, Feuer WJ, et al. Progressive loss of retinal ganglion cell function precedes structural loss by several years in glaucoma suspects. *Investig Ophthalmol Vis Sci*. 2013;54(3):2346-2352. doi:10.1167/iovs.12-11026.

125. Weinstein GW, Odom JV, Cavender S. Visually evoked potentials and electroretinography in neurologic evaluation. *Neurol Clin*. 1991;9(1):225-242. http://www.ncbi.nlm.nih.gov/entrez/query.fcgi?cmd=Retrieve&db=PubMed&dopt=Citation&list_uids=1849226.

126. Fritsches KA, Rosa MGP. Visuotopic organisation of striate cortex in the marmoset monkey (Callithrix jacchus). *J Comp Neurol*. 1996;372(2):264-282. doi:10.1002/(SICI)1096-9861(19960819)372:2<264::AID-CNE8>3.0.CO;2-1.

127. Halliday AM, Mcdonald WI, Mushin J. Delayed Visual Evoked Response in Optic Neuritis. *Lancet*. 1972;299(7758):982-985. doi:10.1016/S0140-6736(72)91155-5.

128. Wilson WB. Visual-evoked response differentiation of ischemic optic neuritis from the optic neuritis of multiple sclerosis. *AmJ Ophthalmol*. 1978;86(4):530-535.

129. Halliday AM, Halliday E, Kriss A, McDonald WI, Mushin J. The pattern-evoked potential in compression of the anterior visual pathways. *Brain*. 1976;99(2):357-374. http://www.ncbi.nlm.nih.gov/pubmed/990902.

130. Howe JW, Mitchell KW. Visual evoked cortical potential to paracentral retinal stimulation in chronic glaucoma, ocular hypertension, and an age-matched group of normals. *Doc Ophthalmol*. 1986;63(1):37-44. http://www.ncbi.nlm.nih.gov/pubmed/3732011.

131. Cappin JM, Nissim S. Visual evoked responses in the assessment of field defects in glaucoma. *Arch Ophthalmol*. 1975;93(1):9-18. doi:10.1001/archopht.1975.01010020013002.

132. Huber C, Wagner T. Electrophysiological evidence for glaucomatous lesions in the optic nerve. *Ophthal Res*. 1978;10:22-29.

133. Krogh E. VER in intraocular hypertension. Short communication. *Acta Ophthalmol*. 1980;58(6):929-932.

134. Bodis-Wollner I. *Electrophysiological and Psychophysical Testing of Vision in Glaucoma.* Survey of ophthalmology 33 Suppl, 301-307 (1989).

135. Schmeisser ET, Smith TJ. High-frequency flicker visual-evoked potential losses in glaucoma. *Ophthalmology*. 1989;96(5):620-623.

136. Ducati A, Fava E, Motti EDF. Neuronal generators of the visual evoked potentials: intracerebral recording in awake humans. *Electroencephalogr Clin Neurophysiol Evoked Potentials*. 1988;71(2):89-99. doi:10.1016/0168-5597(88)90010-X.

137. Tobimatsu S, Tomoda H, Kato M. Human VEPs to isoluminant chromatic and achromatic sinusoidal gratings: Separation of parvocellular components. In: *Brain Topography*. Vol 8. ; 1996:241-243. doi:10.1007/BF01184777.

138. Horn FK, Bergua A, Jünemann A, Korth M. Visual evoked potentials under luminance contrast and color contrast stimulation in glaucoma diagnosis. *J Glaucoma*. 2000;9(6):428-437.

139. Horn FK, Jonas JB, Budde WM, J??nemann AM, Mardin CY, Korth M. Monitoring glaucoma progression with visual evoked potentials of the blue-sensitive pathway. *Investig Ophthalmol Vis Sci*. 2002;43(6):1828-1834.

140. Graham SL, Wong T, Drance SM, Mikelberg FS. Pattern Electroretinograms From Hemifields in Normal Subjects and Patients With Glaucoma. 2016;35(9):3347-3356.

141. Baseler H a., Sutter EE, Klein S a., Carney T. The topography of visual evoked response properties across the visual field. *Electroencephalogr Clin Neurophysiol*. 1994;90(1):65-81. doi:10.1016/0013-4694(94)90114-7.

142. Sutter EE. The fast m-transform A fast computation of cross-correlations with binary m-sequences. *SIAM J Comput*. 1991;20(4):686-694. doi:10.1137/0220043.

143. Klistorner AI, Graham SL, Grigg JR, Billson F a. Multifocal topographic visual evoked potential: Improving objective detection of local visual field defects. *Investig Ophthalmol Vis Sci*. 1998;39(6):937-950.

144. Hood DC, Zhang X, Greenstein VC, et al. An interocular comparison of the multifocal VEP: A possible technique for detecting local damage to the optic nerve. *Investig Ophthalmol Vis Sci*. 2000;41(6):1580-1587.

145. Graham SL, Klistorner AI, Grigg JR, Billson FA. Objective VEP perimetry in glaucoma: asymmetry analysis to identify early deficits. *J Glaucoma*. 2000;9(1):10-19. doi:10.1097/00061198-200002000-00004.

146. Hasegawa S, Abe H. Mapping of Glaucomatous Visual Field Defects by. *Invest Ophthalmol*. 2001;42(13):3341-3348.

147. Goldberg I, Graham SL, Klistorner AI. Multifocal objective perimetry in the detection of glaucomatous field loss. *Am J Ophthalmol*. 2002;133(1):29-39. doi:10.1016/S0002-9394(01)01294-6.

148. Baseler H a., Sutter EE. M and P components of the VEP and their visual field distribution. *Vision Res*. 1997;37(6):675-690. doi:10.1016/S0042-6989(96)00209-X.

149. Cowey a, Rolls ET. Human cortical magnification factor and its relation to visual acuity. *Exp Brain Res*. 1974;21(5):447-454. doi:10.1007/BF00237163.

150. Kitano M, Niiyama K, Kasamatsu T, Sutter EE, Norcia a M. Retinotopic and nonretinotopic field potentials in cat visual cortex. *Vis Neurosci*. 1994;11(5):953-977. doi:10.1017/S0952523800003904.

151. McFadzean R, Brosnahan D, Hadley D, Mutlukan E. Representation of the Visual-Field in the Occipital Striate Cortex. *Br J Ophthalmol*. 1994;78(3):185-190. doi:10.1136/bjo.78.3.185.

152. Di Russo F, Martínez A, Sereno MI, Pitzalis S, Hillyard SA. Cortical sources of the early components of the visual evoked potential. *Hum Brain Mapp*. 2002;15(2):95-111. doi:10.1002/hbm.10010.

153. Sutter EE, Tran D. The field topography of ERG components in man-I. The photopic luminance response. *Vision Res*. 1992;32(3):433-446. doi:10.1016/0042-6989(92)90235-B.

154. Baseler H a, Morland a B, Wandell B a. Topographic organization of human visual areas in the absence of input from primary cortex. *J Neurosci*. 1999;19(7):2619-2627.

155. Fortune B, Hood DC. Conventional pattern-reversal VEPs are not equivalent to summed multifocal VEPs. *Investig Ophthalmol Vis Sci*. 2003;44(3):1364-1375. doi:10.1167/iovs.02-0441.

156. Graham SL, Klistorner A, Grigg JR, Billson F a., Ao. Objective perimetry in glaucoma: Recent advances with multifocal stimuli. *Surv Ophthalmol*. 1999;43(6 SUPPL.):199-209. doi:10.1016/S0039-6257(99)00011-9.

157. Alshowaeir D, Yiannikas C, Garrick R, et al. Latency of multifocal visual evoked potentials in nonoptic neuritis eyes of multiple sclerosis patients associated with optic radiation lesions. *Investig Ophthalmol Vis Sci*. 2014;55(6):3758-3764. doi:10.1167/iovs.14-14571.

158. Rodarte C, Hood DC, Yang EB, et al. The effects of glaucoma on the latency of the multifocal visual evoked potential. *Br J Ophthalmol*. 2006;90(9):1132-1136. doi:10.1136/bjo.2006.097592.

159. Hood DC, Greenstein VC. Multifocal VEP and ganglion cell damage: Applications and limitations for the study of glaucoma. *Prog Retin Eye Res*. 2003;22(2):201-251. doi:10.1016/S1350-9462(02)00061-7.

160. Hood DC, Zhang X. Multifocal ERG and VEP responses and visual fields: comparing disease-related changes. *Doc Ophthalmol*. 2000;100(2-3):115-137. http://link.springer.com/10.1023/A:1002727602212%5Cnpapers3://publication/doi/10.1023/A:1002727602212.

161. Sutter EE, Bearse MA. The optic nerve head component of the human ERG. *Vision Res*. 1999;39(May 1998):419-436. doi:10.1016/S0042-6989(98)00161-8.

162. Arvind H, Klistorner A, Graham SL, Grigg JR. Multifocal visual evoked responses to dichoptic stimulation using virtual reality goggles: Multifocal VER to dichoptic stimulation. *Doc Ophthalmol*. 2006;112(3):189-199. doi:10.1007/s10633-006-0005-y.

163. Zhang X, Hood DC, Chen CS, Hong JE. A signal-to-noise analysis of multifocal VEP responses: An objective definition for poor records. *Doc Ophthalmol*. 2002;104(3):287-302. doi:10.1023/A:1015220501743.

164. Maddess T, James AC, Bowman EA. Contrast response of temporally sparse dichoptic multifocal visual evoked potentials. *Vis Neurosci*. 2005;22(2):153-162. doi:10.1017/S0952523805222046.

165. James AC, Ruseckaite R, Maddess T. Effect of temporal sparseness and dichoptic presentation on multifocal visual evoked potentials. *Vis Neurosci*. 2005;22(1):45-54. doi:10.1017/S0952523805221053.

166. Klistorner AI, Graham SL. Effect of eccentricity on pattern-pulse multifocal VEP. *Doc Ophthalmol*. 2005;110(2-3):209-218. doi:10.1007/s10633-005-7309-1.

167. James AC. The pattern-pulse multifocal visual evoked potential. *Investig Ophthalmol Vis Sci*. 2003;44(2):879-890. doi:10.1167/iovs.02-0608.

168. Pieh C, Hoffmann MB, Bach M. The influence of defocus on multifocal visual evoked potentials. *Graefe's Arch Clin Exp Ophthalmol*. 2005;243(1):38-42. doi:10.1007/s00417-004-0969-9.

169. Klistorner A, Graham SL, Martins A, et al. Multifocal Blue-on-Yellow Visual Evoked Potentials in Early Glaucoma. *Ophthalmology*. 2007;114(9):1613-1621. doi:10.1016/j.ophtha.2006.11.037.

170. Klistorner A, Fraser C, Garrick R, Graham S, Arvind H. Correlation between full-field and multifocal VEPs in optic neuritis. *Doc Ophthalmol*. 2008;116(1):19-27. doi:10.1007/s10633-007-9072-y.

171. Hood DC, Chen JY, Yang EB, et al. The role of the multifocal visual evoked potential (mfVEP) latency in understanding optic nerve and retinal diseases. *Trans Am Ophthalmol Soc*. 2006;104:71-77.

172. Klistorner A, Arvind H, Garrick R, Graham SL, Paine M, Yiannikas C. Interrelationship of optical coherence tomography and multifocal visual-evoked potentials after optic neuritis. *Investig Ophthalmol Vis Sci*. 2010;51(5):2770-2777. doi:10.1167/iovs.09-4577.

173. Fortune B, Zhang X, Hood DC, Demirel S, Johnson C a. Normative ranges and specificity of the multifocal VEP. *Doc Ophthalmol*. 2004;109(1):87-100. doi:10.1007/s10633-004-3300-5.

174. Nakamura M, Kato K, Kamata S, Ishikawa K, Nagai T. Effect of refractive errors on

multifocal VEP responses and standard automated perimetry tests in a single population. *Doc Ophthalmol*. 2014;128(3):179-189. doi:10.1007/s10633-014-9431-4.

175. Fortune B, Demirel S, Zhang X, Hood DC, Johnson C a. Repeatability of normal multifocal VEP: implications for detecting progression. *J Glaucoma*. 2006;15(2):131-141. doi:10.1097/00061198-200604000-00010.

176. Chen CS, Hood DC, Zhang X, et al. Repeat reliability of the multifocal visual evoked potential in normal and glaucomatous eyes. *J Glaucoma*. 2003;12(5):399-408. doi:10.1097/00061198-200310000-00002.

177. Narayanan D, Cheng H, Tang RA, Frishman LJ. Reproducibility of multifocal visual evoked potential and traditional visual evoked potential in normal and multiple sclerosis eyes. *Doc Ophthalmol*. 2014;130(1):31-41. doi:10.1007/s10633-014-9467-5.

178. Klistorner a., Graham SL. Intertest variability of mfVEP amplitude: Reducing its effect on the interpretation of sequential tests. *Doc Ophthalmol*. 2005;111(3):159-167. doi:10.1007/s10633-005-5363-3.

179. Zhang X, Hood DC. A principal component analysis of multifocal pattern reversal VEP. *J Vis*. 2004;4(1):32-43. doi:10:1167/4.1.4.

180. Klistorner a I, Graham SL, Grigg J, Balachandran C. Objective perimetry using the multifocal visual evoked potential in central visual pathway lesions. *Br J Ophthalmol*. 2005;89(6):739-744. doi:10.1136/bjo.2004.053223.

181. Hood DC, Thienprasiddhi P, Greenstein VC, et al. Detecting Early to Mild Glaucomatous Damage: A Comparison of the Multifocal VEP and Automated Perimetry. *Investig Ophthalmol Vis Sci*. 2004;45(2):492-498. doi:10.1167/iovs.03-0602.

182. Thienprasiddhi P, Greenstein VC, Chen CS, Liebmann JM, Ritch R, Hood DC. Multifocal visual evoked potential responses in glaucoma patients with unilateral hemifield defects. *Am J Ophthalmol*. 2003;136(1):34-40. doi:10.1016/S0002-9394(03)00080-1.

183. Johnson C a. Recent Developments In Automated Perimetry In Glaucoma Diagnosis and Management. *Curr Opin Ophthalmol*. 2002;13:77-84. doi:10.1097/00055735-200204000-00004.

184. Atkin a., Bodis-Wollner I, Podos SM, Wolkstein M, Mylin L, Nitzberg S. Flicker threshold and pattern VEP latency in ocular hypertension and glaucoma. *Investig Ophthalmol Vis Sci*. 1983;24(11):1524-1528.

185. Towle VL, Moskowitz A, Sokol S, Schwartz B. The visual evoked potential in glaucoma and ocular hypertension: Effects of check size, field size, and stimulation rate. *Investig Ophthalmol Vis Sci*. 1983;24(2):175-183.

186. Parisi V, Miglior S, Manni G, Centofanti M, Bucci MG. Clinical ability of pattern electroretinograms and visual evoked potentials in detecting visual dysfunction in ocular hypertension and glaucoma. *Ophthalmology*. 2006;113(2):216-228. doi:10.1016/j.ophtha.2005.10.044.

187. Grippo TM, Hood DC, Kanadani FN, et al. A comparison between multifocal and conventional VEP latency changes secondary to glaucomatous damage. *Investig Ophthalmol Vis Sci*. 2006;47(12):5331-5336. doi:10.1167/iovs.06-0527.

188. Hood DC, Ohri N, Yang BE, et al. Determining abnormal latencies of multifocal visual evoked potentials: A monocular analysis. *Doc Ophthalmol*. 2004;109(2):189-199. doi:10.1007/s10633-004-5512-0.

189. Hood DC, Zhang X, Rodarte C, et al. Determining abnormal interocular latencies of multifocal visual evoked potentials. *Doc Ophthalmol*. 2004;109(2):177-187. doi:10.1007/s10633-004-5511-1.

190. Korth M, Nguyen NX, Junemann A, Martus P, Jonas JB. VEP test of the blue-sensitive pathway in glaucoma. *Investig Ophthalmol Vis Sci*. 1994;35(5):2599-2610.

191. Sample PA, Weinreb RN, Boynton RM. Acquired dyschromatopsia in glaucoma. *Surv Ophthalmol*. 1986;31(1):54-64. doi:10.1016/0039-6257(86)90051-2.

192. Horn FK, Jonas JB, Budde WD, Al E. Monitoring glaucoma progression with visual evoked potentials of the blue sensitive pathway. *Invest Ophthalmol Vis Sci*. 2002;43:1828-1834.

193. Arvind H, Graham S, Leaney J, et al. Identifying Preperimetric Functional Loss in Glaucoma. A Blue-on-Yellow Multifocal Visual Evoked Potentials Study. *Ophthalmology*. 2009;116(6):1134-1141. doi:10.1016/j.ophtha.2008.12.041.

194. Shapley R. Visual sensitivity and parallel retinocortical channels. *Annu Rev Psychol*.

1990;41:635-658. doi:10.1146/annurev.psych.41.1.635.

195. Kogure S, Toda Y, Tsukahara S. Prediction of future scotoma on conventional automated static perimetry using frequency doubling technology perimetry. *Br J Ophthalmol*. 2006;90(3):347-352. doi:10.1136/bjo.2005.077065.

196. Ferreras A, Polo V, Larrosa JM, et al. Can frequency-doubling technology and short-wavelength automated perimetries detect visual field defects before standard automated perimetry in patients with preperimetric glaucoma? *J Glaucoma*. 2007;16(4):372-383. doi:10.1097/IJG.0b013e31803bbb17.

197. Klistorner a., Crewther DP, Crewther SG. Separate magnocellular and parvocellular contributions from temporal analysis of the multifocal VEP. *Vision Res*. 1997;37(15):2161-2169. doi:10.1016/S0042-6989(97)00003-5.

198. Klistorner AI, Graham SL. Early magnocellular loss in glaucoma demonstrated using the pseudorandomly stimulated flash visual evoked potential. *J Glaucoma*. 1999;8(2):140-148. http://www.ncbi.nlm.nih.gov/pubmed/10209732.

199. Arvind H, Klistorner A, Grigg J, Graham SL. Low-luminance contrast stimulation is optimal for early detection of glaucoma using multifocal visual evoked potentials. *Investig Ophthalmol Vis Sci*. 2011;52(6):3744-3750. doi:10.1167/iovs.10-6057.

200. Sriram P, Klistorner A, Graham S, Grigg J, Arvind H. Optimizing the detection of preperimetric glaucoma by combining structural and functional tests. *Investig Ophthalmol Vis Sci*. 2015;56(13):7794-7800. doi:10.1167/iovs.15-16721.

201. Airaksinen PJ, Drance SM, Douglas GR, Schulzer M, Wijsman K. Visual field and retinal nerve fiber layer comparisons in glaucoma. *Arch Ophthalmol*. 1985;103(2):205-207. http://www.ncbi.nlm.nih.gov/pubmed/3977691.

202. Kanamori A, Nakamura M, Escano MFT, Seya R, Maeda H, Negi A. Evaluation of the glaucomatous damage on retinal nerve fiber layer thickness measured by optical coherence tomography. *Am J Ophthalmol*. 2003;135(4):513-520. doi:10.1016/S0002-9394(02)02003-2.

203. Alencar LM, Zangwill LM, Weinreb RN, et al. A comparison of rates of change in neuroretinal rim area and retinal nerve fiber layer thickness in progressive glaucoma. *Investig Ophthalmol Vis Sci*. 2010;51(7):3531-3539. doi:10.1167/iovs.09-4350.

204. Strouthidis NG, Vinciotti V, Tucker AJ, Gardiner SK, Crabb DP, Garway-Heath DF. Structure and function in glaucoma: The relationship between a functional visual field map and an anatomic retinal map. *Investig Ophthalmol Vis Sci*. 2006;47(12):5356-5362. doi:10.1167/iovs.05-1660.

205. Medeiros F a., Leite MT, Zangwill LM, Weinreb RN. Combining structural and functional measurements to improve detection of glaucoma progression using Bayesian hierarchical models. *Investig Ophthalmol Vis Sci*. 2011;52(8):5794-5803. doi:10.1167/iovs.10-7111.

206. Medeiros FA, Zangwill LM, Bowd C, Mansouri K, Weinreb RN. The structure and function relationship in glaucoma: Implications for detection of progression and measurement of rates of change. *Investig Ophthalmol Vis Sci*. 2012;53(11):6939-6946. doi:10.1167/iovs.12-10345.

207. Meira-Freitas D, Lisboa R, Tatham A, et al. Predicting progression in glaucoma suspects with longitudinal estimates of retinal ganglion cell counts. *Investig Ophthalmol Vis Sci*. 2013;54(6):4174-4183. doi:10.1167/iovs.12-11301.

208. Gardiner SK, Johnson C a., Cioffi G a. Evaluation of the structure-function relationship in glaucoma. *Investig Ophthalmol Vis Sci*. 2005;46(10):3712-3717. doi:10.1167/iovs.05-0266.

209. Hood DC, Anderson SC, Wall M, Kardon RH. Structure versus function in glaucoma: An application of a linear model. *Investig Ophthalmol Vis Sci*. 2007;48(8). doi:10.1167/iovs.06-1401.

210. Chen TC. Spectral domain optical coherence tomography in glaucoma: qualitative and quantitative analysis of the optic nerve head and retinal nerve fiber layer (an AOS thesis). *Trans Am Ophthalmol Soc*. 2009;107:254-281. http://www.pubmedcentral.nih.gov/articlerender.fcgi?artid=2814580&tool=pmcentrez&rendertype=abstract.

211. Danthurebandara VM, Sharpe GP, Hutchison DM, et al. Enhanced structure–function relationship in glaucoma with an anatomically and geometrically accurate neuroretinal rim measurement. *Investig Ophthalmol Vis Sci*. 2015;56(1):98-105. doi:10.1167/iovs.14-15375.

212. Garway-Heath DF, Poinoosawmy D, Fitzke FW, Hitchings RA. Mapping the visual

field to the optic disc in normal tension glaucoma eyes. *Ophthalmology*. 2000;107(10):1809-1815. doi:10.1016/S0161-6420(00)00284-0.

213. Omodaka K, Takada N, Yamaguchi T, Takahashi H, Araie M, Nakazawa T. Characteristic correlations of the structure-function relationship in different glaucomatous disc types. *Jpn J Ophthalmol*. 2015;59(4):223-229. doi:10.1007/s10384-015-0379-z.

214. Thienprasiddhi P, Greenstein VC, Chu DH, et al. Detecting early functional damage in glaucoma suspect and ocular hypertensive patients with the multifocal VEP technique. *J Glaucoma*. 2006;15(4):321-327. doi:10.1097/01.ijg.0000212237.26466.0e.

215. Bengtsson B. Evaluation of VEP perimetry in normal subjects and glaucoma patients. *Acta Ophthalmol Scand*. 2002;80(6):620-626. doi:10.1034/j.1600-0420.2002.800612.x.

216. Laron M, Schiffman JS, Tang RA, Frishman LJ. Comparison of multifocal visual evoked potential, standard automated perimetry and optical coherence tomography in assessing visual pathway in multiple sclerosis patients. *Mult Scler*. 2010;16(4):412-426. doi:10.1177/1352458509359782.

217. Sriram P, Wang C, Yiannikas C, et al. Relationship between Optical Coherence Tomography and Electrophysiology of the Visual Pathway in Non-Optic Neuritis Eyes of Multiple Sclerosis Patients. *PLoS One*. 2014;9(8):e102546. doi:10.1371/journal.pone.0102546.

218. Klistorner A, Arvind H, Nguyen T, et al. Multifocal VEP and OCT in optic neuritis: A topographical study of the structure - Function relationship. *Doc Ophthalmol*. 2009;118(2):129-137. doi:10.1007/s10633-008-9147-4.

219. Greenstein VC, Thienprasiddhi P, Ritch R, Liebmann JM, Hood DC. A method for comparing electrophysiological, psychophysical, and structural measures of glaucomatous damage. *Arch Ophthalmol*. 2004;122(9):1276-1284. doi:10.1001/archopht.122.9.1276.

220. Miglior S, Brigatti L, Lonati C, Rossetti L, Pierrottet C, Orzalesi N. Correlation between the progression of optic disc and visual field changes in glaucoma. *Curr Eye Res*. 1996;15(2):145-149. http://www.ncbi.nlm.nih.gov/pubmed/8670722.

221. Anderson DR PV. Automated static perimetry. *Mosby*. 1999:164. doi:10.1001/archopht.1994.01090180043025.

222. McNaught AI, Crabb DP, Fitzke FW, Hitchings RA. Visual field progression: Comparison of Humphrey Statpac and pointwise linear regression analysis. *Graefe's Arch Clin Exp Ophthalmol*. 1996;234(7):411-418. doi:10.1007/BF02539406.

223. Johnson C a., Sample P a., Cioffi G a., Liebmann JR, Weinreb RN. Structure and function evaluation (SAFE): I. criteria for glaucomatous visual field loss using standard automated perimetry (SAP) and short wavelength automated perimetry (SWAP). *Am J Ophthalmol*. 2002;134(2):177-185. doi:10.1016/S0002-9394(02)01577-5.

224. Polo V, Larrosa JM, Pinilla I, Pablo L, Honrubia FM. Optimum criteria for short-wavelength automated perimetry. *Ophthalmology*. 2001;108(2):285-289. doi:10.1016/S0161-6420(00)00535-2.

225. Bussel I, Wollstein G, Schuman J. OCT for glaucoma diagnosis, screening and detection of glaucoma progression. *Br J Ophthalmol*. 2014;98(Suppl II). doi:10.1136/bjophthalmol-2013-304326.

226. Felleman DJ, Van Essen DC. Distributed hierarchical processing in the primate cerebral cortex. *Cereb Cortex*. 1991;1(1):1-47. doi:10.1093/cercor/1.1.1-a.

227. Hubel DH, Wiesel TN. Functional architecture of macaque monkey visual cortex. *Proc R Soc B Biol Sci*. 1977;198(1130):1-59. doi:10.1098/rspb.1977.0085.

228. Balasubramanian V, Sterling P. Receptive fields and functional architecture in the retina. *J Physiol*. 2009;587(Pt 12):2753-2767. doi:10.1113/jphysiol.2009.170704.

229. Glezer VD. The receptive fields of the retina. *Vision Res*. 1965;5(10-11):497-525. doi:10.1016/0042-6989(65)90084-2.

230. Van Essen DC, Maunsell JHR. Hierarchical organization and functional streams in the visual cortex. *Trends Neurosci*. 1983;6(C):370-375. doi:10.1016/0166-2236(83)90167-4.

231. Quigley HA, Addicks EM, Green WR. Optic nerve damage in human glaucoma. III. Quantitative correlation of nerve fiber loss and visual field defect in glaucoma, ischemic neuropathy, papilledema, and toxic neuropathy. *Arch Ophthalmol (Chicago, Ill 1960)*. 1982;100(1):135-146. doi:10.1001/archopht.1982.01030030137016.

232. Harwerth RS, Carter-Dawson L, Shen F, Smith EL, Crawford MLJ. Ganglion cell

losses underlying visual field defects from experimental glaucoma. *Investig Ophthalmol Vis Sci*. 1999;40(10):2242-2250.

233. Soliman AE, DeJong LAMS, Ismaeil AAA, Van den Berg TJTP, De Smet MD. Standard achromatic perimetry, short wavelength automated perimetry, and frequency doubling technology for detection of glaucoma damage. *Ophthalmology*. 2002;109(3):444-454. doi:10.1016/S0161-6420(01)00988-5.

234. Trible JR, Schultz RO, Robinson JC, Rothe TL. Accuracy of glaucoma detection with frequency-doubling perimetry. *Am J Ophthalmol*. 2000;129(6):740-745. doi:10.1016/S0002-9394(00)00354-8.

235. Brusini P, Busatto P. Frequency doubling perimetry in glaucoma early diagnosis. *Acta Ophthalmol Scand Suppl*. 1998;(227):23-24. doi:10.1097/00061198-200202000-00009.

236. Spry PGD, Johnson C a, Mansberger SL, Cioffi G a. Psychophysical investigation of ganglion cell loss in early glaucoma. *J Glaucoma*. 2005;14(1):11-19. doi:10.1097/01.ijg.0000145813.46848.b8.

237. WMA. *Declaration of Helsinki.* Vol 353. 1974. doi:10.2471/BLT.08.057737.

238. Whitehouse GM. The effect of cataract on Accumap multifocal objective perimetry. *Am J Ophthalmol*. 2003;136(1):209-212. doi:10.1016/S0002-9394(02)02276-6.

239. Costagliola C, De Simone C, Giacoia A, Iuliano G, Landolfo V. Influence of lens opacities on visual field indices. *Ophthalmol J Int d'ophtalmologie Int J Ophthalmol Zeitschrift f{ü}r Augenheilkd*. 1990;201(4):180-186. http://www.ncbi.nlm.nih.gov/pubmed/2077454.

240. Cai Y, Lim BA, Chi L, et al. [Effects of lens opacity on AccuMap multifocal objective perimetry in glaucoma]. *Zhonghua Yan Ke Za Zhi*. 2006;42(11):972-976. http://www.ncbi.nlm.nih.gov/pubmed/17386132.

241. Herbik A, Hölzl GC, Reupsch J, Hoffmann MB. Differential effects of optic media opacities on mfERGs and mfVEPs. *Clin Neurophysiol*. 2013;124(6):1225-1231. doi:10.1016/j.clinph.2012.11.020.

242. Hood DC, Ghadiali Q, Zhang JC, Graham N V, Wolfson SS, Zhang X. Contrast-response functions for multifocal visual evoked potentials: a test of a model relating V1 activity to multifocal visual evoked potentials activity. *J Vis*. 2006;6(5):580-593.

doi:10.1167/6.5.4.

243. Pointer JS, Hess RF. The contrast sensitivity gradient across the human visual field: With emphasis on the low spatial frequency range. *Vision Res*. 1989;29(9):1133-1151. doi:10.1016/0042-6989(89)90061-8.

244. Quigley HA, Sanchez RM, Dunkelberger GR, L'Hernault NL, Baginski TA. Chronic glaucoma selectively damages large optic nerve fibers. *Investig Ophthalmol Vis Sci*. 1987;28(6):913-920.

245. Parisi V. Impaired visual function in glaucoma. *Clin Neurophysiol*. 2001;112(2):351-358. doi:10.1016/S1388-2457(00)00525-3.

246. Hasnain MK, Fox PT, Woldorff MG. Intersubject variability of functional areas in the human visual cortex. *Hum Brain Mapp*. 1998;6(4):301-315. doi:10.1002/(SICI)1097-0193(1998)6:4<301::AID-HBM8>3.0.CO;2-7.

247. Hood DC. Assessing retinal function with the multifocal technique. *Prog Retin Eye Res*. 2000;19(5):607-646. doi:10.1016/S1350-9462(00)00013-6.

248. Rademacher J, Rademacher J, Caviness VS, Steinmetz H, Galaburda AM. Topographical variation of the human primary cortices: implications for neuroimaging, brain mapping, and neurobiology. *Cereb Cortex*. 1993;3(4):313-329. doi:10.1093/cercor/3.4.313.

249. Klistorner AI, Graham SL. Multifocal pattern VEP perimetry: Analysis of sectoral waveforms. *Doc Ophthalmol*. 1999;98(2):183-196. doi:10.1023/A:1002449304052.

250. Heijl A, Leske MC, Bengtsson B, Bengtsson B, Hussein M. Measuring visual field progression in the Early Manifest Glaucoma Trial. *Acta Ophthalmol Scand*. 2003;81(3):286-293. doi:070 [pii].

251. Burnstein Y, Ellish NJ, Magbalon M, Higginbotham EJ. Comparison of frequency doubling perimetry with Humphrey visual field analysis in a glaucoma practice. *Am J Ophthalmol*. 2000;129(3):328-333. doi:10.1016/S0002-9394(99)00364-5.

252. Medeiros FA, Sample PA, Weinreb RN. Frequency doubling technology perimetry abnormalities as predictors of glaucomatous visual field loss. *Am J Ophthalmol*. 2004;137(5):863-871. doi:10.1016/j.ajo.2003.12.009.

253. Meira-Freitas D, Tatham AJ, Lisboa R, et al. Predicting progression of glaucoma from

rates of frequency doubling technology perimetry change. *Ophthalmology*. 2014;121(2):498-507. doi:10.1016/j.ophtha.2013.09.016.

254. Johnson CA, Samuels SJ. Screening for glaucomatous visual field loss with frequency-doubling perimetry. *Investig Ophthalmol Vis Sci*. 1997;38(2):413-425.

255. Arend KO, Plange N. [Diagnostic approaches for early detection of glaucoma progression]. *Klin Monbl Augenheilkd*. 2006;223(3):194-216. doi:10.1055/s-2005-858734.

256. Sponsel WE, Arango S, Trigo Y, Mensah J. Clinical classification of glaucomatous visual field loss by frequency doubling perimetry. *Am J Ophthalmol*. 1998;125(6):830-836. doi:10.1016/S0002-9394(98)00047-6.

257. Spry PGD, Hussin HM, Sparrow JM. Clinical evaluation of frequency doubling technology perimetry using the Humphrey Matrix 24-2 threshold strategy. *Br J Ophthalmol*. 2005;89(8):1031-1035. doi:10.1136/bjo.2004.057778.

258. Kim KE, Jeoung JW, Kim DM, Ahn SJ, Park KH, Kim SH. Long-term follow-up in preperimetric open-angle glaucoma: Progression rates and associated factors. *Am J Ophthalmol*. 2015;159(1):160-168.e2. doi:10.1016/j.ajo.2014.10.010.

259. Leung CK, Ye C, Weinreb RN, et al. Retinal nerve fiber layer imaging with spectral-domain optical coherence tomography a study on diagnostic agreement with Heidelberg Retinal Tomograph. *Ophthalmology*. 2010;117(2):267-274. doi:10.1016/j.ophtha.2009.06.061.

260. Hood DC, Greenstein VC, Odel JG, et al. Visual field defects and multifocal visual evoked potentials: evidence of a linear relationship. *Arch Ophthalmol*. 2002;120(12):1672-1681.

261. Sung KR, Kim DY, Park SB, Kook MS. Comparison of Retinal Nerve Fiber Layer Thickness Measured by Cirrus HD and Stratus Optical Coherence Tomography. *Ophthalmology*. 2009;116(7). doi:10.1016/j.ophtha.2008.12.045.

262. Tan O, Chopra V, Lu ATH, et al. Detection of Macular Ganglion Cell Loss in Glaucoma by Fourier-Domain Optical Coherence Tomography. *Ophthalmology*. 2009;116(12). doi:10.1016/j.ophtha.2009.05.025.

263. Medeiros FA, Zangwill LM, Bowd C, Vessani RM, Susanna R, Weinreb RN.

Evaluation of retinal nerve fiber layer, optic nerve head, and macular thickness measurements for glaucoma detection using optical coherence tomography. *Am J Ophthalmol*. 2005;139(1):44-55. doi:10.1016/j.ajo.2004.08.069.

264. Na JH, Sung KR, Lee JR, et al. Detection of glaucomatous progression by spectral-domain optical coherence tomography. *Ophthalmology*. 2013;120(7):1388-1395. doi:10.1016/j.ophtha.2012.12.014.

265. Miki A, Medeiros FA, Weinreb RN, et al. Rates of retinal nerve fiber layer thinning in glaucoma suspect eyes. *Ophthalmology*. 2014;121(7):1350-1358. doi:10.1016/j.ophtha.2014.01.017.

266. Hood DC, Kardon RH. A framework for comparing structural and functional measures of glaucomatous damage. *Prog Retin Eye Res*. 2007;26(6):688-710. doi:10.1016/j.preteyeres.2007.08.001.

267. Landers J a, Goldberg I, Graham SL. Detection of early visual field loss in glaucoma using frequency-doubling perimetry and short-wavelength automated perimetry. *Arch Ophthalmol*. 2003;121(12):1705-1710. doi:10.1001/archopht.121.12.1705.

268. Chauhan BC, Garway-Heath DF, Goñi FJ, et al. Practical recommendations for measuring rates of visual field change in glaucoma. *Br J Ophthalmol*. 2008;92(4):569-573. doi:10.1136/bjo.2007.135012.

269. Suda K, Hangai M, Akagi T, et al. Comparison of longitudinal changes in functional and structural measures for evaluating progression of glaucomatous optic neuropathy. *Investig Ophthalmol Vis Sci*. 2015;56(9):5477-5484. doi:10.1167/iovs.15-16704.

270. Zangwill LM, Bowd C, Berry CC, et al. Discriminating Between Normal and Glaucomatous Eyes Using the Heidelberg Retina Tomograph, GDx Nerve Fiber Analyzer, and Optical Coherence Tomograph. *Arch Ophthalmol*. 2001;119(7):985. doi:10.1001/archopht.119.7.985.

271. Shpak AA, Sevostyanova MK, Ogorodnikova SN, Shormaz IN. Comparison of measurement error of Cirrus HD-OCT and Heidelberg Retina Tomograph 3 in patients with early glaucomatous visual field defect. *Graefe's Arch Clin Exp Ophthalmol*. 2012;250(2):271-277. doi:10.1007/s00417-011-1808-4.

272. Jampel HD, Friedman D, Quigley H, et al. Agreement Among Glaucoma Specialists in Assessing Progressive Disc Changes From Photographs in Open-Angle Glaucoma

Patients. *Am J Ophthalmol*. 2009;147(1). doi:10.1016/j.ajo.2008.07.023.